Research with Synchrotron Radiation

R. Gehrke
HASYLAB
Summerstudent Lecture, July 28, 2010

- **Synchrotron Radiation at DESY**
- **Some Examples for Research with Synchrotron Radiation**

First observation of Synchrotron Radiation

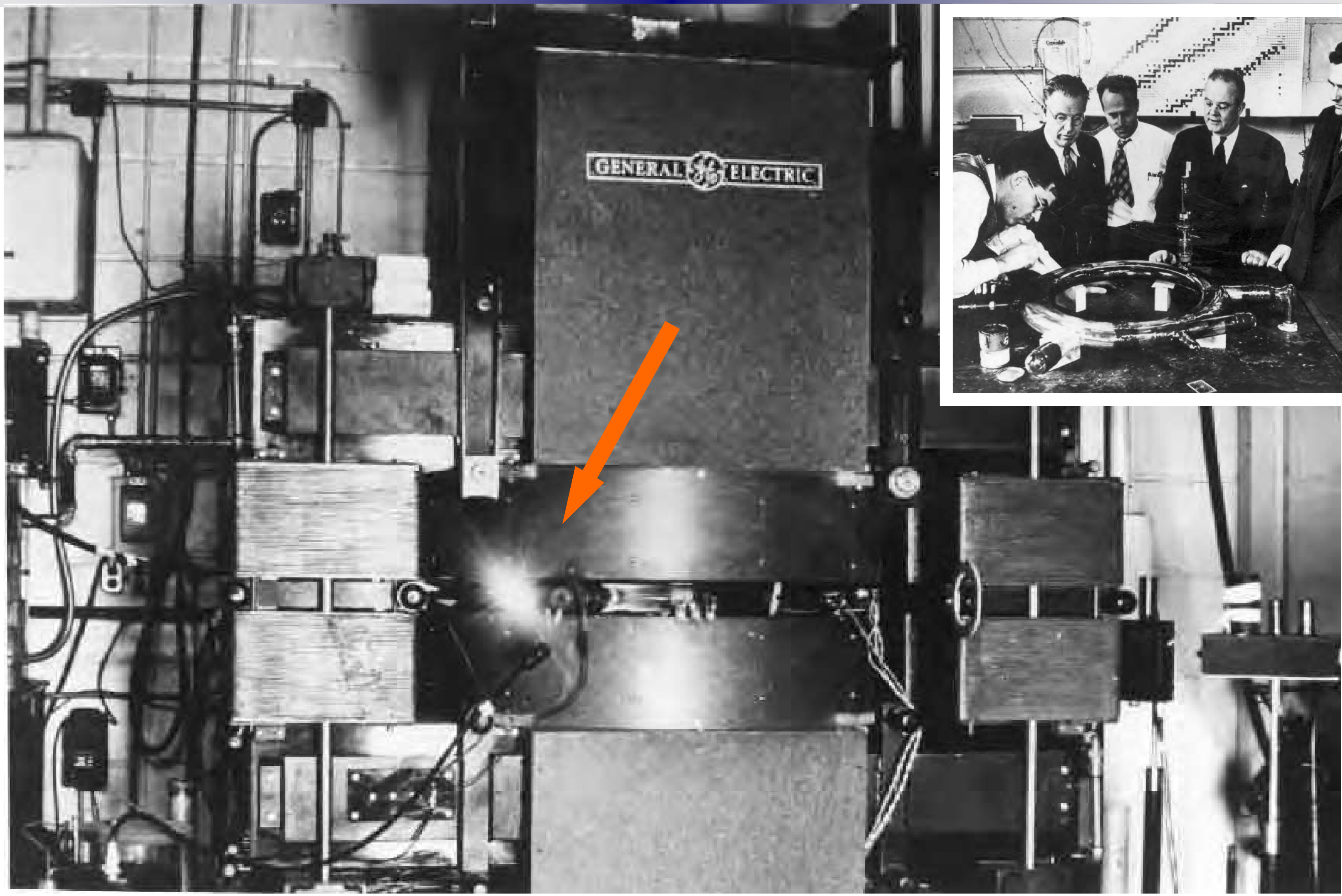

April 24, 1947: First observation of SR at General Electric 70 MeV synchrotron
(Langmuir, Elder, Gurewitch, Charlton, Pollock)

The DORIS III storage ring

Beam Energy	4.5 GeV
Beam Current	150 mA
Power consumption	5 MW
HF Power	1 MW
Radiated Power	200 kW

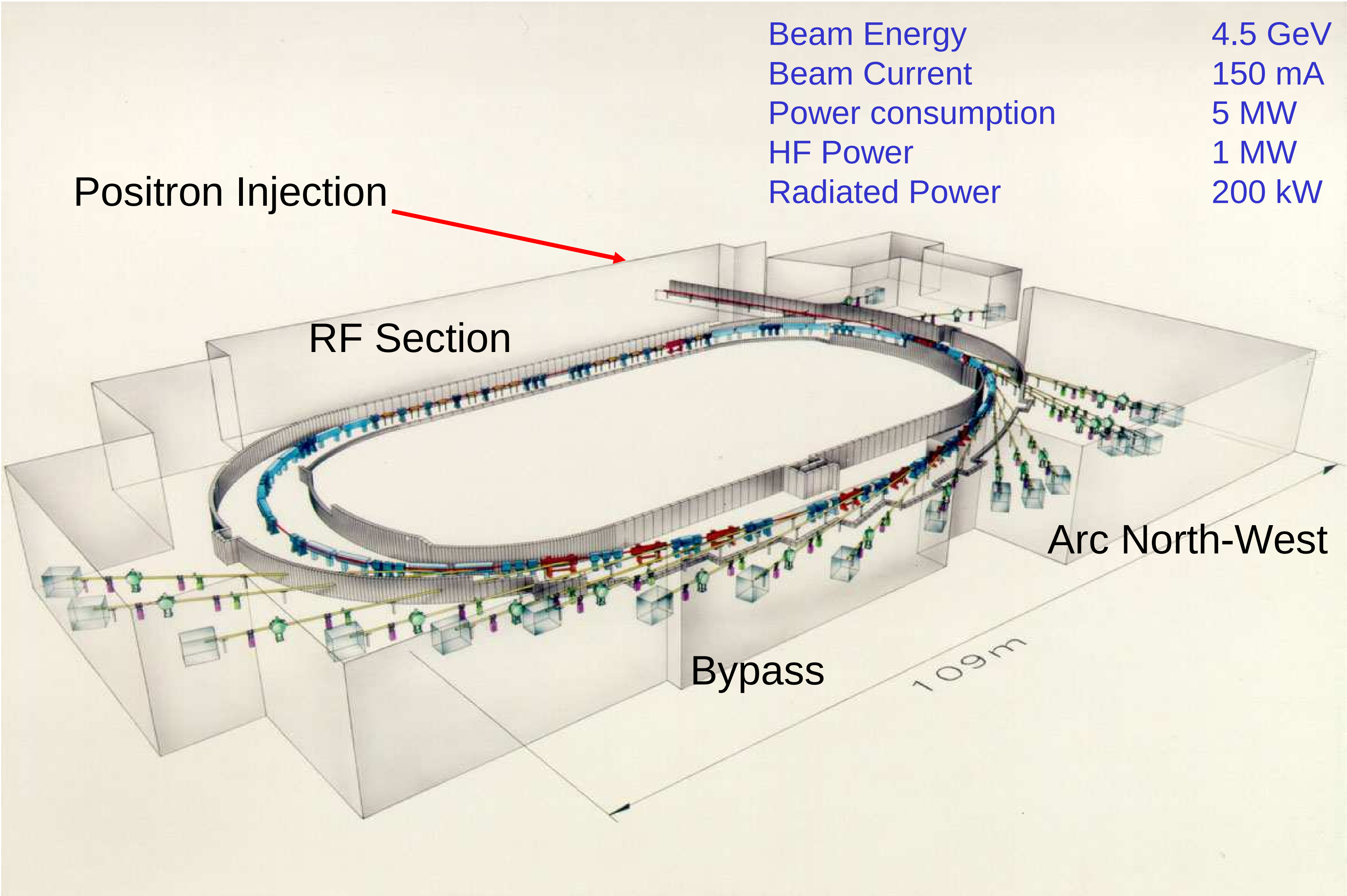

Key Properties of Radiation Emitted by Relativistic Electrons on a Curved Path

1. High photon flux

$$P_{circular} = \frac{2q^2}{3m_0^4 c^7} \cdot \frac{E^4}{R^2}$$

2. High degree of collimation (brilliance) $\Theta = 0.608/\gamma$ = 0.07 mrad at 4.5 GeV and λ=0.1nm

($\gamma = E / m_0 c^2$)

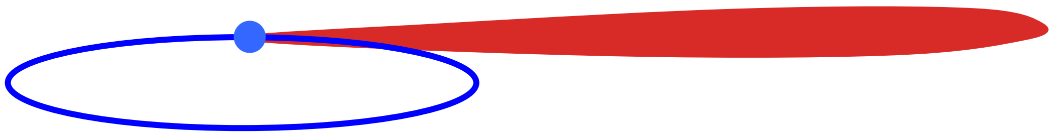

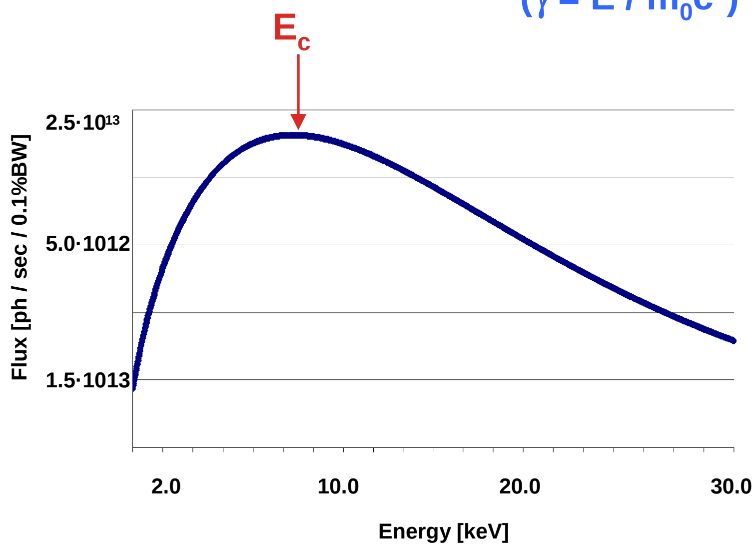

3. Continuous spectrum (IR to hard X-rays)

$$E_c = 0.665 \cdot E^2 [GeV] \cdot B[T]$$

4. Polarization (linear in ring plane, circular above and below)

5. Time structure

6. Clean light pulses

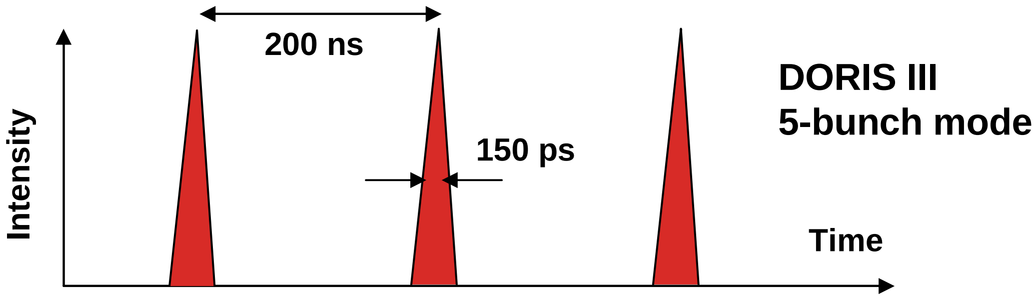

Insertion Devices

Wiggler

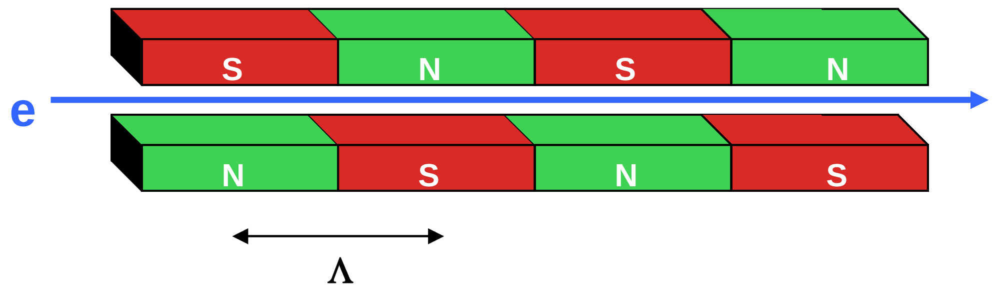

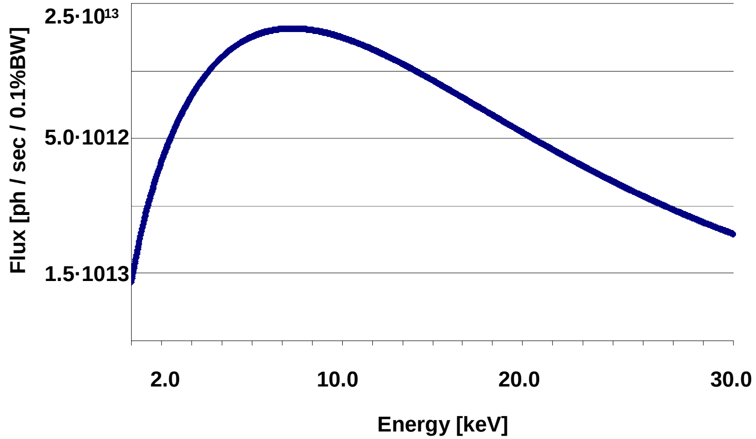

Flux I ∝ N·n

Divergence Θ ∝ 1/γ

Undulator

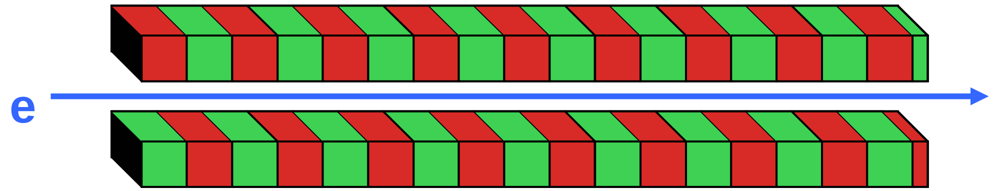

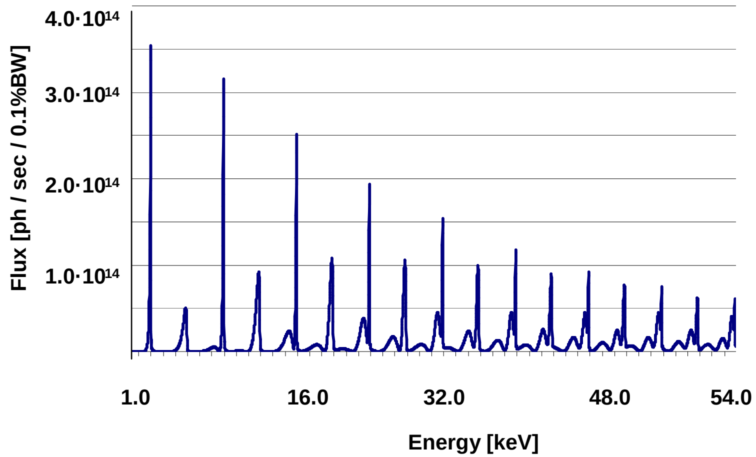

Flux I ∝ N^2 · n

Divergence Θ ∝ $1/\sqrt{\gamma^2 \cdot N \cdot n}$

Undulator in the DORIS III Bypass

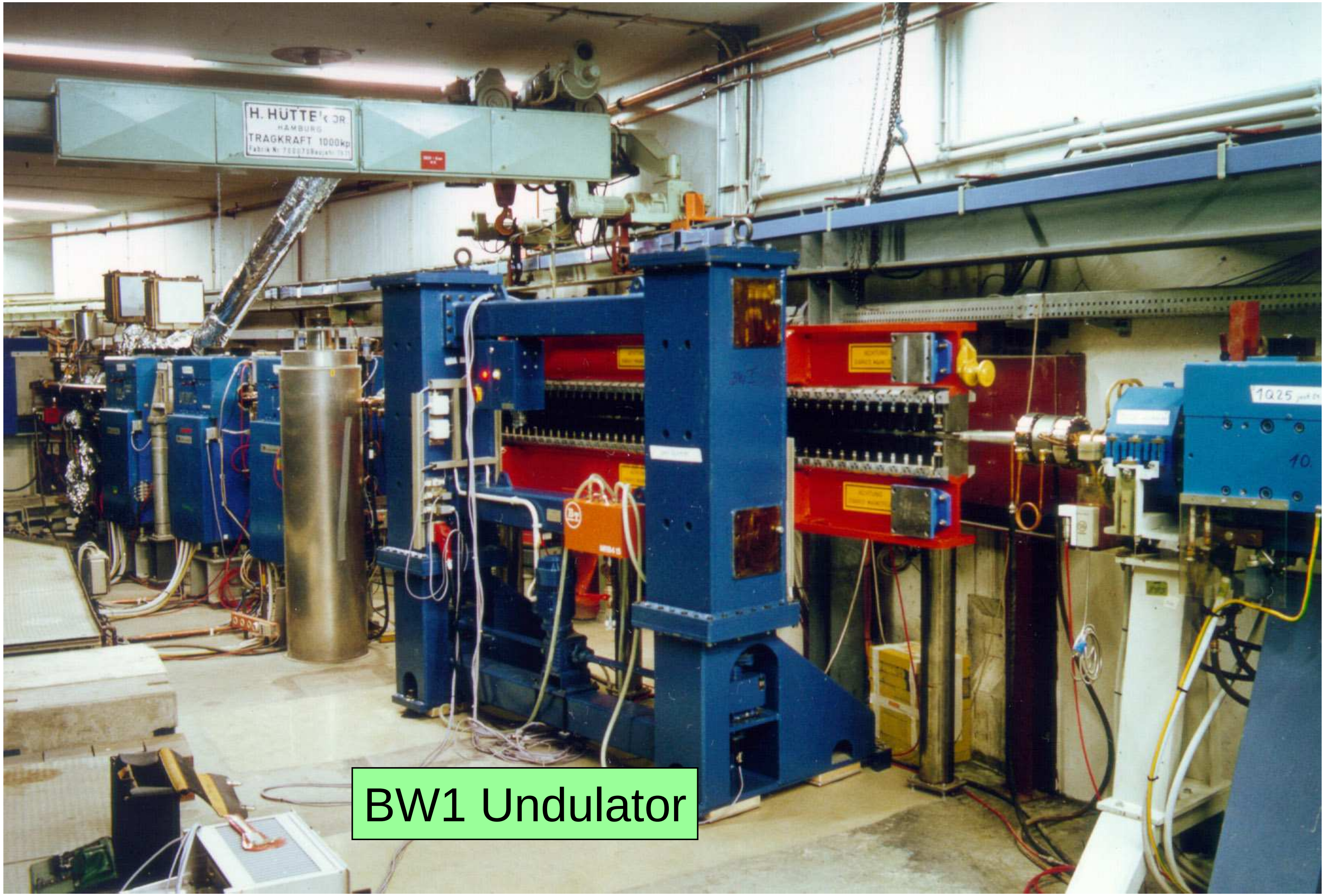

The SASE-principle for free electron lasers

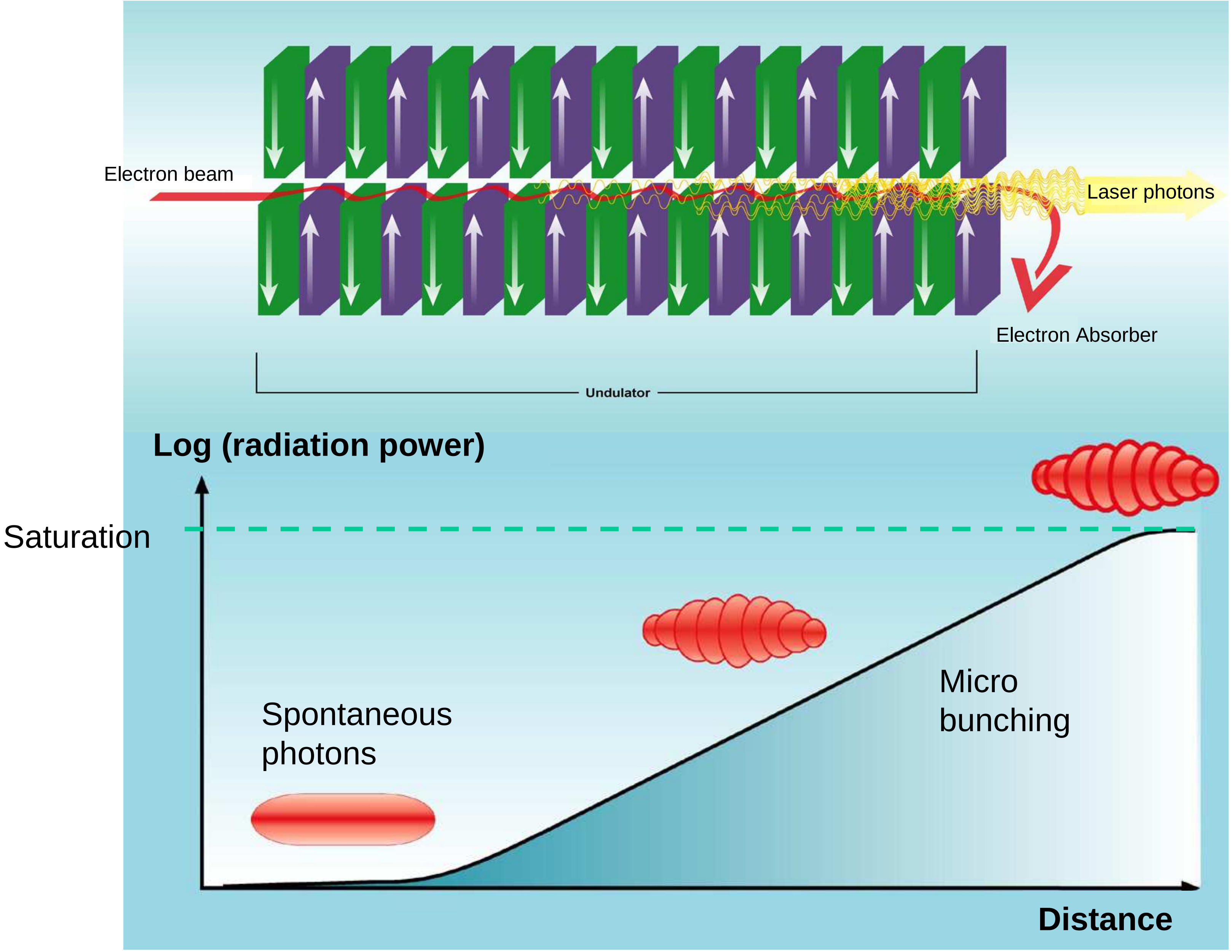

SASE undulators

SASE – Undulator (Free Electron Laser)

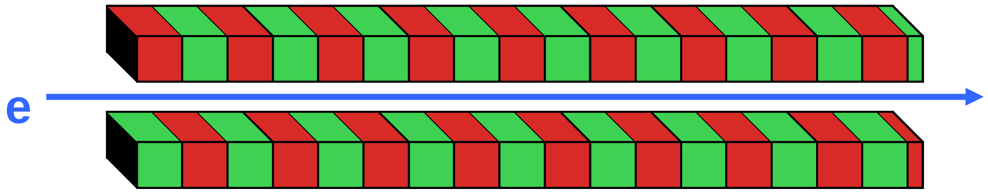

Flux I ∝ $N^2 \cdot$ n²

Divergence $\Theta \propto 1/\sqrt{\gamma^2 \cdot N \cdot n}$

Plus:

- Extreme short pulses (< 100 fsec)
- $10^{12} – 10^{13}$ photons/puls
- Up to 40000 pulses/sec
- 0.1% intrinsic energy resolution
- Full coherence

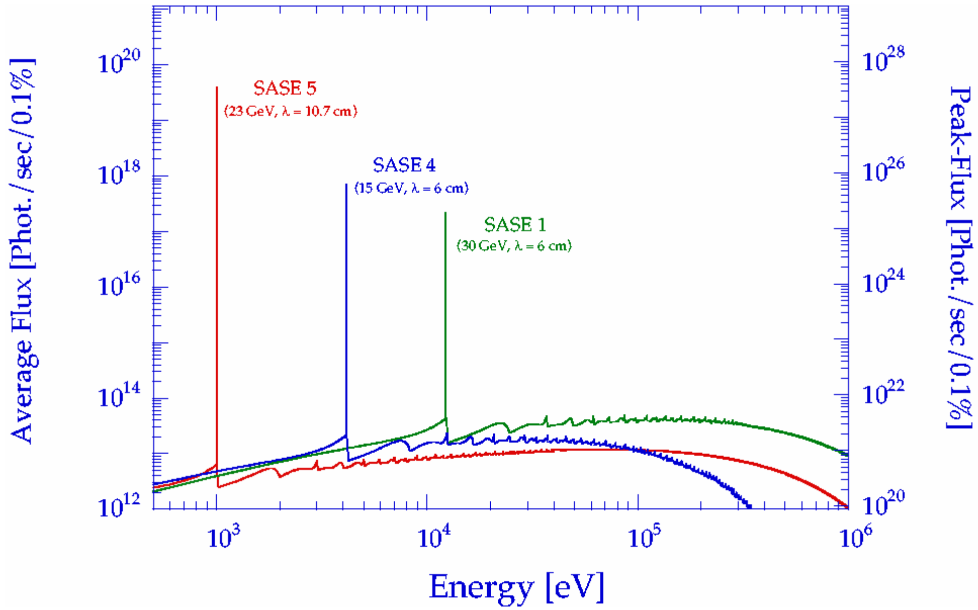

The FLASH free electron laser

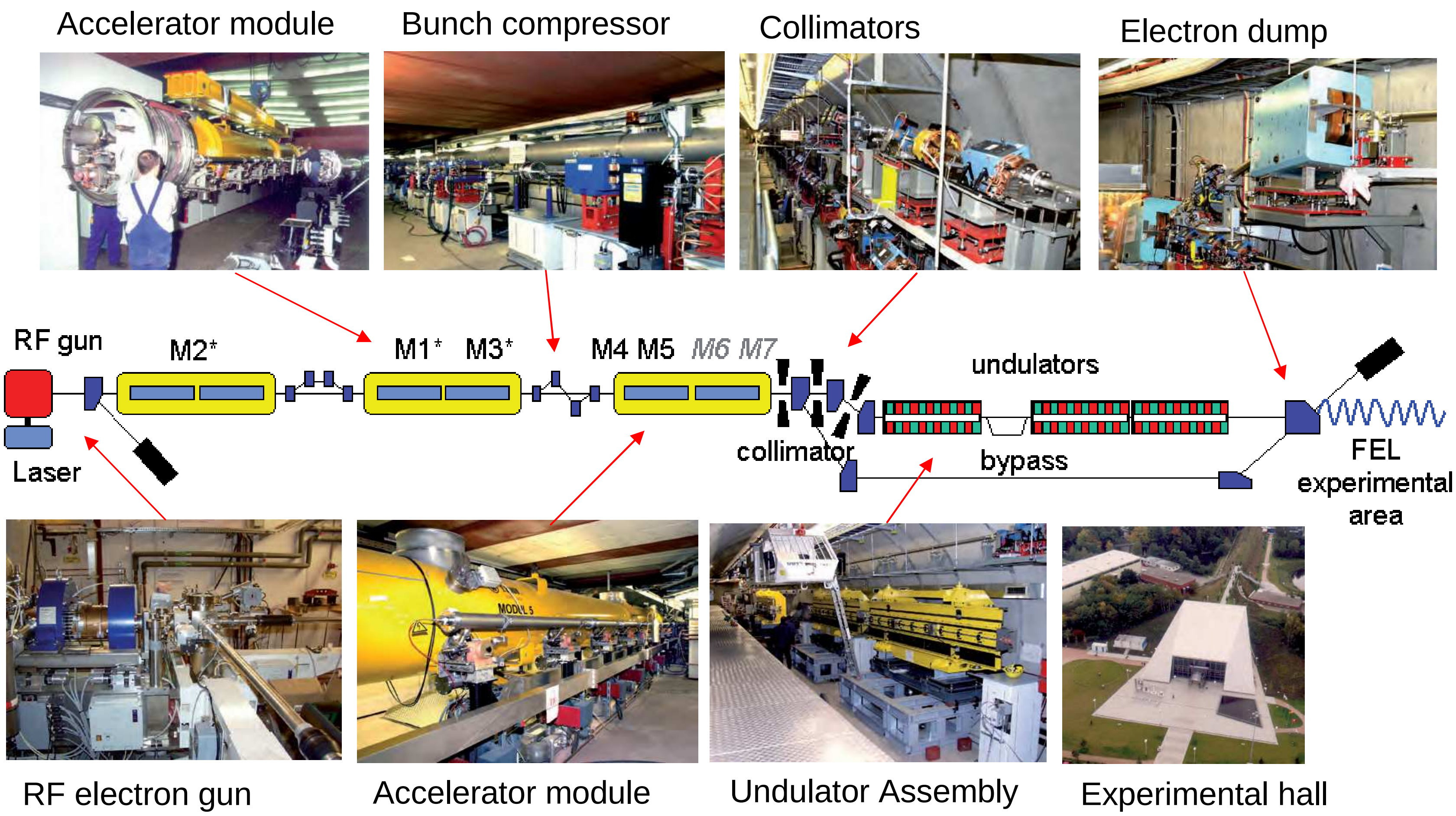

SASE Undulator Assembly at FLASH

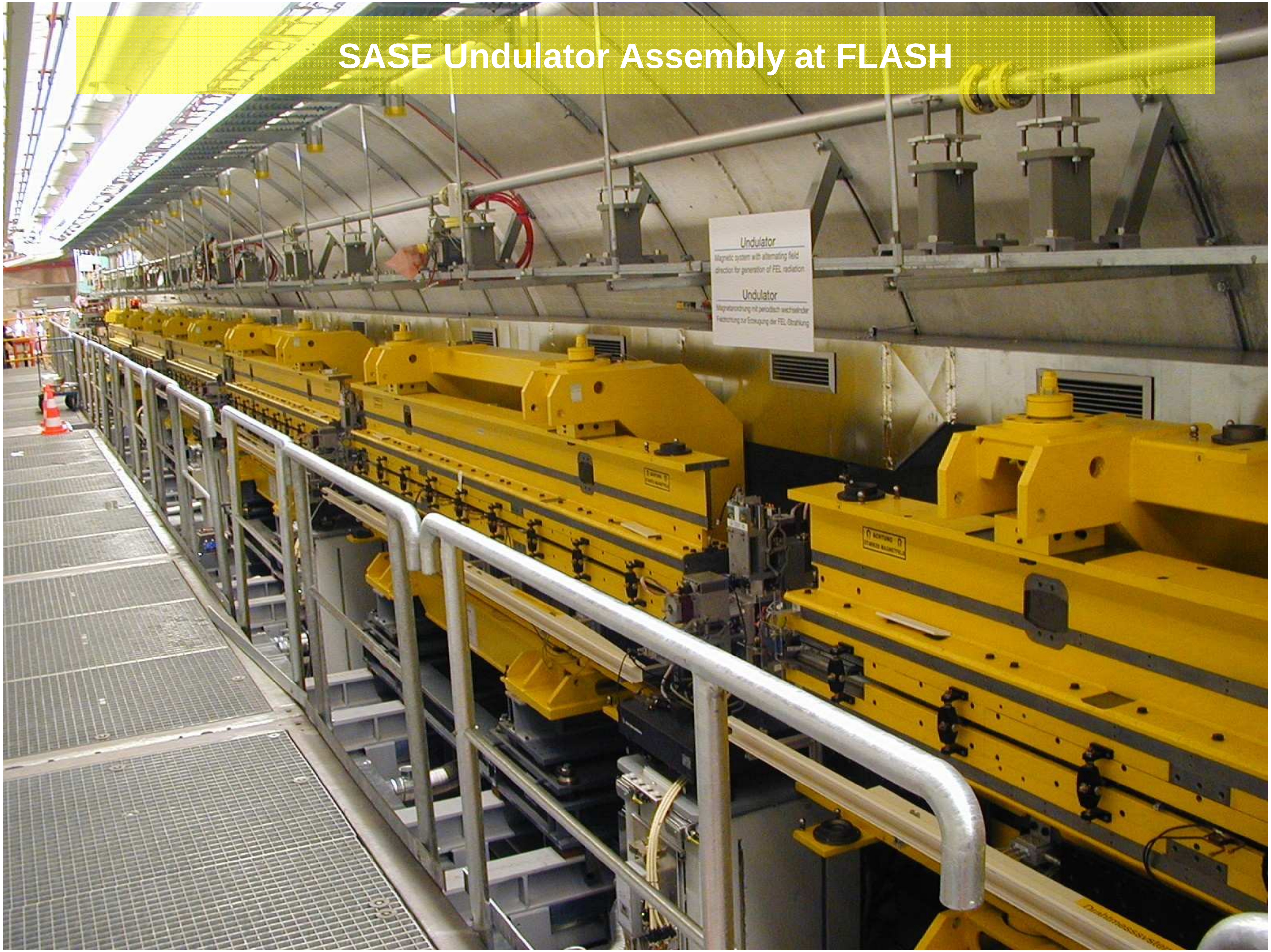

Different quantities to describe photon intensity

Total Flux *F*
number of photons
per time and energy interval

$$[F_{tot}] = \frac{Number\ \ of\ \ photons}{s}$$

Spectral Flux
number of photons
per time, energy, and solid angle

$$[F] = \frac{Number\ of\ \ photons}{s \cdot 0.1\% BW}$$

Brilliance *B*
number of photons
per time, energy, solid angle
and source area

$$[B] = \frac{Number\ \ of\ \ photons}{s \cdot mm^2 \cdot mrad^2 \cdot 0.1\% BW}$$

Peak brilliance B^{peak}
brilliance scaled to pulse duration

$$B^{peak} = \frac{B}{\tau \times f}$$

Evolution of Brilliance

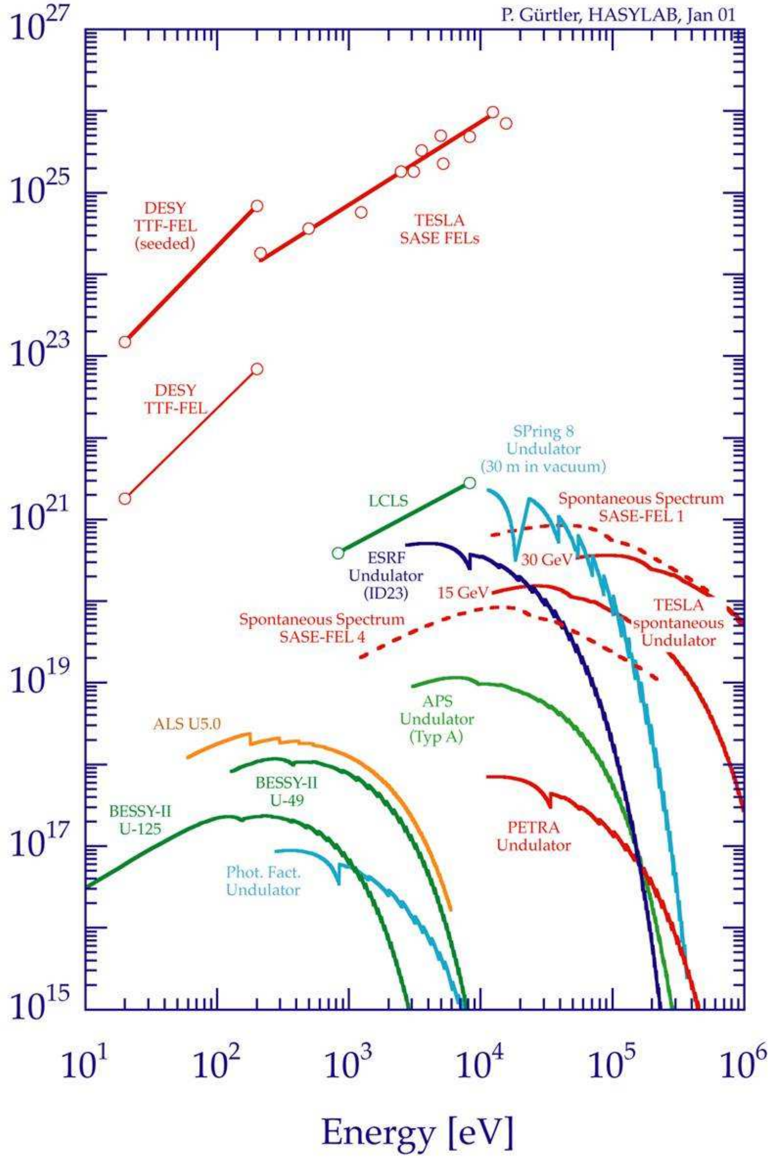

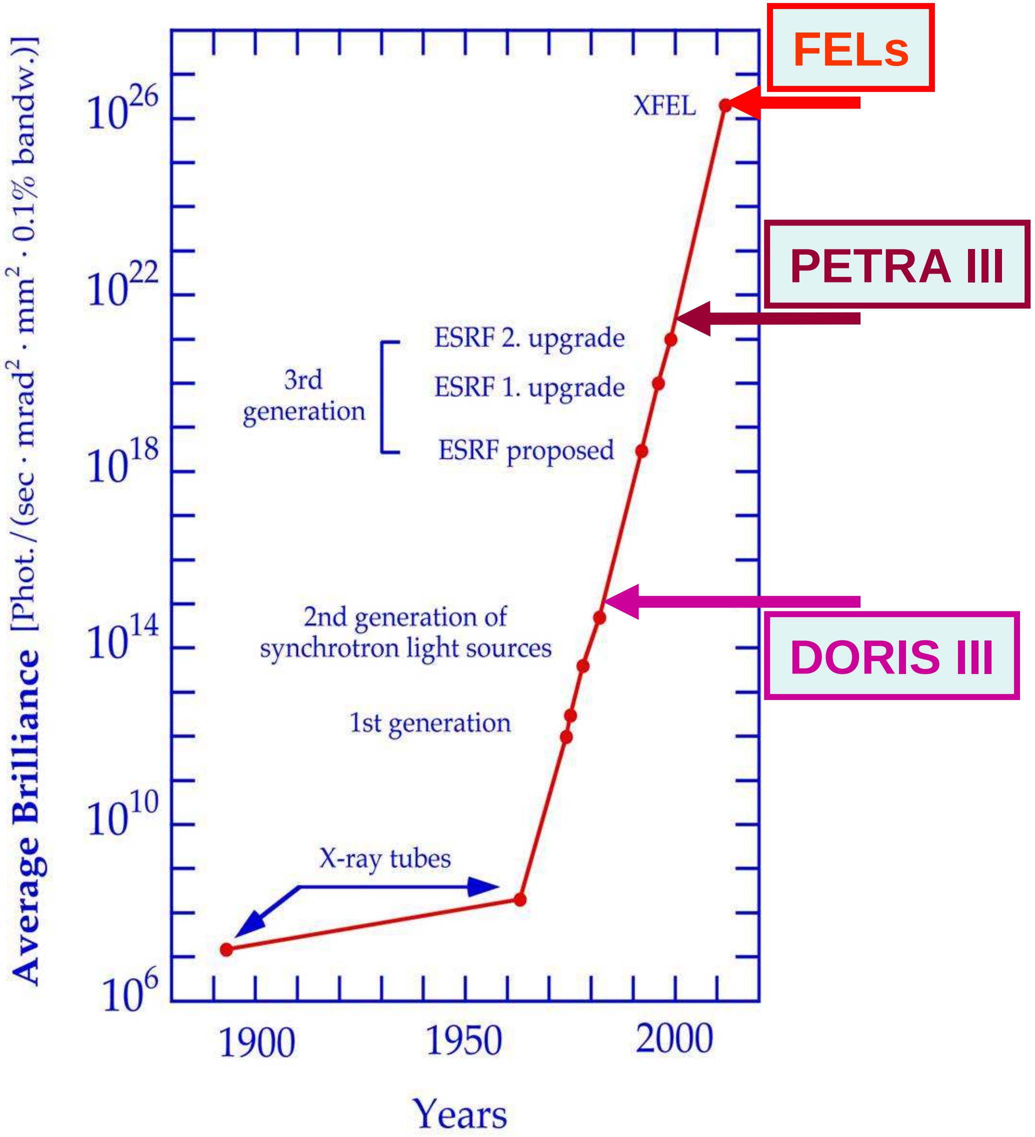

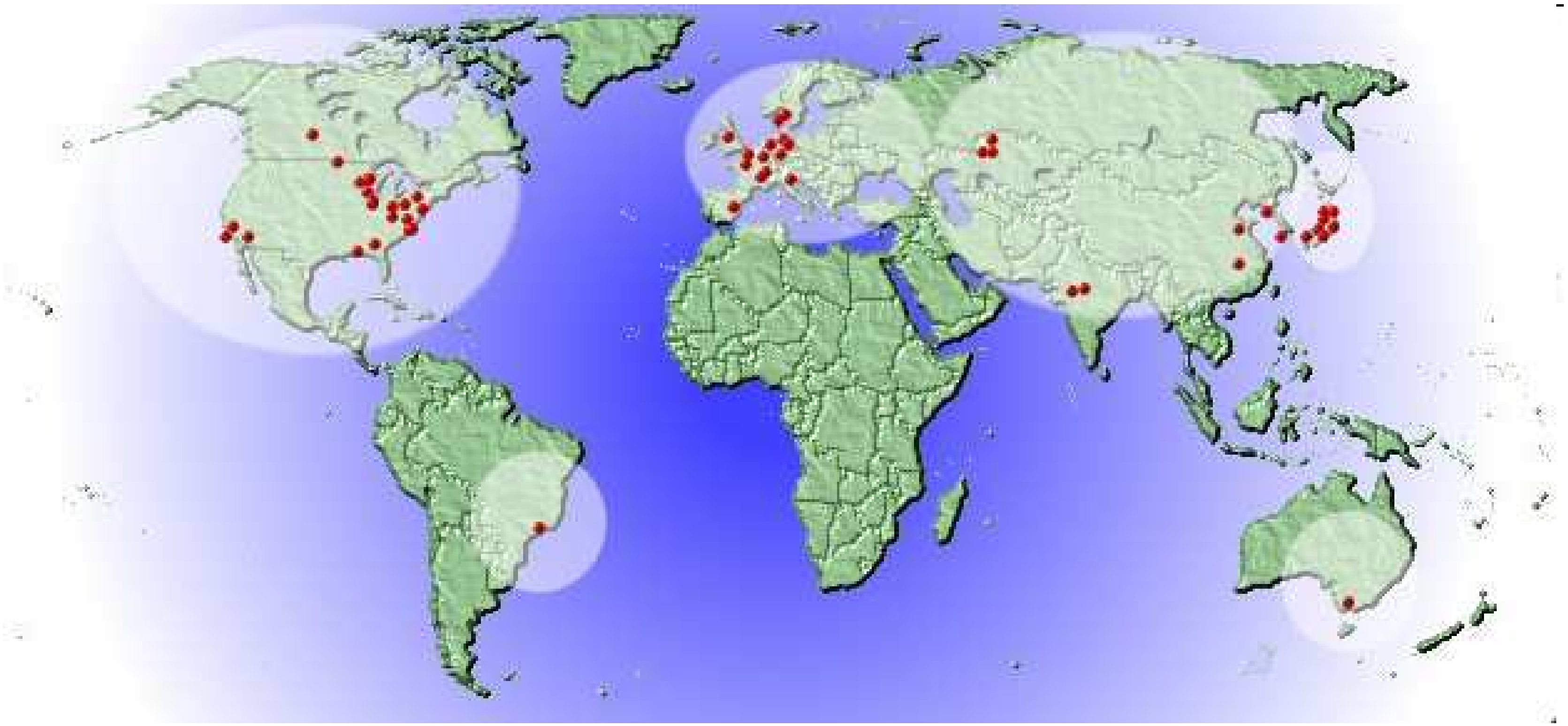

About 70 large and small SR-Facilities worldwide

Synchrotron Radiation Sources in Europe

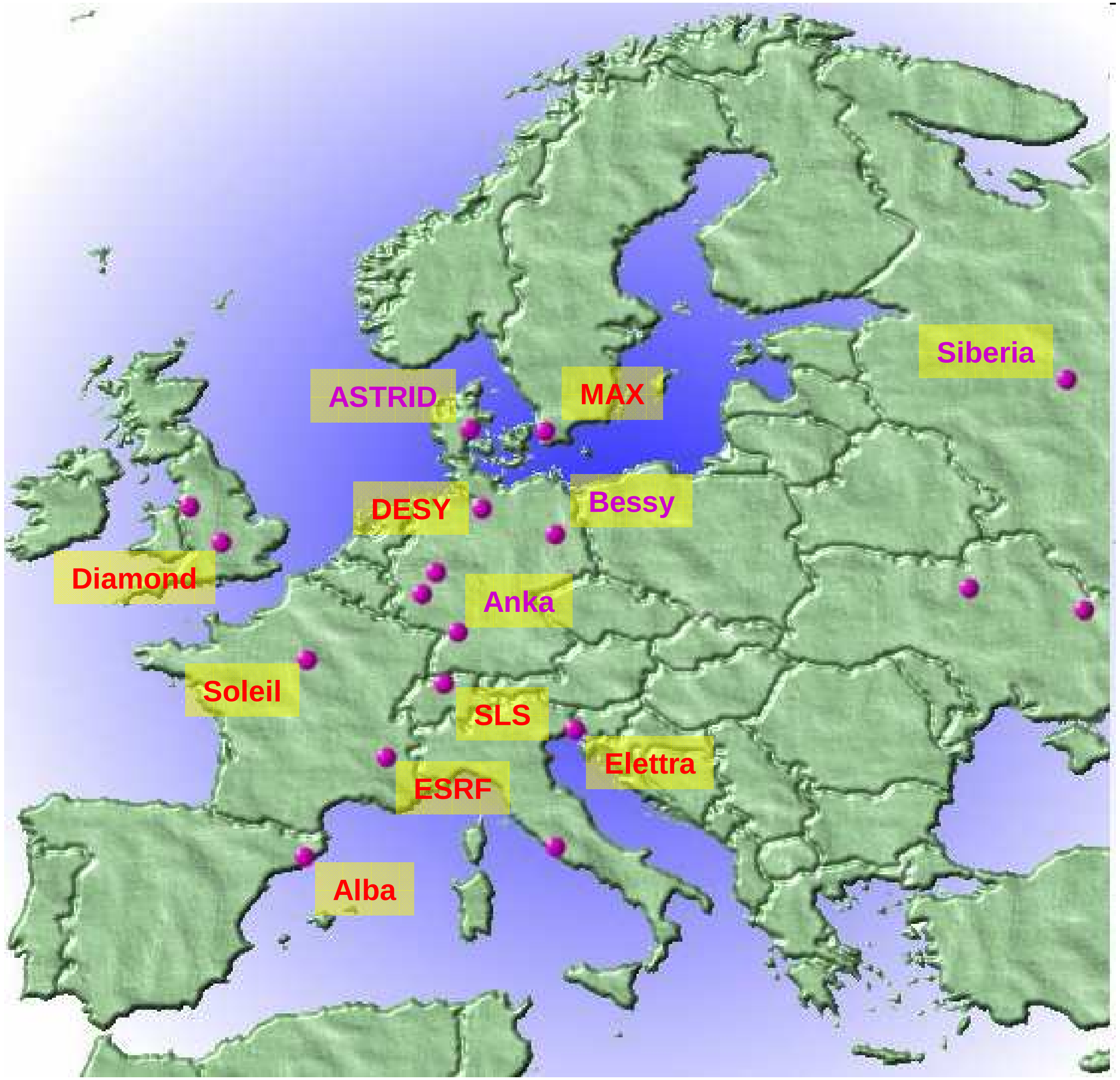

Photon Facilities at DESY

DORIS III

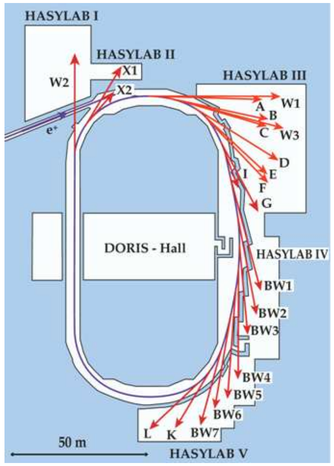

FLASH

PETRA III

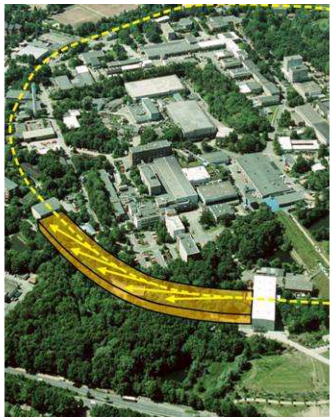

European XFEL

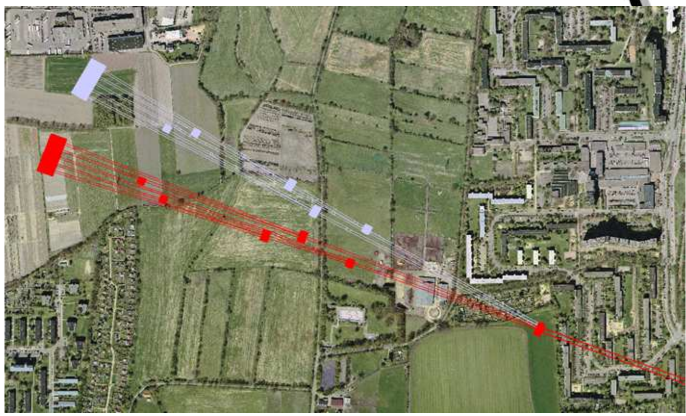

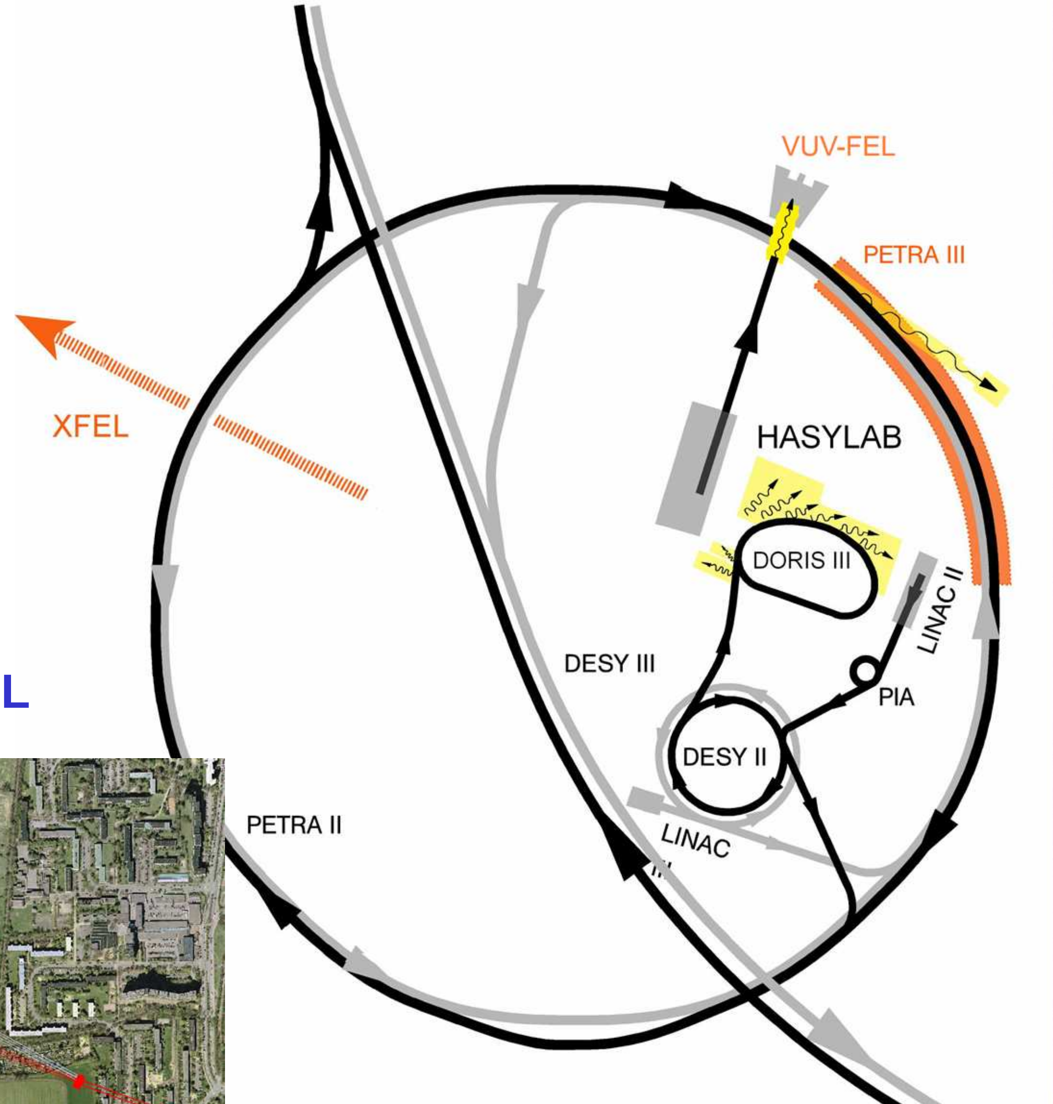

Beamlines at DORIS III

38 beamlines, 70 experimental stations

11 Stations operated by external organizations:
- **EMBL: 7**
- **MPG: 1**
- **GKSS: 1**
- **GFZ: 2**

16 stations operated with support from external institutions:
- **BMBF-Verbundforschung**
- **FZ Jülich**
- **University Hamburg**
- **University Kiel**
- **University Aachen**
- **Debye Inst. Utrecht**
- **RISØ**
- **MPI Golm**

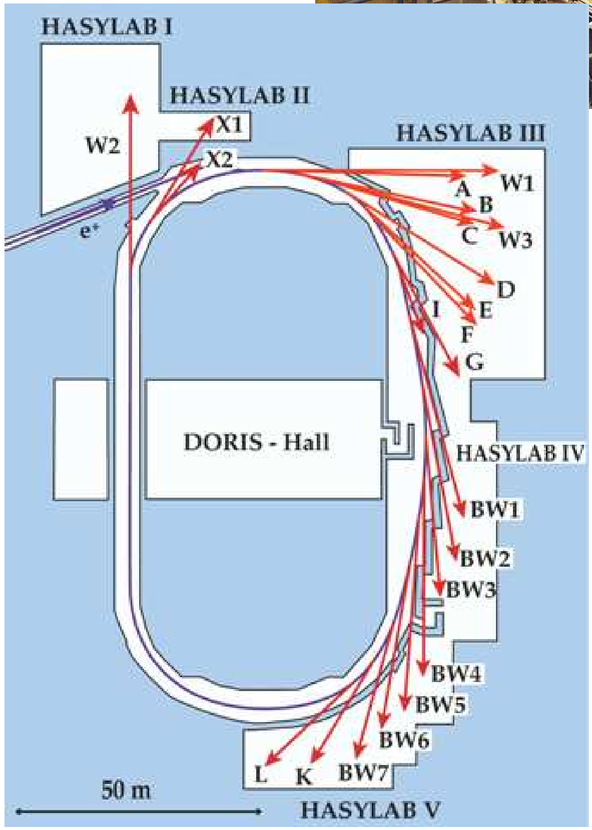

The PETRA III Project

http://petra3.desy.de

The PETRA III Project

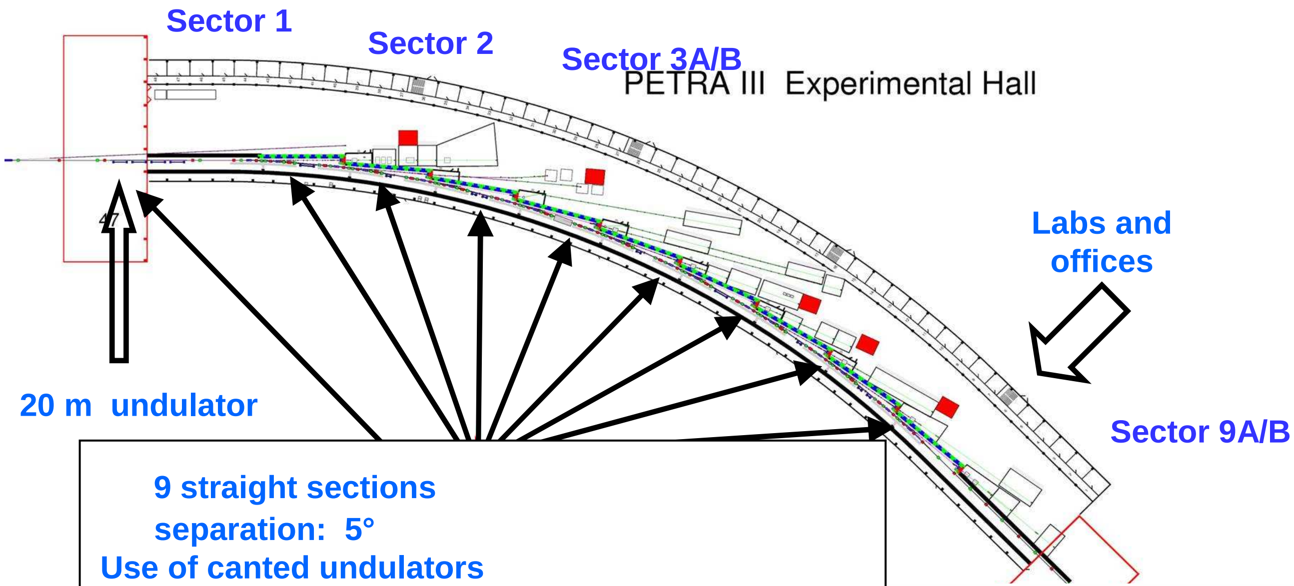

9 straight sections
separation: 5°
Use of canted undulators
(5 mrad, 2 m device length): → 14 separate undulator BLs

Parameters:

- rebuild of 1/8 of PETRA
- refurbishment of 7/8 of PETRA
- energy: 6 GeV
- current: 100 mA
- emittance: 1 nmrad
- undulators: 14
- undulator length: 2, 5, 20 m
- max. BL-length 100 m
- top up operation mode

Phase 1 of beamline construction concentrates on instruments using primary beam size in the micrometer to nanometer range

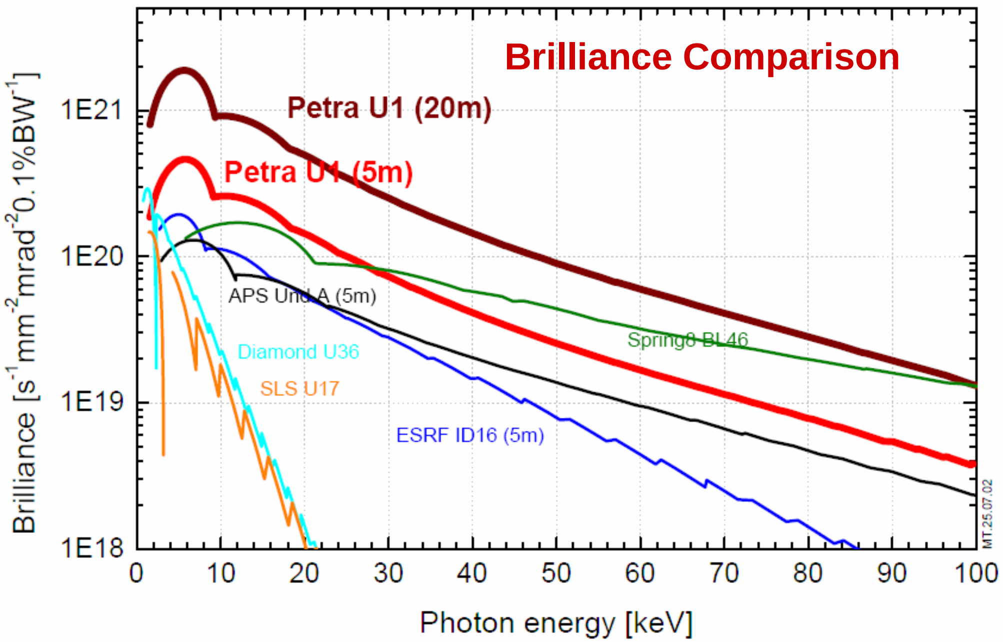

Achieved performance at VUV-FEL (phase 1):

Radiation wavelength	6.9 - 125 nm
Radiation pulse energy at saturation	10 - 100 μJ
Radiation pulse duration (FWHM)	10-50 fs
Radiation peak power	1 - 5 GW
Spectrum width (FWHM)	1%
Radiation spot size [FWHM]	200 μm
Radiation angular divergence [FWHM]	260 μrad
Radiation peak brilliance up to	10^{30}
Number of photons per bunch	10^{12} - 10^{13}

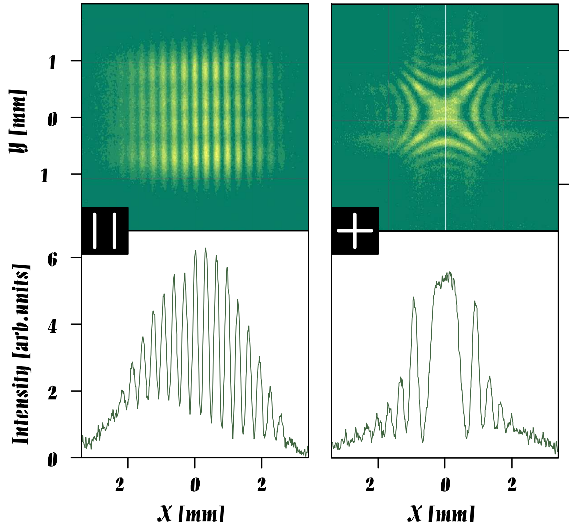

transverse coherence

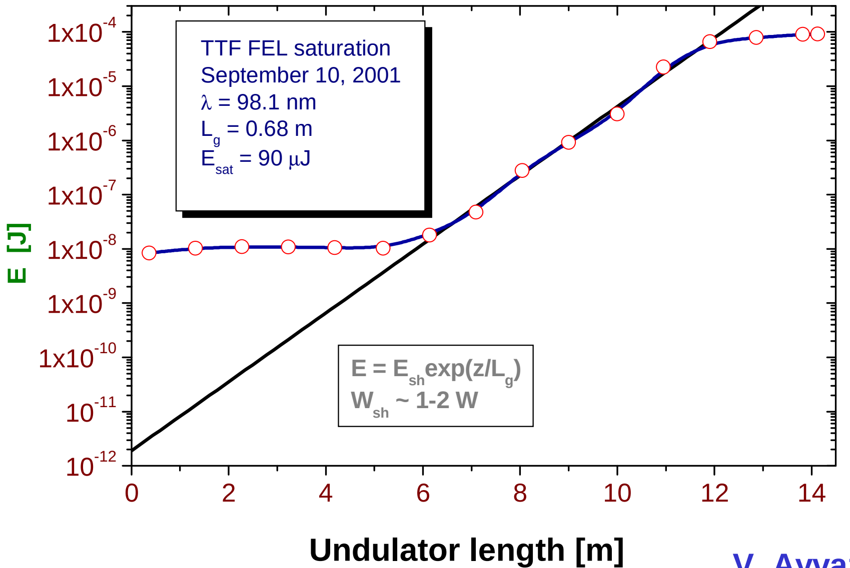

VUV-FEL (phase 1) in saturation at 98nm

V. Ayvazyan et al., PRL 88(2002)104802

The FLASH II User Facility

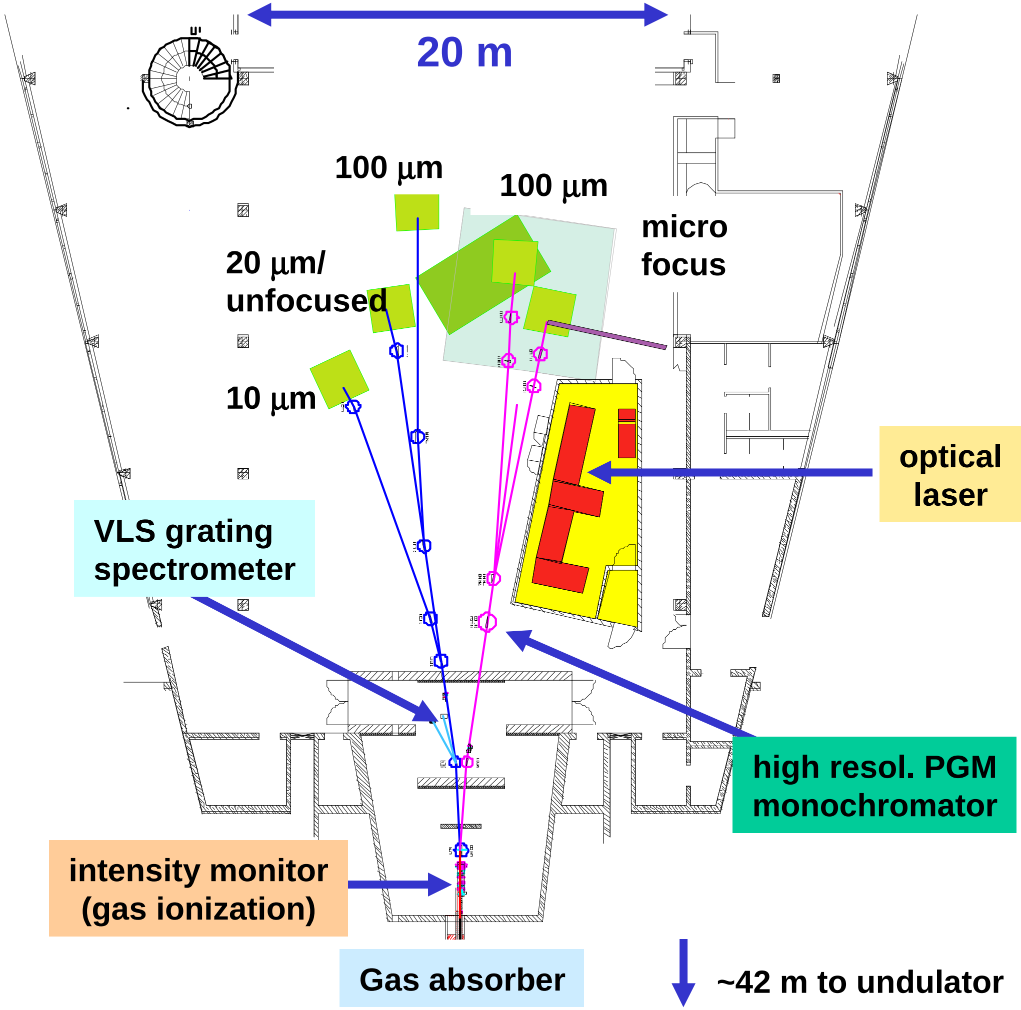

Start of user Operation: 2005

superconducting linac: 1 GeV
minimal wavelength: 6nm
five experimental platforms with different focal spots/optics

FLASH II experimental hall

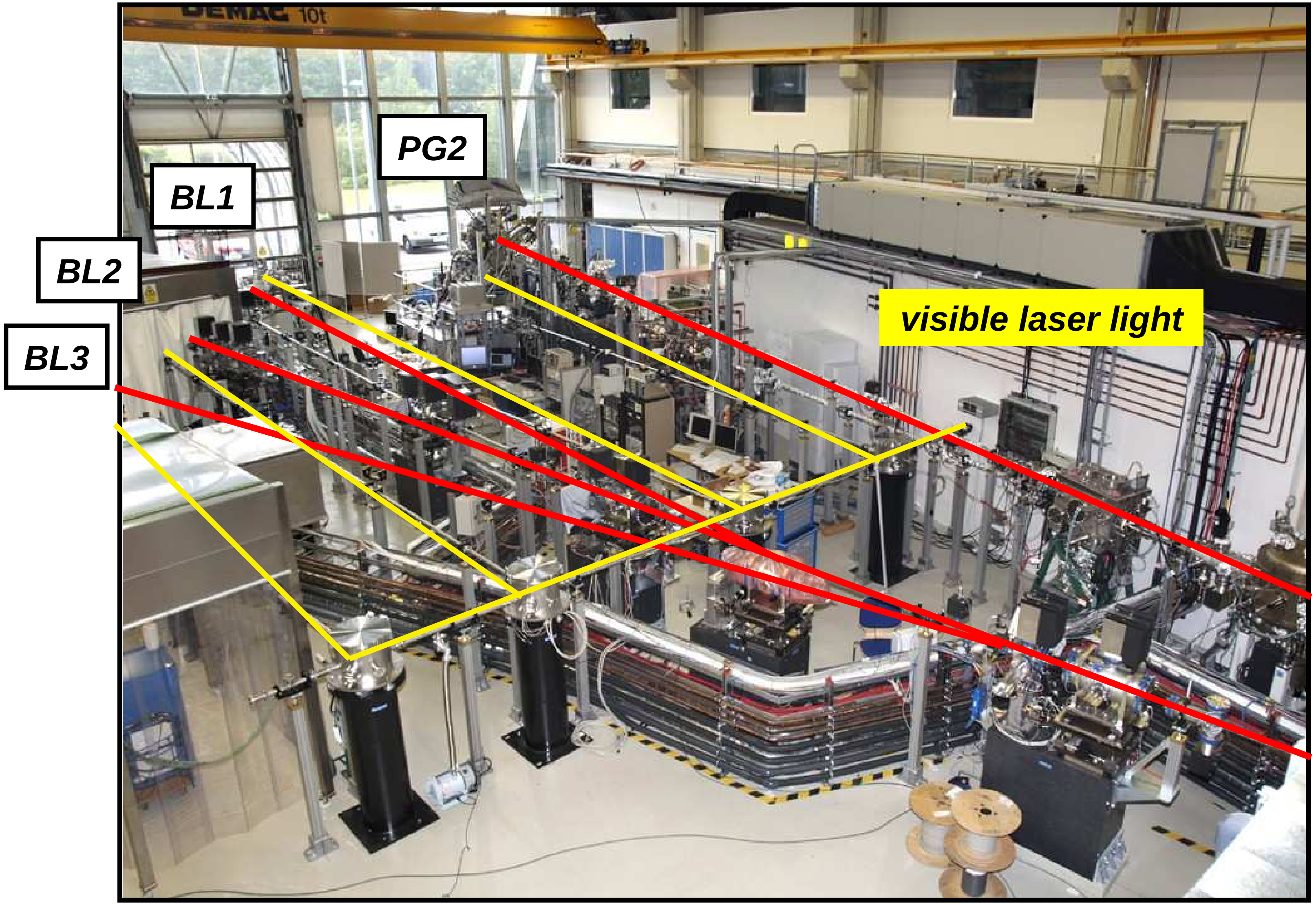

European XFEL Project

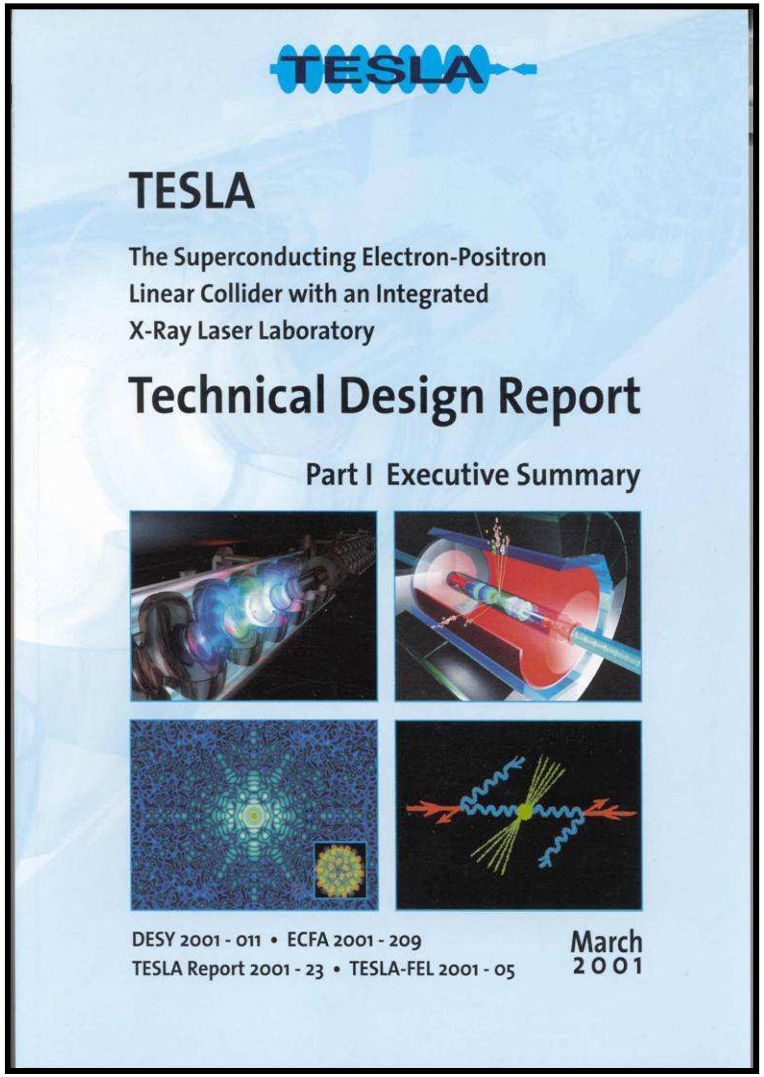

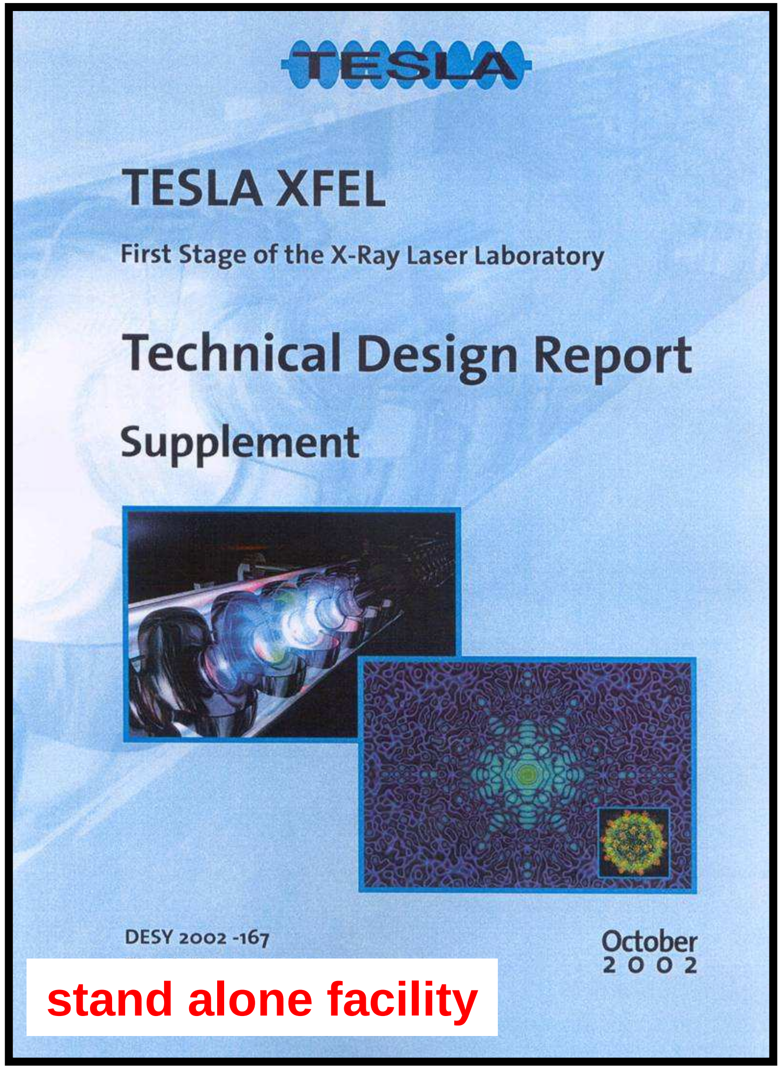

stand alone facility

XFEL: Schematic Layout

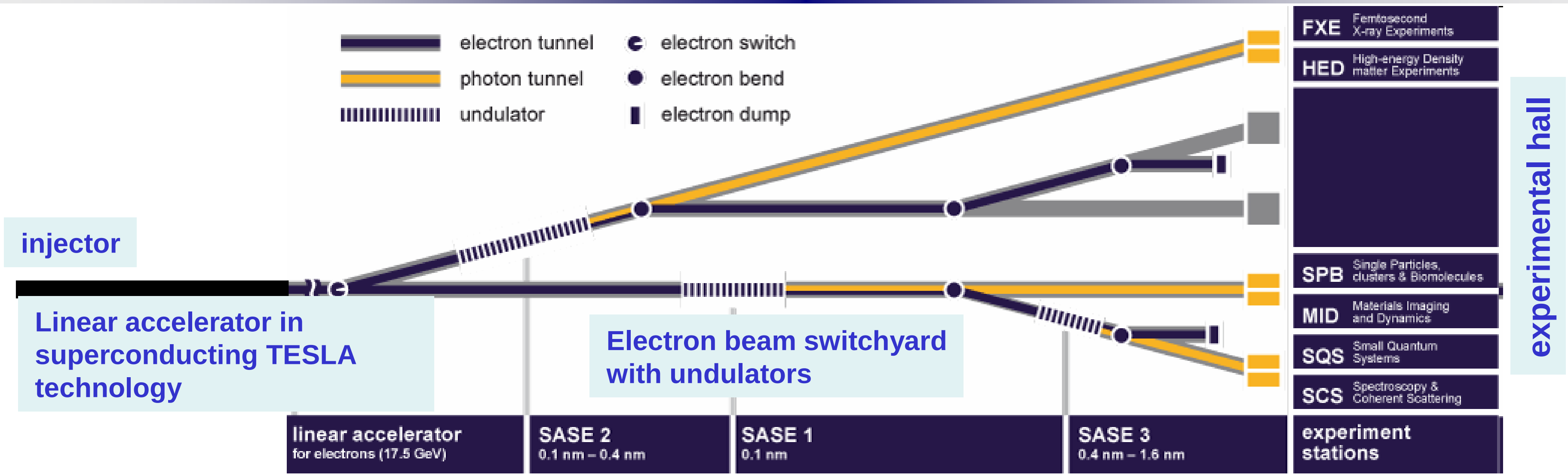

Linac: **20GeV**
min. wavelength: **~1Å**
Average Brilliance: **~10^{25}**
Peak Brilliance: **~10^{33}**

pulse length: **~100 fs**

2 X-ray SASE FELs,
1 SASE XUV-FELs, and
2 beamlines for short pulse physics using spontaneous radiation
10 experimental stations

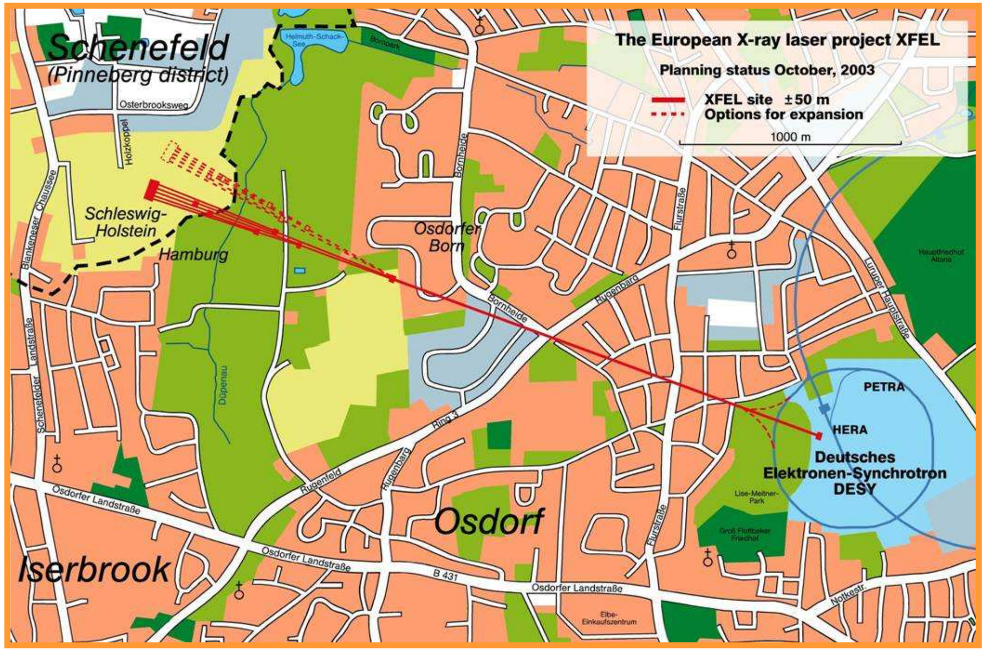

Beamline Components: Collimators and Mirrors

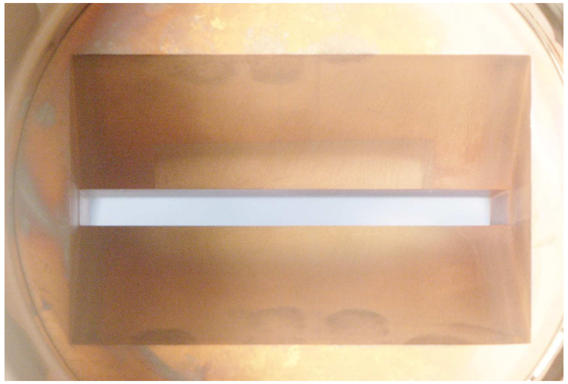

View into the vertical part of the high power slit system installed at DORIS-III ID-beamlines

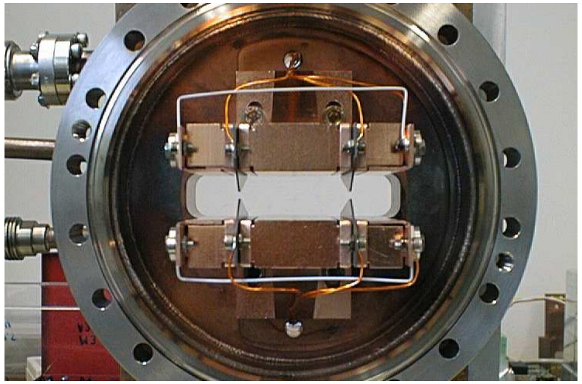

4 blade photon beam position monitor

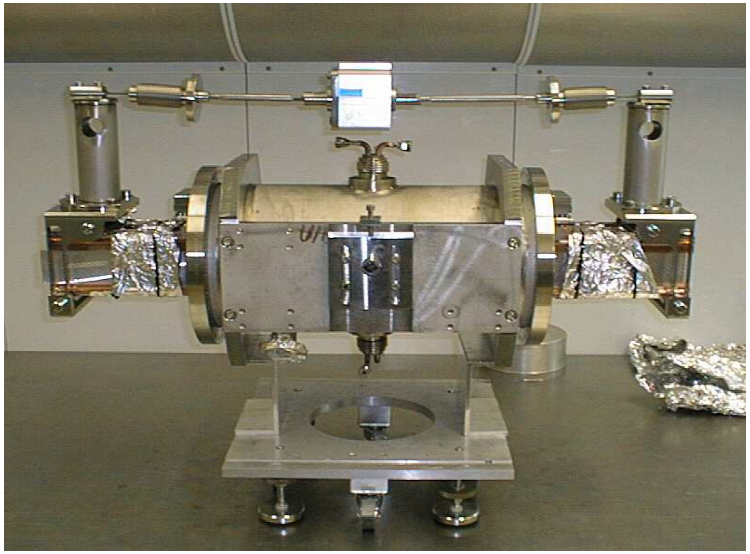

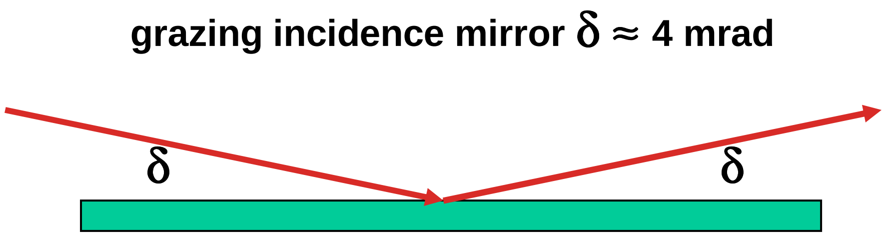

Pneumatically driven bender with cooled mirror (1m) for white beam applications

Beamline Components: Monochromators

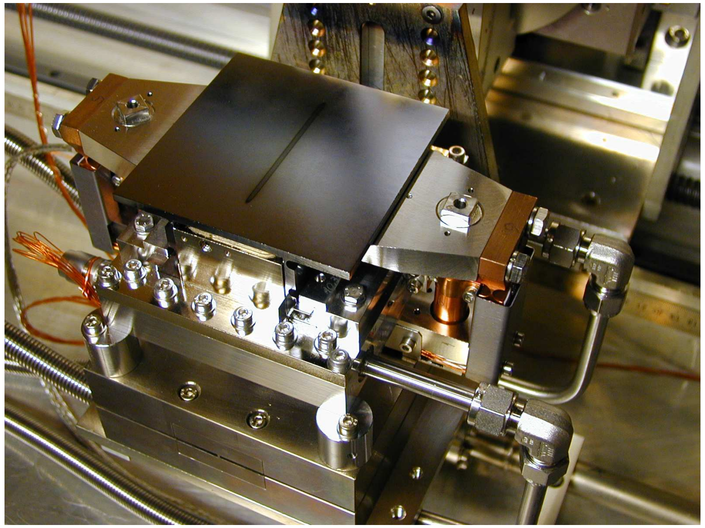

Torii: adaptable high heat load monochromator at W1, W2, BW1, BW2, BW4
MPG-BW6
PSI-Material Science
Maxlab-Material-Science-I811 (licensed to ACCEL)

H. Schulte-Schrepping, G. Materlik, J. Heuer, Th. Teichmann, „Monochromatorkristall-Einrichtung für Synchrotronstrahlung“, Patent Nr. 4425594

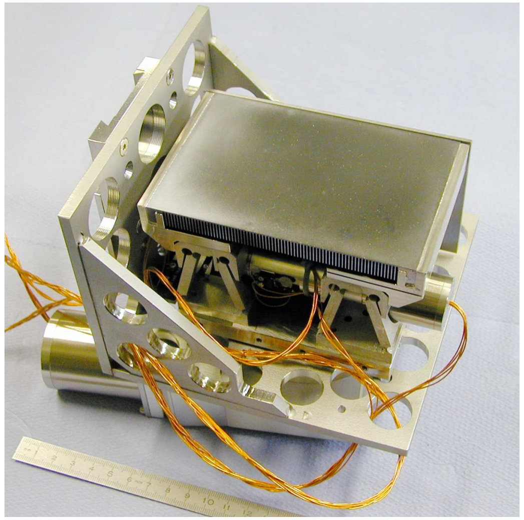

Sagittal bender adapted from ESRF design. Si-111,220, and 311 assembly available for high energy electron spectroscopy at BW2

Diamond crystal and holder at the PETRA-II undulator beamline. Attached to the water-cooled heat exchanger ΔT=5K measured at the crystal support

Beamline Components: Detectors

Integrating pixel detector
Readout time 2.5 s
Dark current 0.01 e^-/pixel/s
Readout noise 10 per pixel
Dynamic range 10^4
(limited by dark current and
pixel saturation)

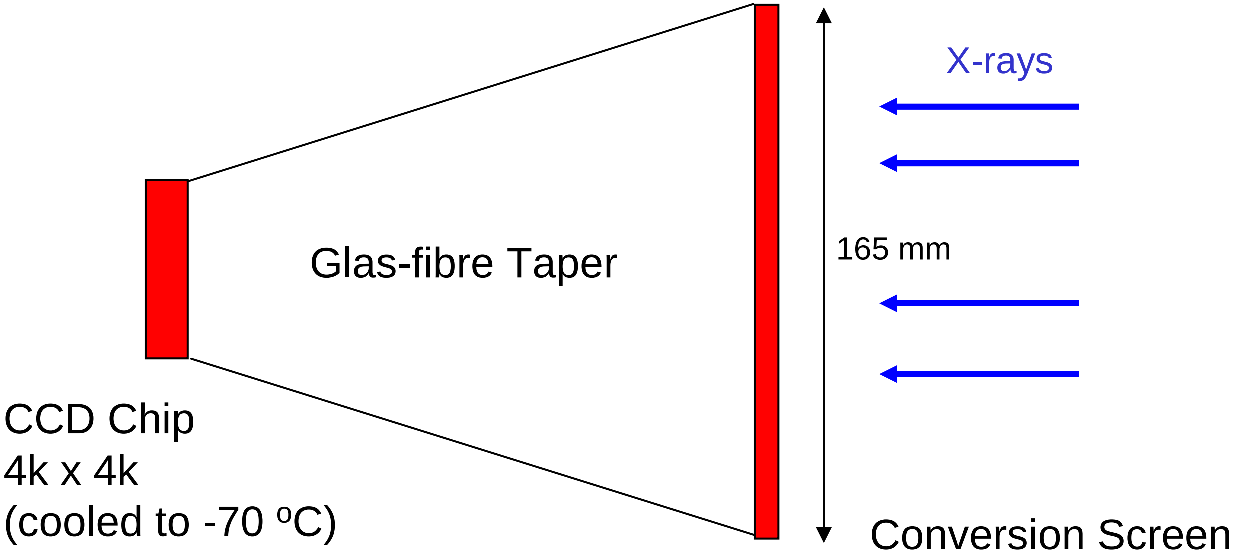

Beamline Components: Detectors

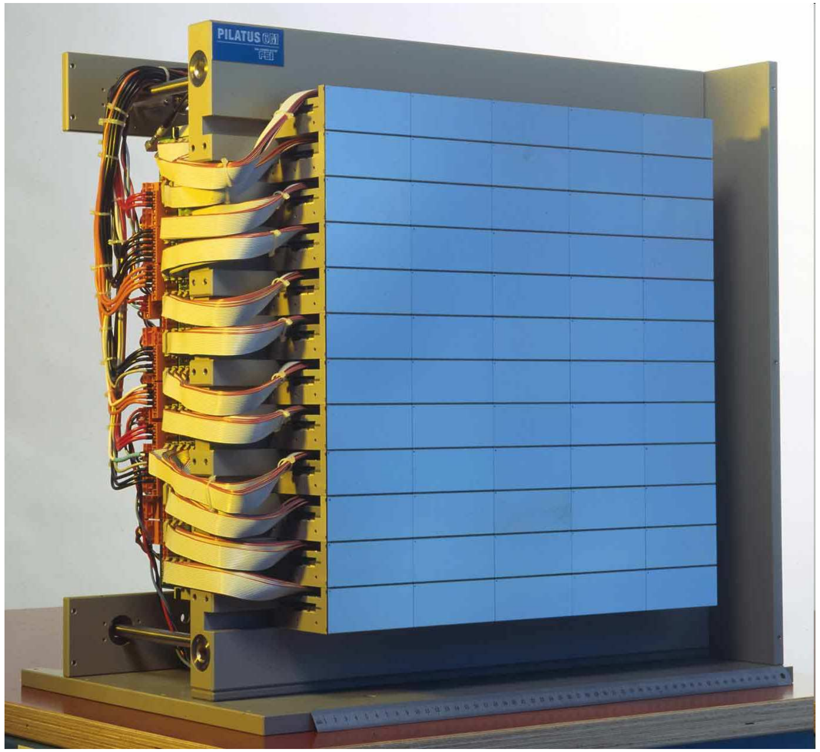

Pilatus 6M

2-D Hybrid Pixel Array

Single Chip: 60 x 97 pixel (pixel size 0.17 mm)
Each pixel with preamp, treshhold adjustment, and 20-bit counter (count rate 1.5 MHz)

Single Module: 8 x 2 Chips
Parallel readout (readout time 2 ms)

6M Detector: 12 x 5 Modules
(2463 x 2527 pixel)

Efficiency: 100% @ 8 keV, 50% @ 16 keV

Single photon counting pixels:
- No readout noise
- Discrimination of fluorescence background
- High dynamic range (10^6, limited by counter)

Scientific Experiments with photons at DESY

40 Beamlines (10 at Wigglers and Undulators)
1500 (440) Scientists from 270 (140) Institutes
about 5000 hours of beamtime/year

Physics, Chemistry,
Earth Science, Biology,
Medicine

- **XUV Fluorescence Spectroscopy**
- **X-Ray Absorption Spectroscopy**
- **Small Angle X-Ray Scattering** (SAXS, USAXS, GISAXS, ASAXS)
- **Diffraction and Crystallography** (General, Powders, Proteins, High Pressure, Surfaces)
- **Microtomography**
- **X-Ray Micro Fluorescence**
- **X-Ray Photoemission Spectroscopy**
- **Nuclear Resonant Scattering**
- **High Energy X-Ray Scattering**
- **X-Ray Holography**
- **X-Ray Standing Wave Interferometry**
- **X-Ray Reflectometry**
- **X-Ray Topography**

Weak Signals
- e.g. High Collimation
- e.g. Small Samples

Time resolved measurements
Tunable wavelength
Time Structure

$$\rho(\mathbf{r}) \longrightarrow I(\mathbf{k}) = I_e \cdot |F[\rho(\mathbf{r})]|^2$$

Fourier Transformation

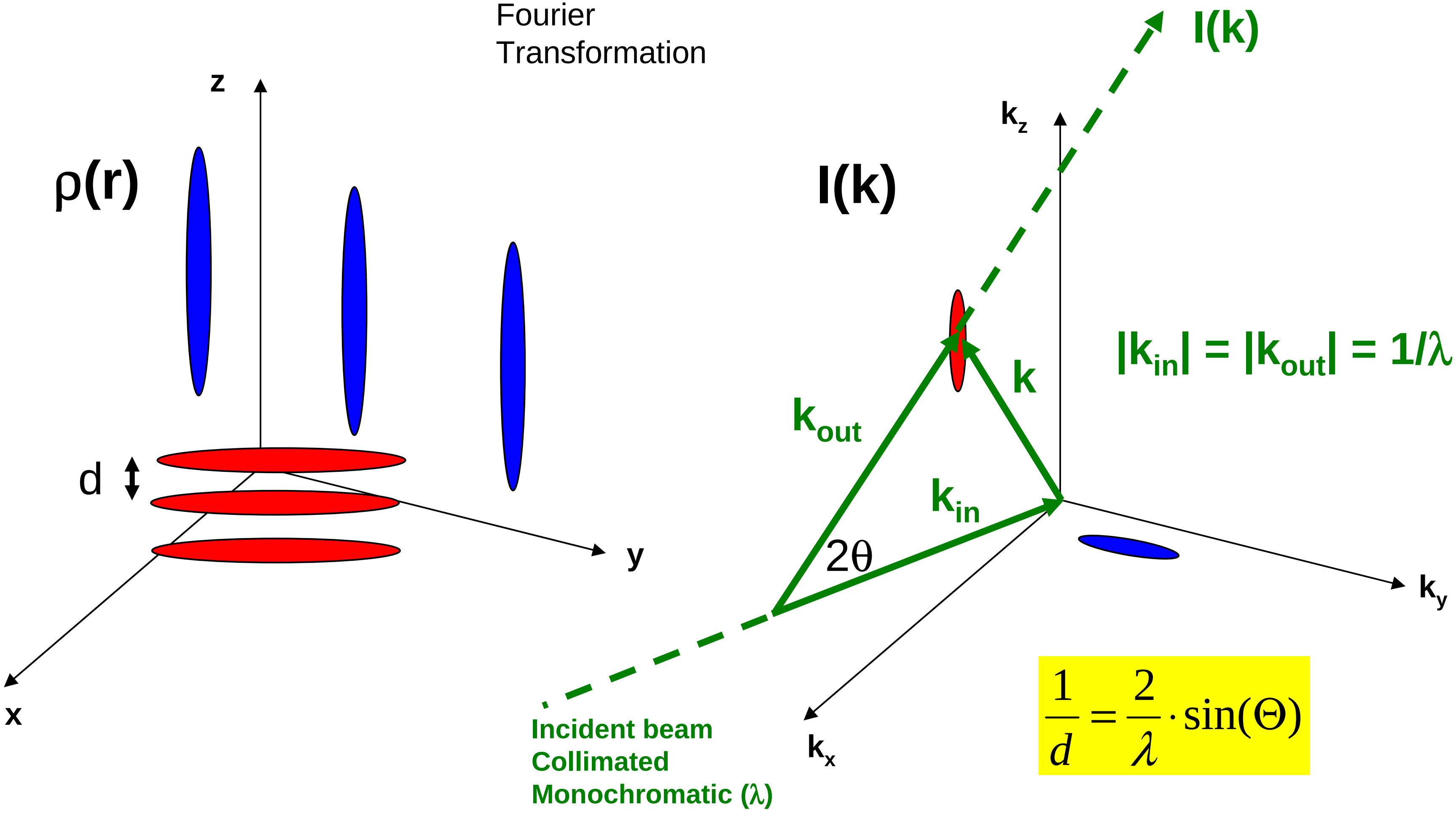

$$\frac{1}{d} = \frac{2}{\lambda} \cdot \sin(\Theta)$$

Real space

Reciprocal space

No direct back-transformation possible, because phase is lost!

Basics of X-ray Spectroscopy

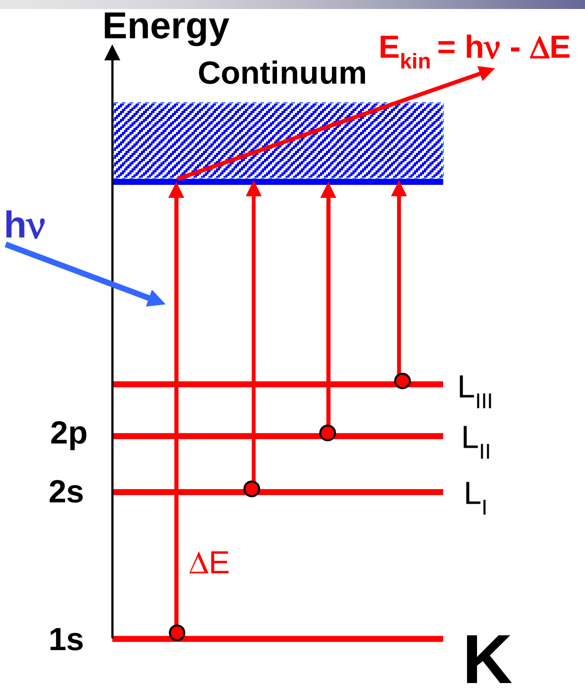

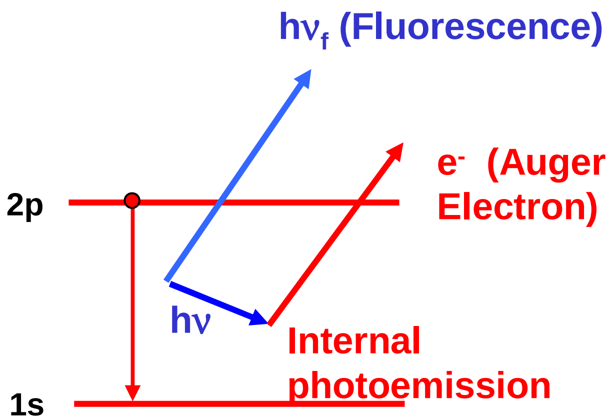

X-Ray Absorption Edges
(example Titanium K-Edge)

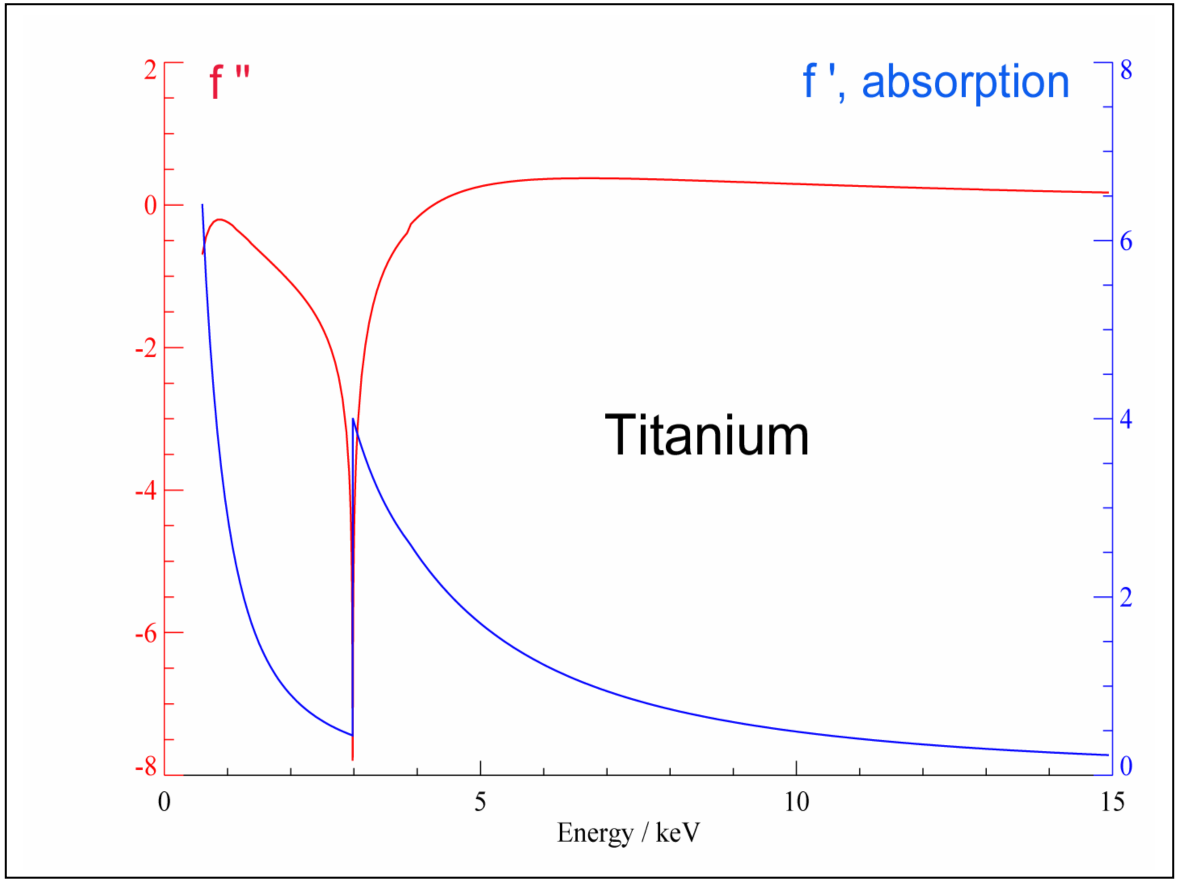

$$f(s,E) = f_0 + f\,'(E) + i\,f\,''(E)$$

Atomic scattering Amplitude

Protein Crystallography (PX)

Tiny samples
Huge unit cells
Light elements
Sensitive to radiation damage
High resolution necessary
- narrow energy band
- high degree of collimation

→ High brilliance required


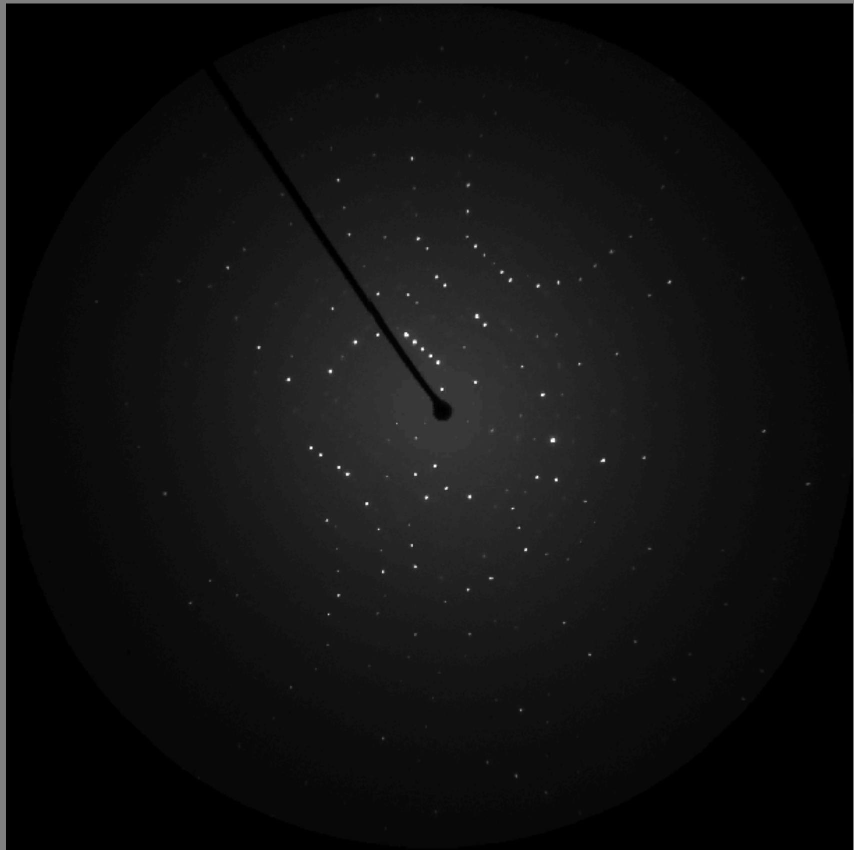

Monochromatic beam

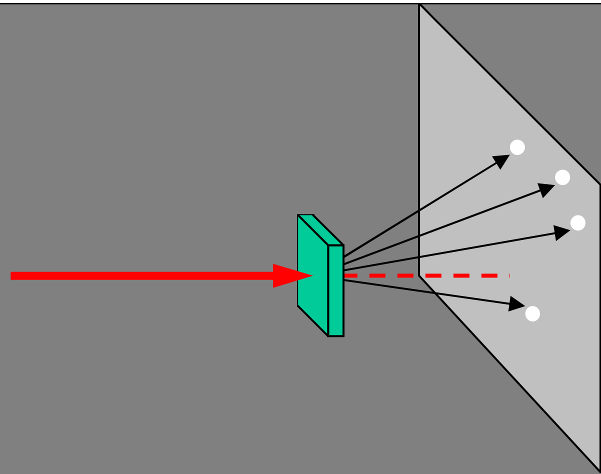

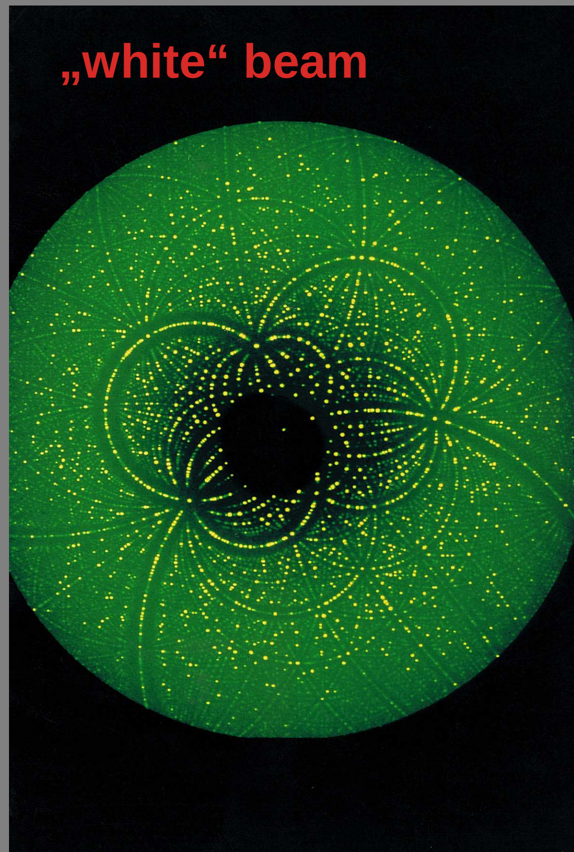

Protein crystal: Yeast Proteasome (50000 Atoms/unit cell)

Resolution 0.09 nm, mean position error 0.001 nm
Even Position of Hydrogene Atoms resolved!

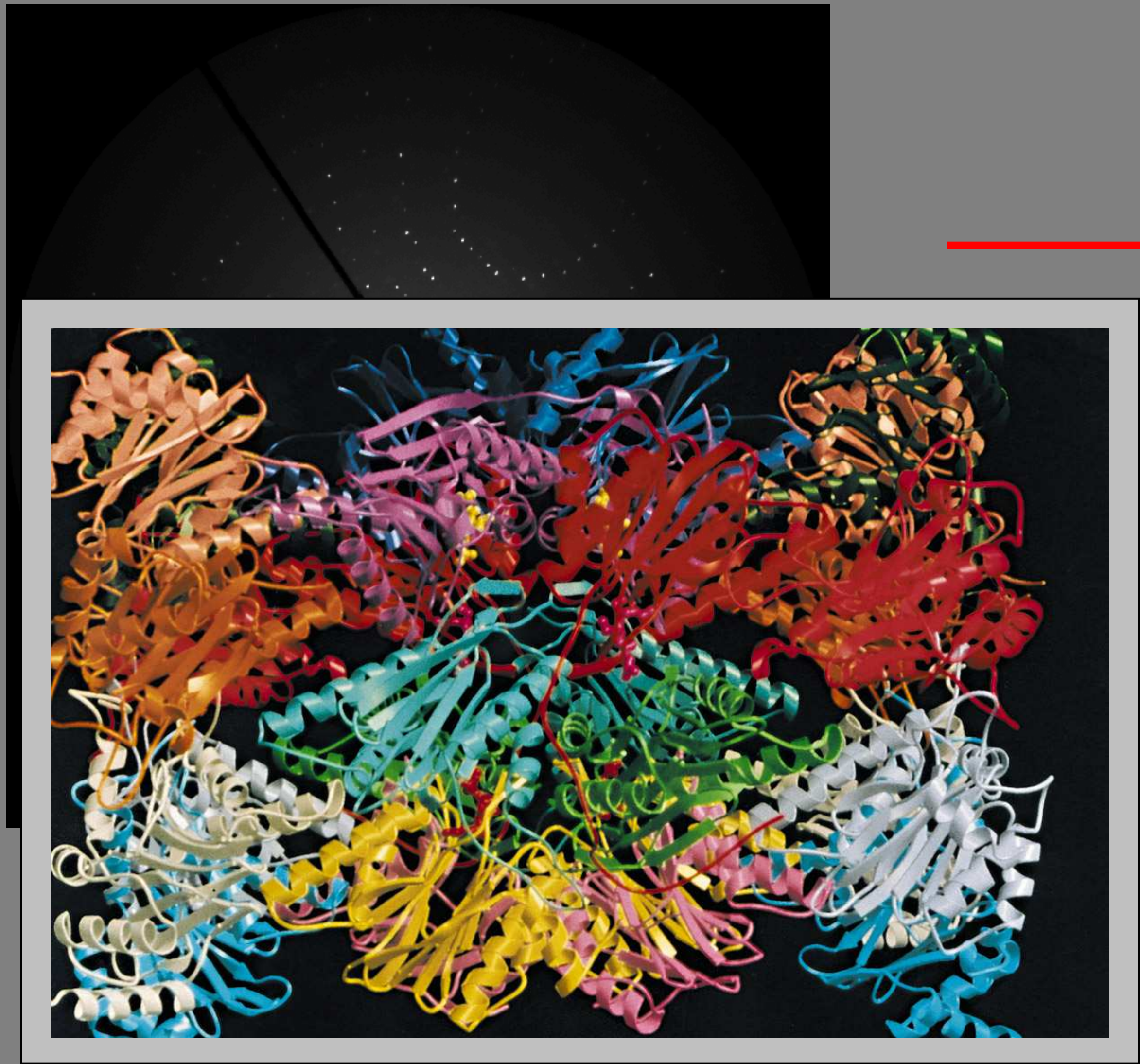

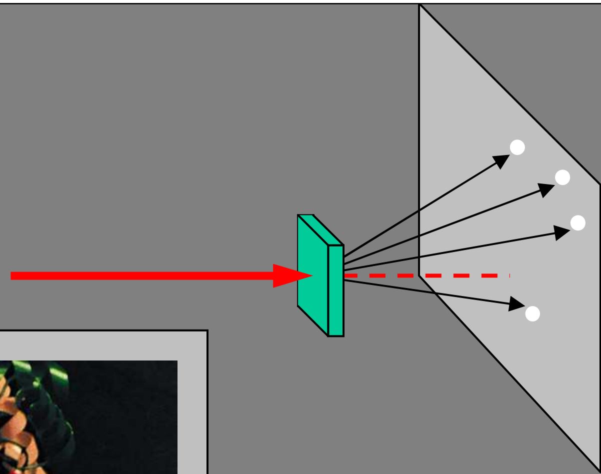

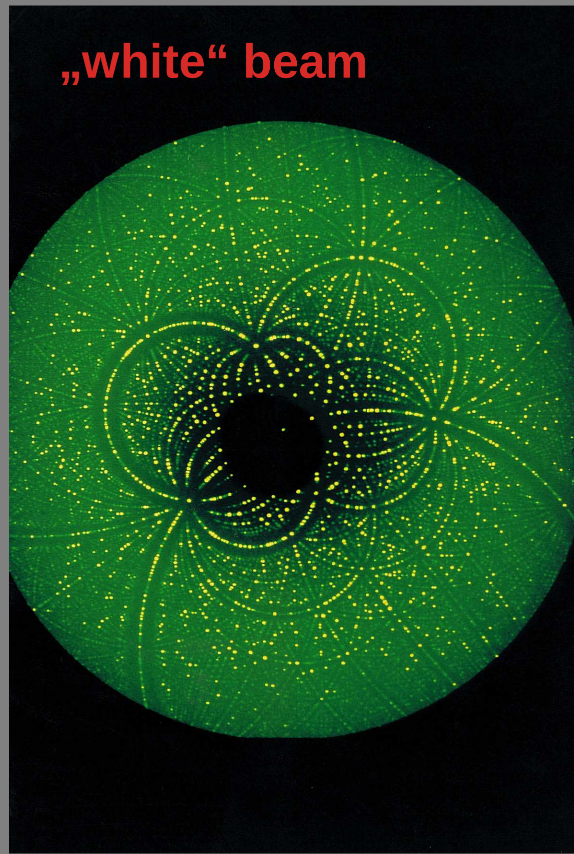

Protein crystal: Yeast Proteasome (50000 Atoms/unit cell)

Resolution 0.09 nm, mean position error 0.001 nm
Even Position of Hydrogene Atoms resolved!

Layout of a SAXS Instrument (BW4 at DORIS III)

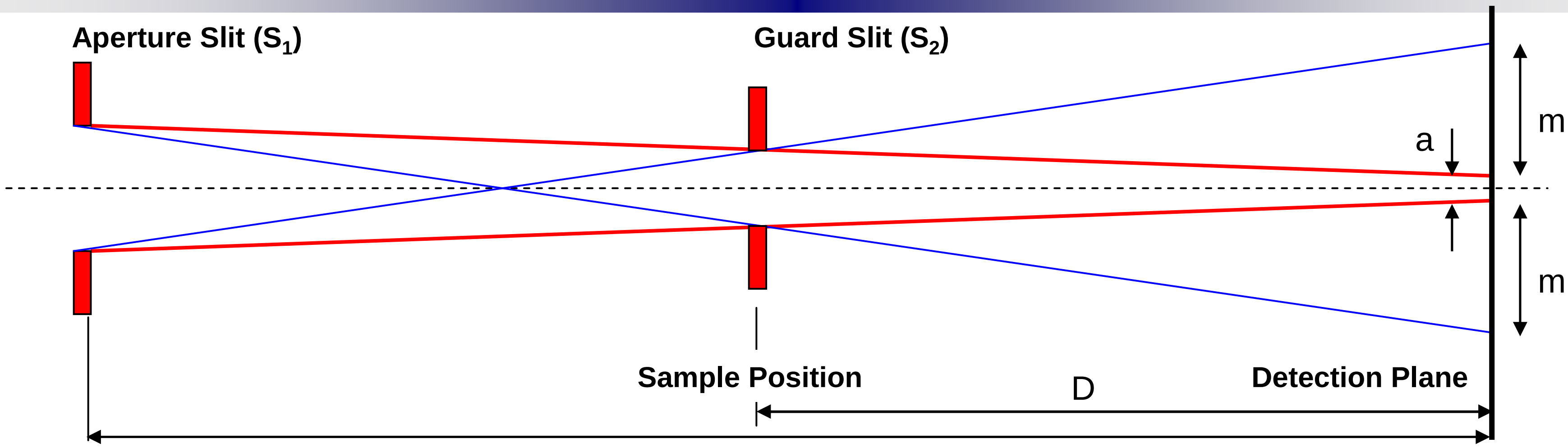

Resolution (maximum observed correlation distances) depends on sample to detector distance: 90 nm to 700 nm, photon flux $5 \cdot 10^9$ sec^{-1} (monocromatic)

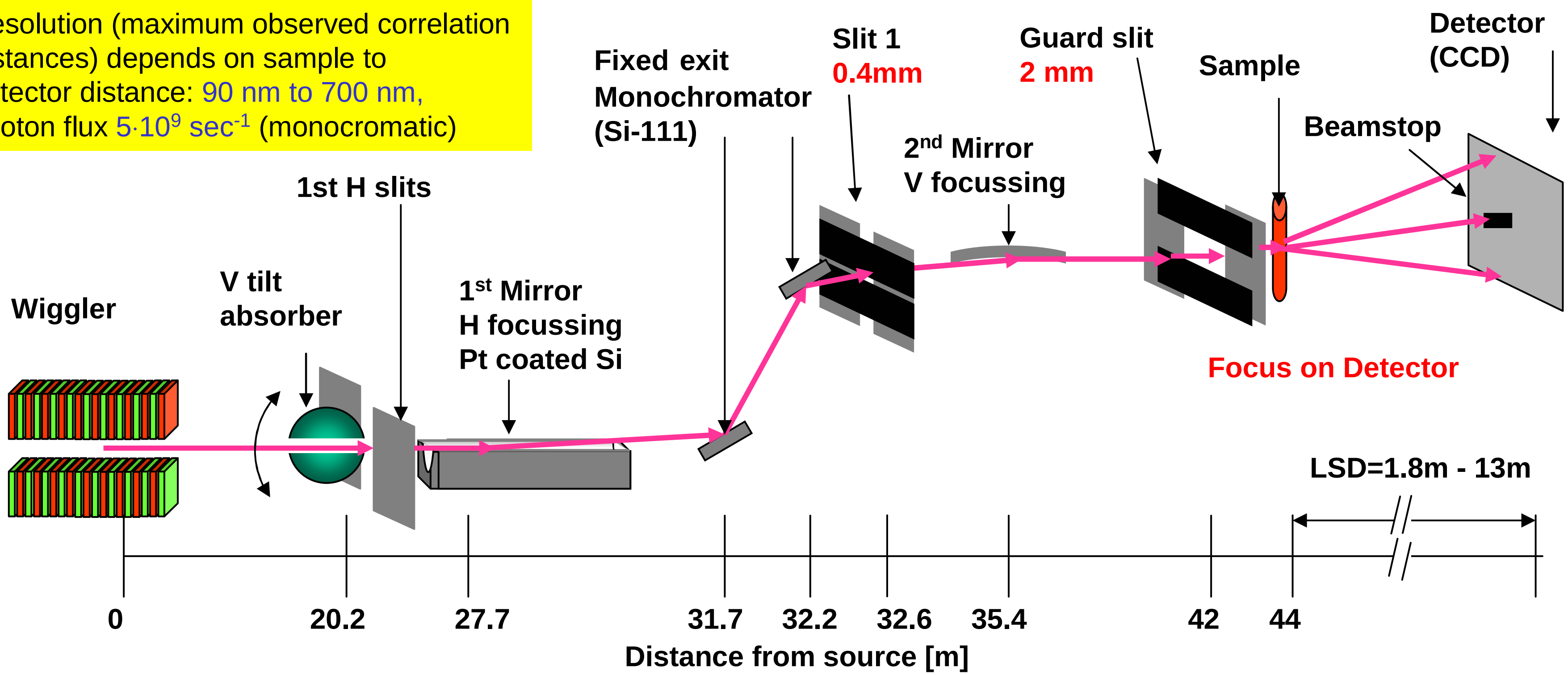

SAXS/WAXS at lamellar polymer systems

Example: Polyethylenterephtalate (PET)

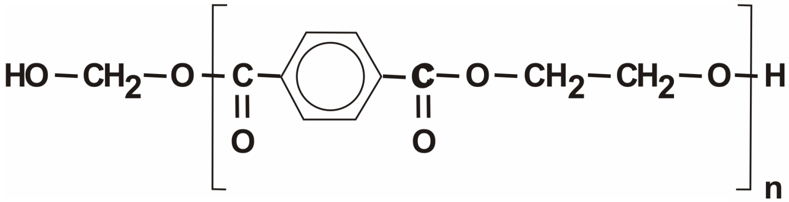

$$q_{max} = \frac{4\pi}{\lambda} \cdot \sin(\theta_{max}) \approx \frac{4\pi}{\lambda} \cdot \theta_{max}$$

Long Period

$$L = \frac{2\pi}{q_{max}}$$

$$Q = \int I(q) q^2 dq = 2\pi^2 \cdot \Phi \cdot (1 - \Phi) \cdot (\Delta\rho)^2$$

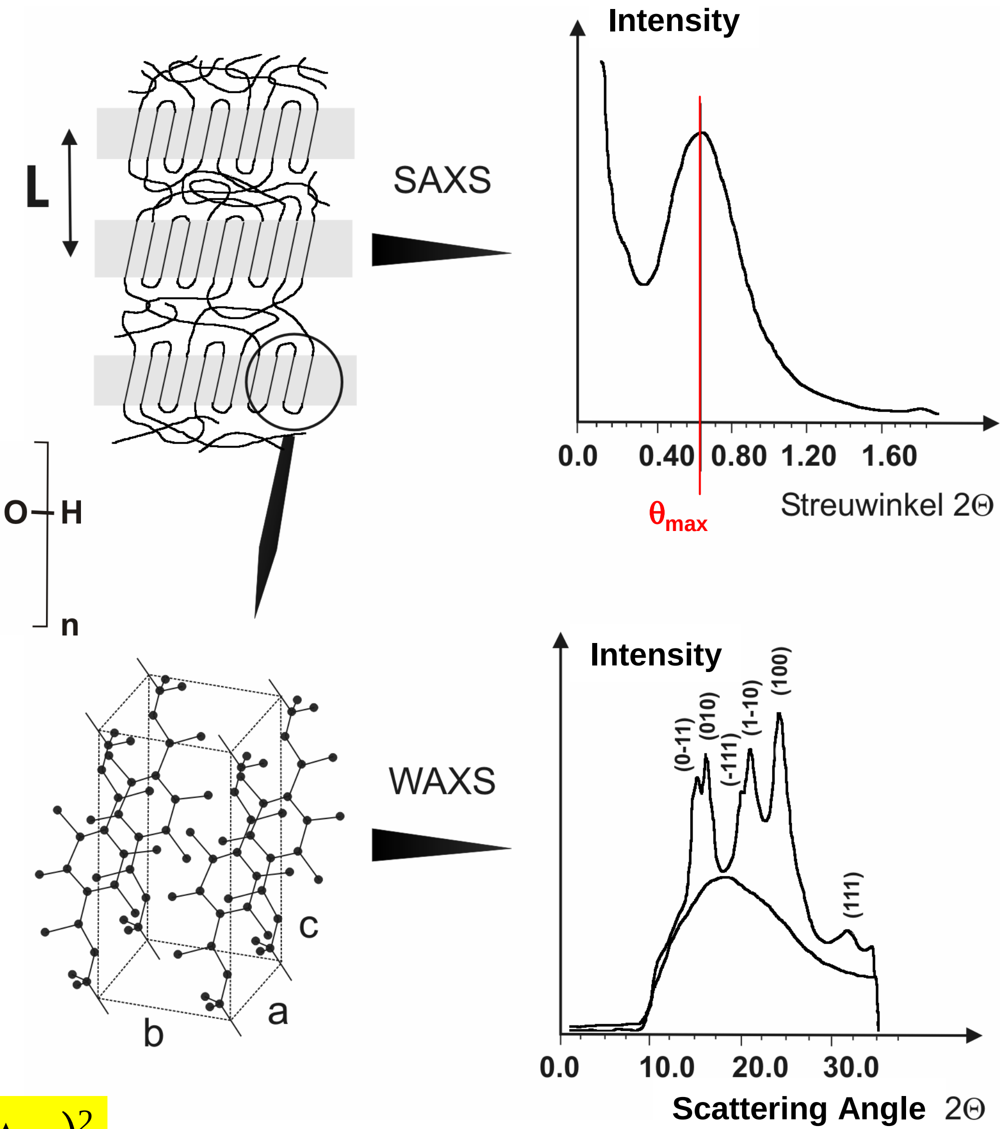

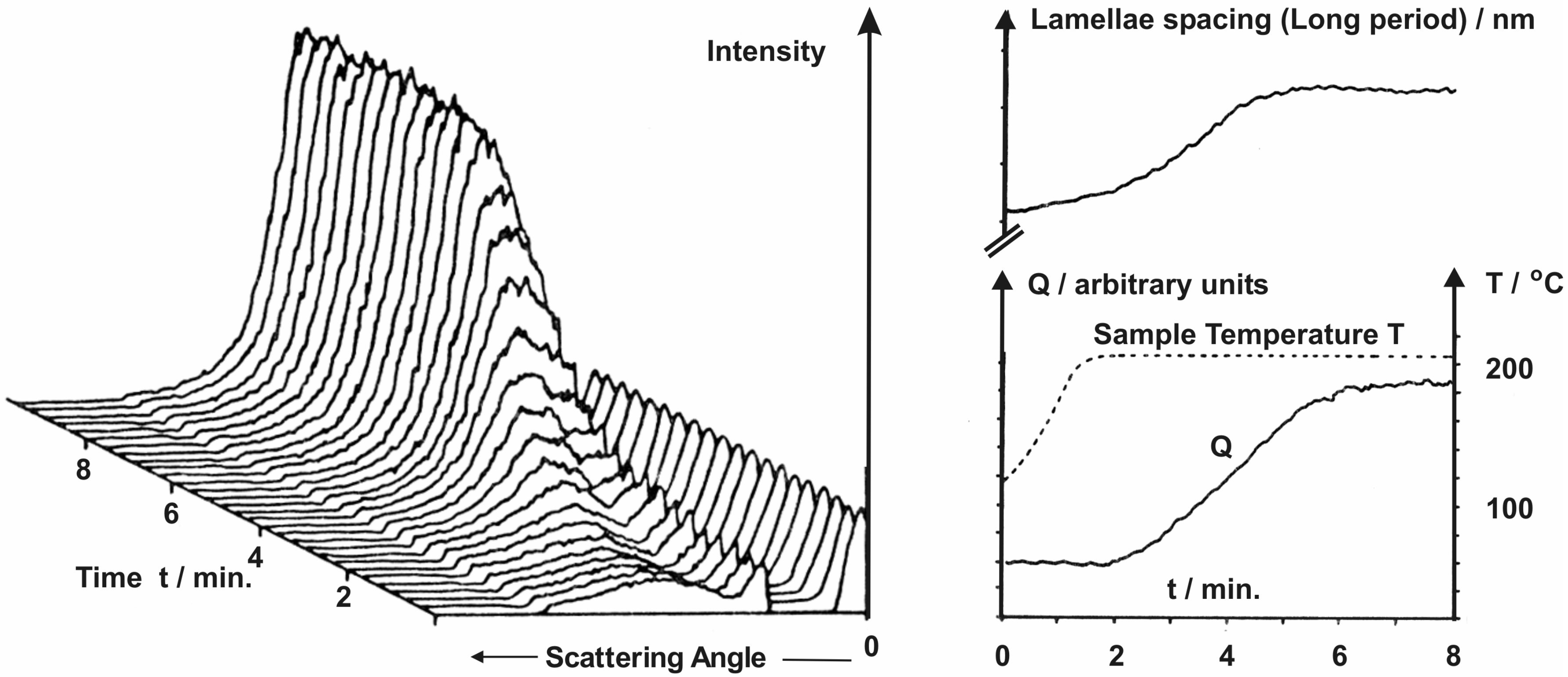

Annealing of PET, previously crystallised at T_1=130°C, recrystallisation at T_2=230°C

Scattering of Anisotropically Oriented materials

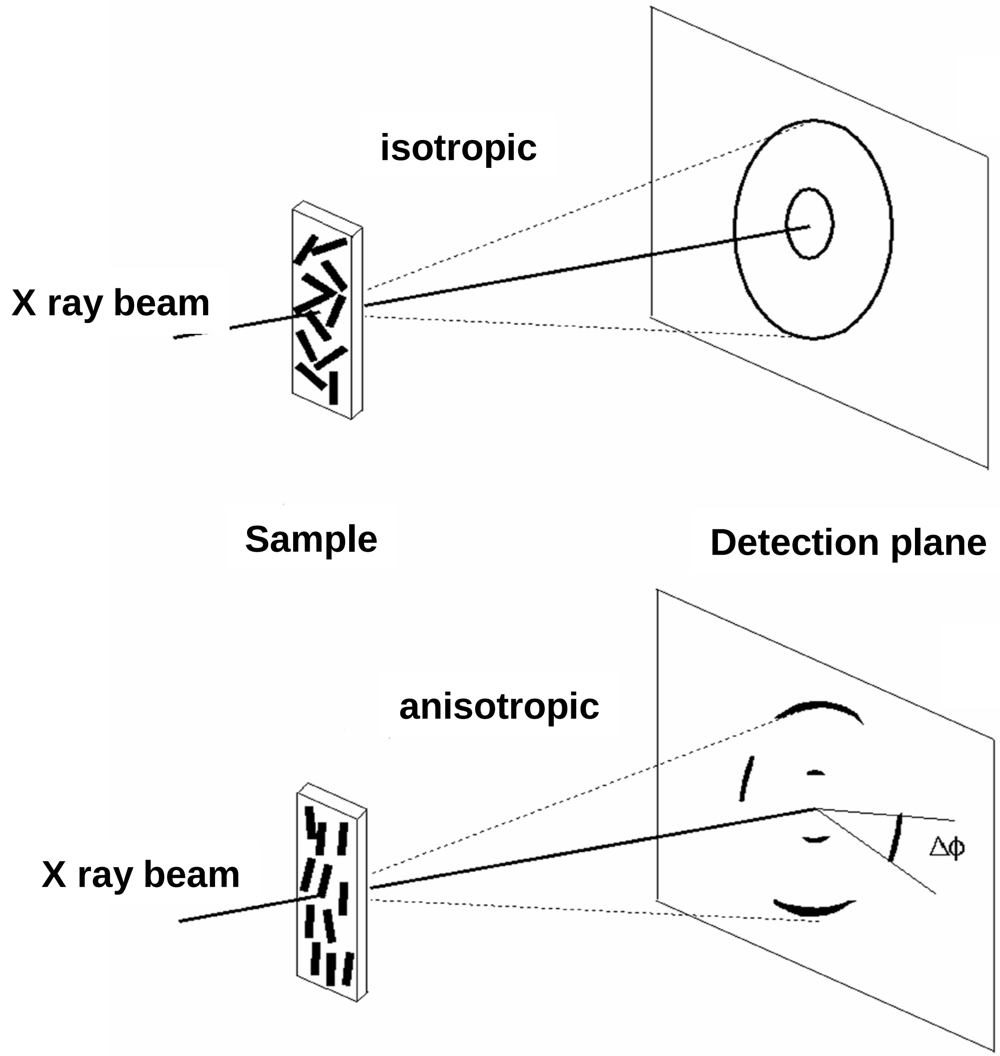

Deformation of an SBS-Triblock Copolymer (Thermoplastic Elastomer)

$$\lambda \equiv \frac{L_{final}}{L_{initial}} = 1 \qquad \lambda = 2 \qquad \lambda = 6$$

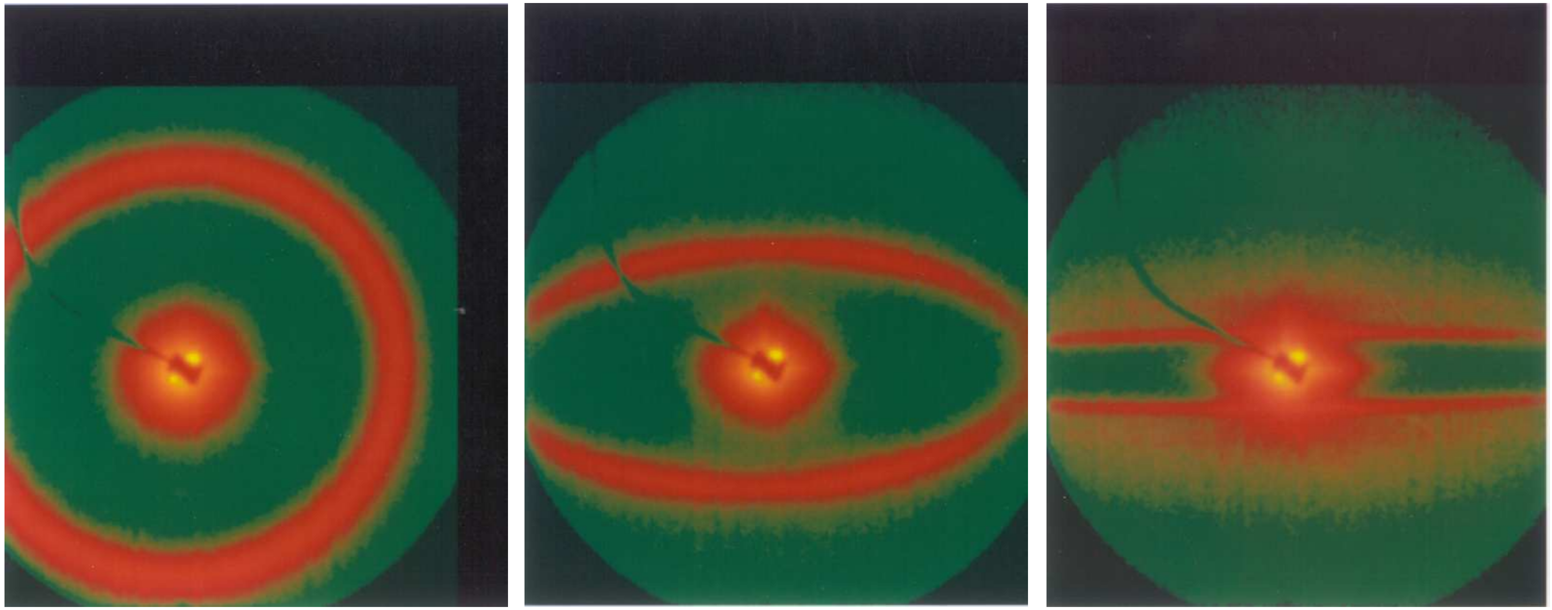

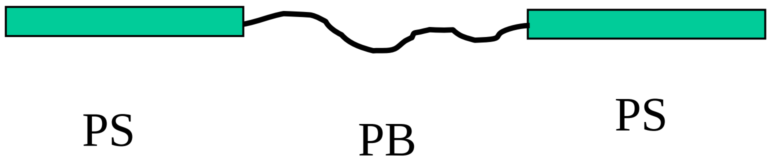

80% Polystyrene
20% Polybutadiene
→ PS cylinders in PB-Matrix

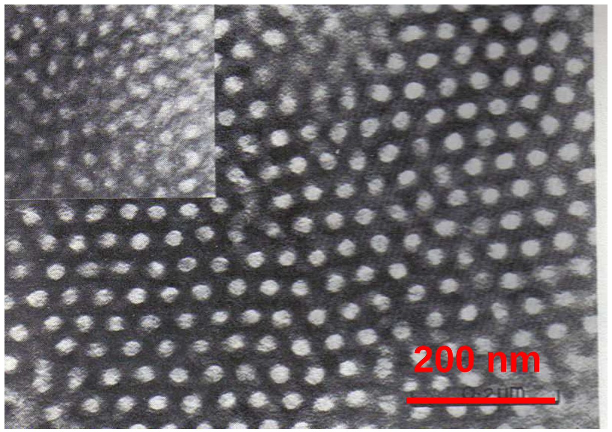

Electron micrograph

Wood - Determination of the microfibril angle (Microfocus SAXS and WAXS)

Picea abies (spruce)

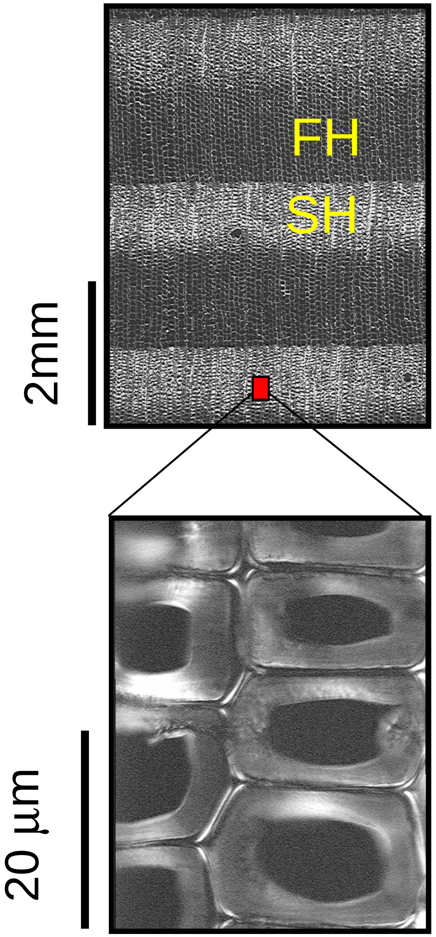

Focus 2x2µm^2

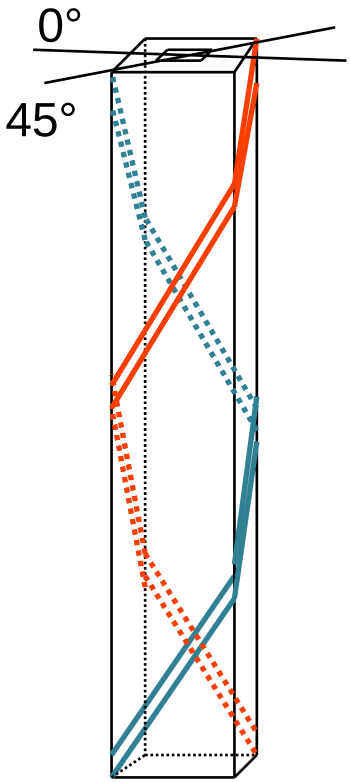

Fiber geometry

SAXS | **WAXS**

ω = 0°

ω = 45°

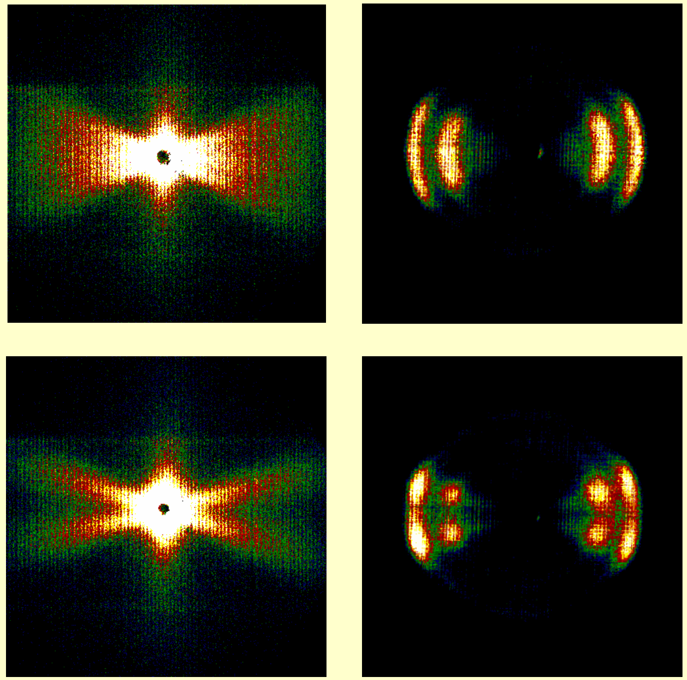

$\mu = 20.4°(\pm 0.6°)$ | $\mu = 20.0°(\pm 0.6°)$

Lichtenegger et al. *J. Struct. Biol.* (1999)

Helical arrangement of cellulose fibers in the wood cell wall (Scanning Microfocus SAXS)

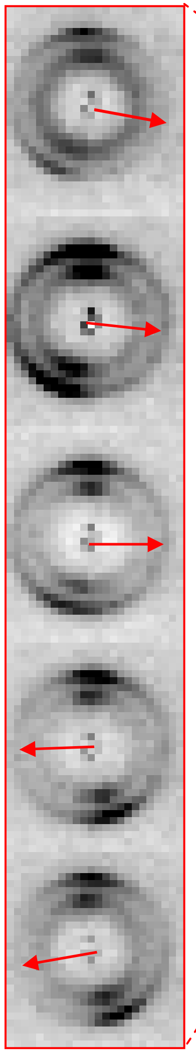

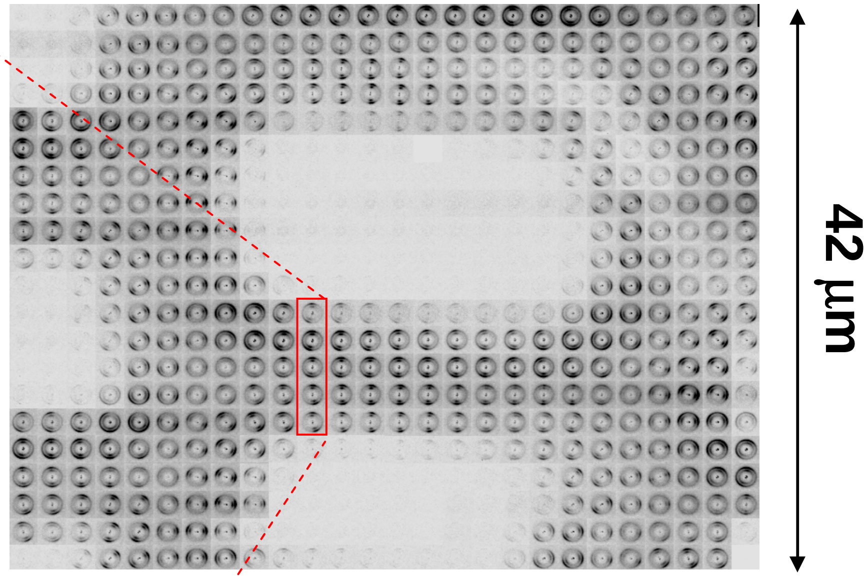

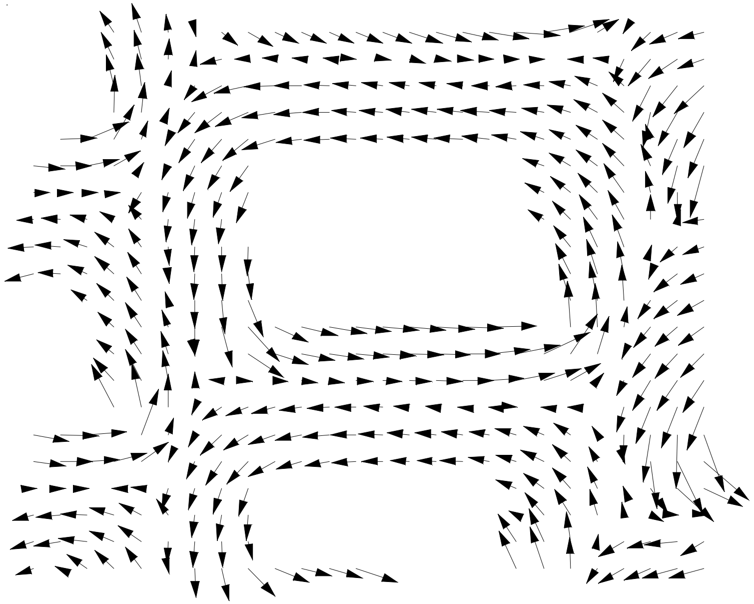

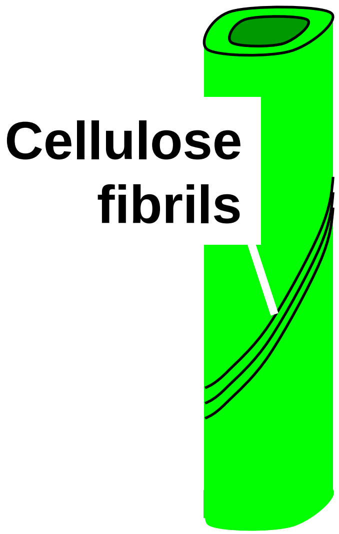

Z-Helix

Focus 2x2μm^2

Lichtenegger, Müller, Paris, Riekel & Fratzl
J. Appl. Cryst. (1999)

Contrast variation with anomalous scattering (ASAXS)

Atomic scattering factor

Structure factor
(interatomic interferences)

$$I(s)=|f(s)|^2\cdot|F(s)|^2$$

$$f(s,E) = f_0 + f'(E) + i\,f''(E)$$

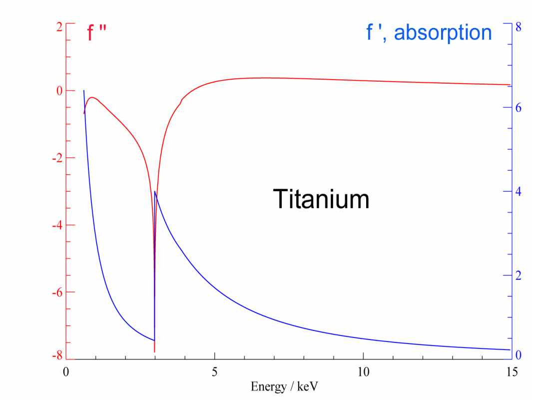

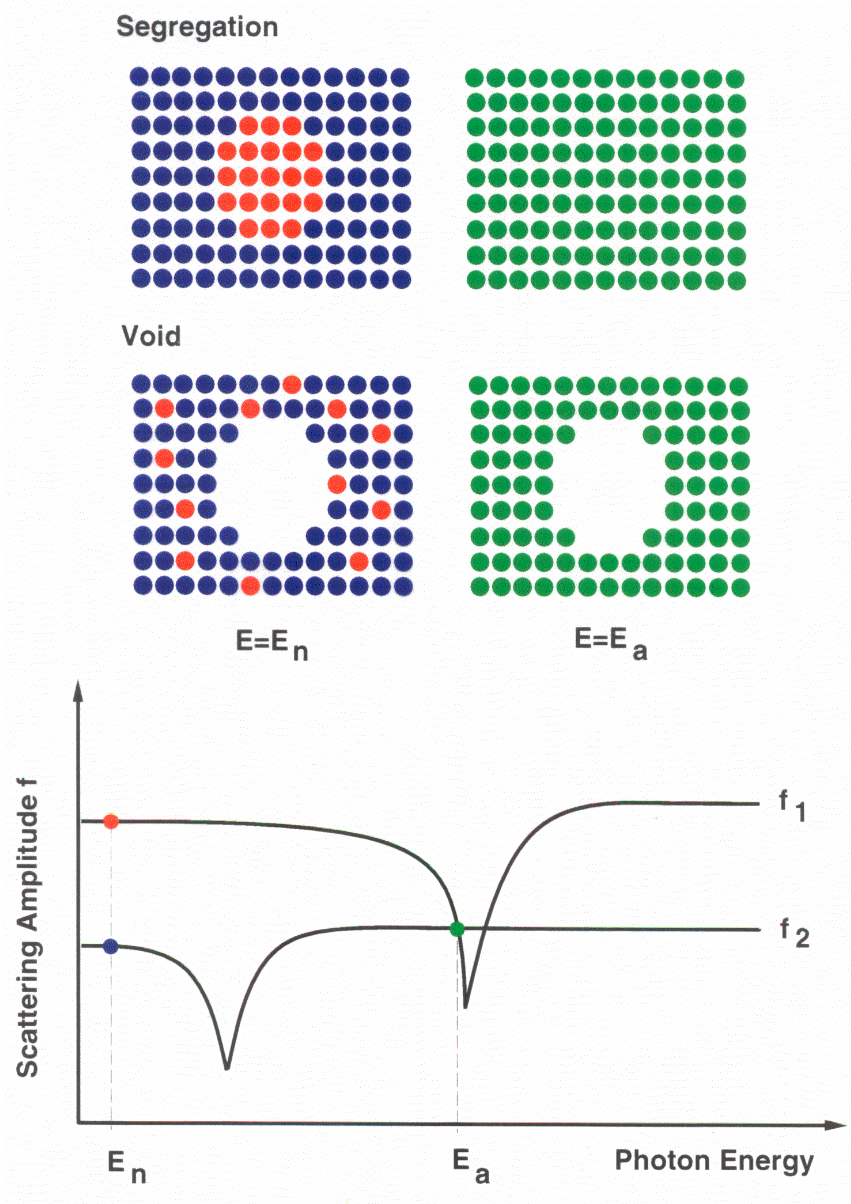

Sr-Counterion Condensation in Diluted Solutions of Na-Polyacrylates – Evidence for Pearl-Necklace Structure

K.Huber[1], R.Schweins[2]
[1]Universität Paderborn, Fakultät für Naturwissenschaften, Department Chemie, F.R.Germany, [2]Institute Laue-Langevin, Large Scale Structures Group, France

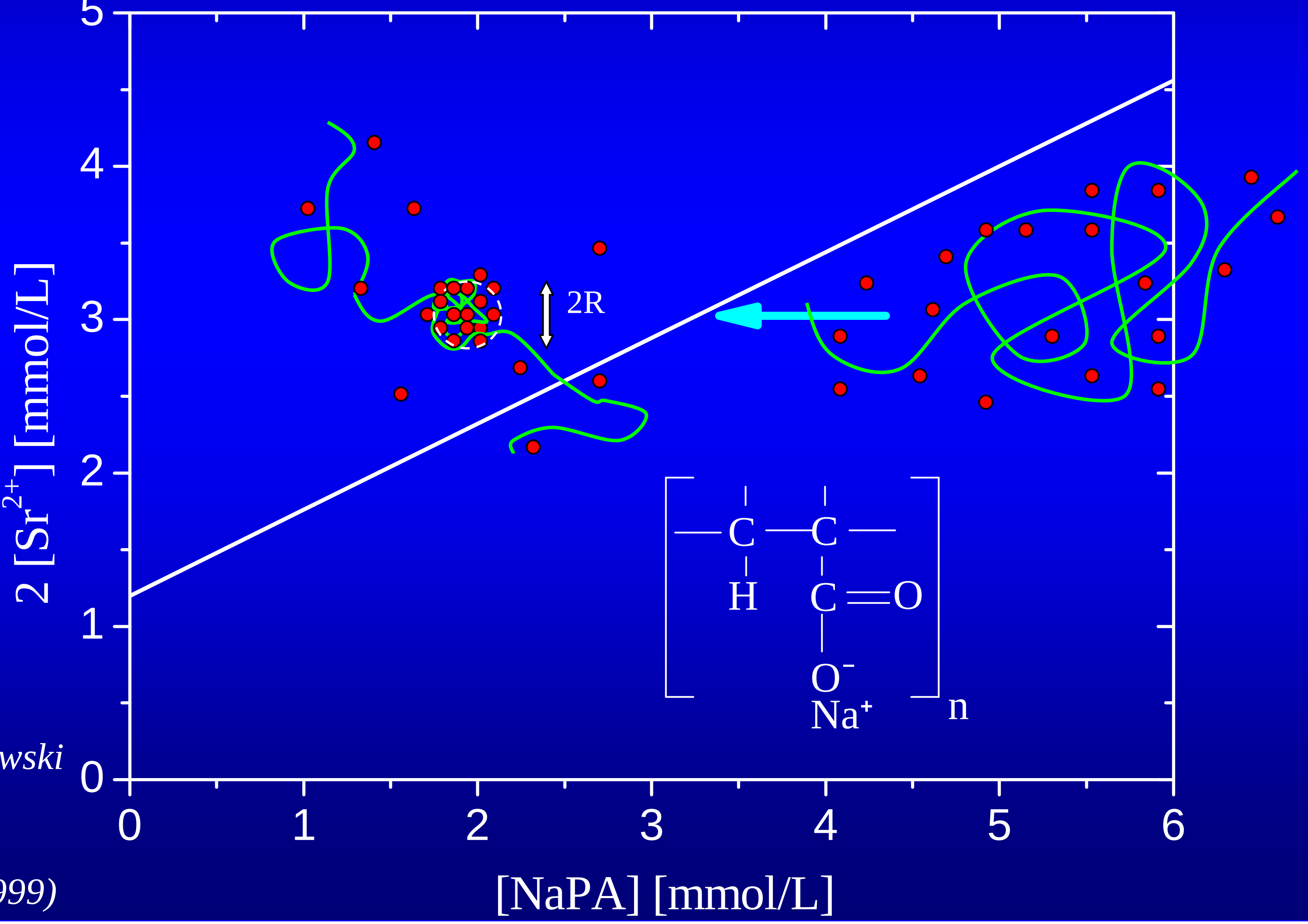

A.P.Chodanowski and S.Stoll, J.Chem.Phys. ***111,****609 ff (1999)*

Results from ASAXS measurements at the Sr-K edge at 16.1 keV

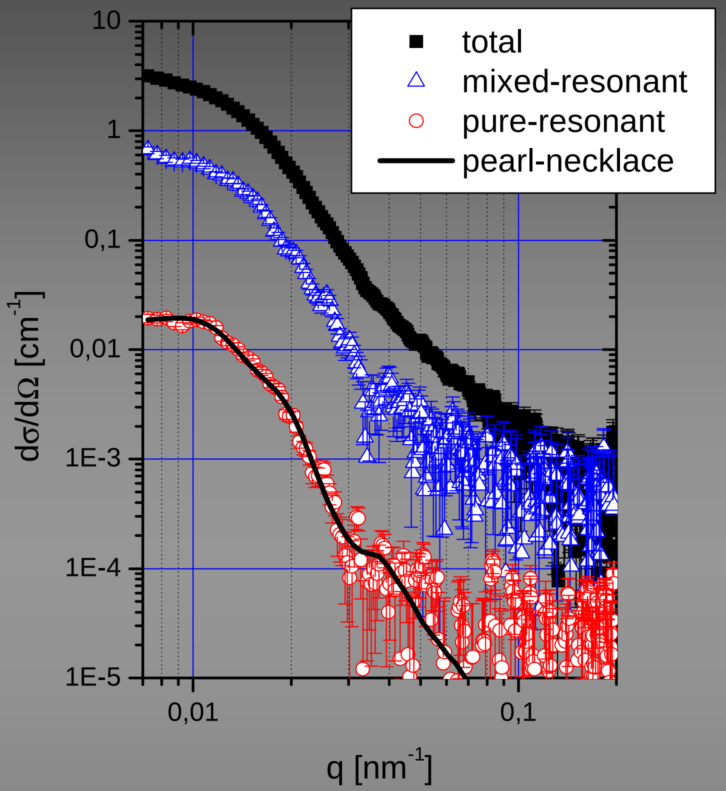

$[Sr^{2+}]/[NaPA]=0.458$

Pearl necklace model of collapsed chains

Pearls with radius R and distance d

R = 14 nm

d = 71 nm

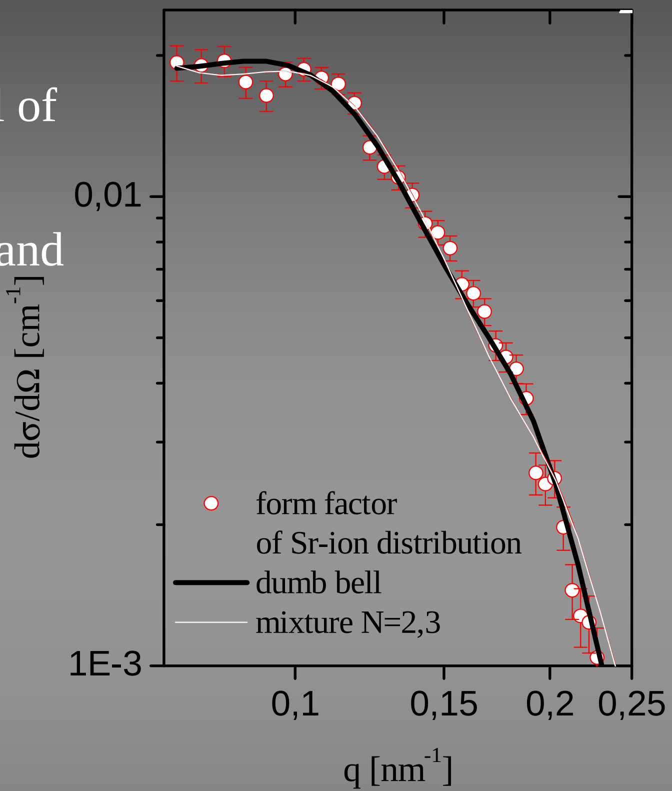

$$S_{Ion}(q) = const \int_0^\infty P(R) \cdot \left(\frac{4\pi R^3}{3} \frac{3(\sin(qR) - qR\cos(qR))}{(qR)^3}\right)^2 \cdot \left(N + 2\sum_{n=1}^{N-1} (N-n)\frac{\sin(nqd)}{nqd}\right) dR$$

$$P(R) = \frac{1}{\sqrt{2\pi}} \cdot \frac{1}{\sigma R} \cdot \exp\left(-\frac{\ln^2 \frac{R}{R_0}}{2\sigma^2}\right)$$

Log-normal size distribution $\sigma = 0.17$, $\Delta R_{FMHW} = 6$ nm

Grazing Incidence Small Angle Scattering (GISAXS)

q_z-dependence
(in-plane)
→height H

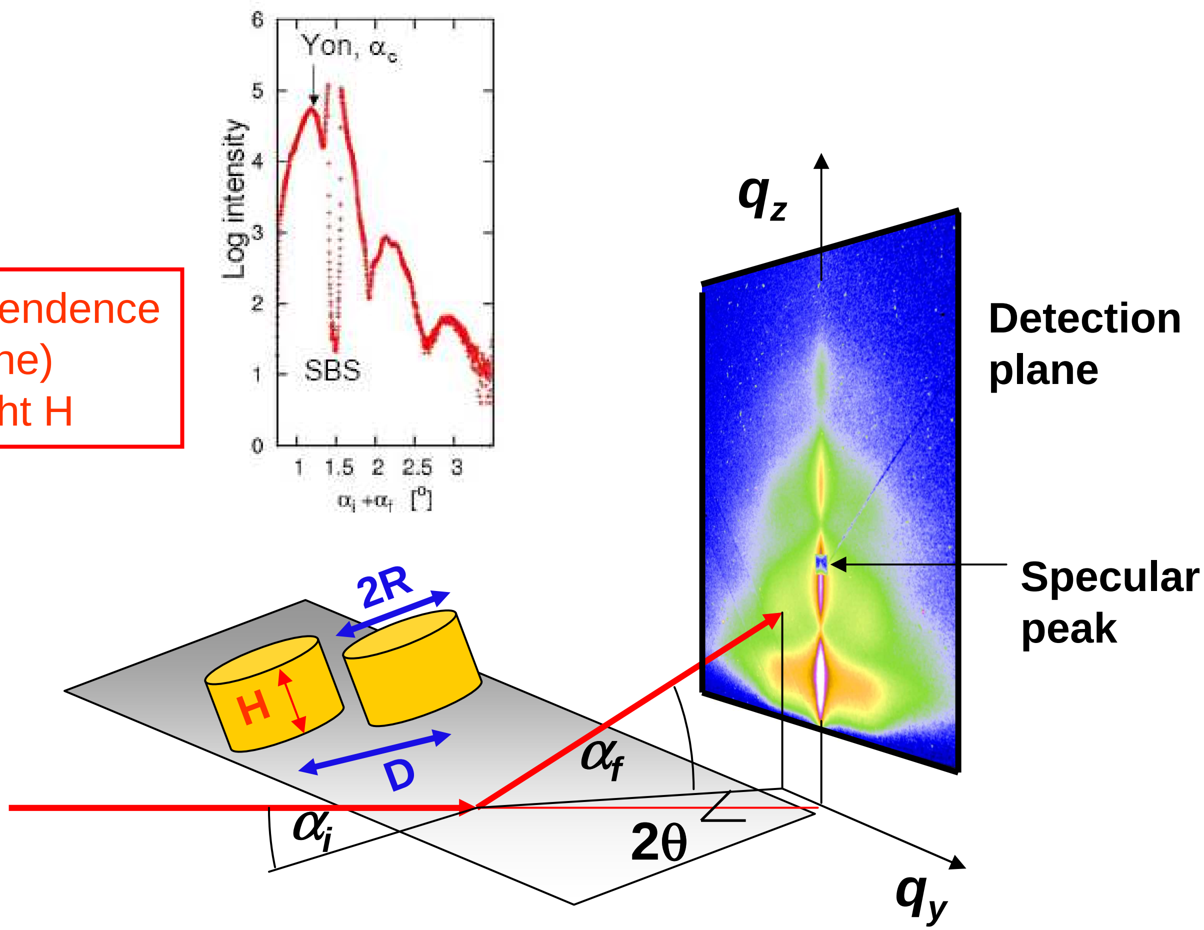

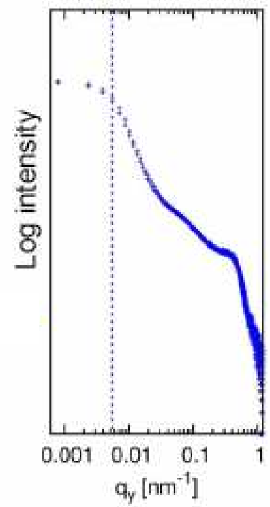

q_y-dependence
(out-of-plane)
→ lateral distance D,
lateral size R

$q_z=2\pi/\lambda \sin(\alpha_i+\alpha_f)$
$q_y=2\pi/\lambda \sin(2\theta)\cos(\alpha_f)$

Method only probes thin layer on surface

Sputtering on nanostructured templates

- Substrate: base-cleaned Silicon (Si) wafer
- Polystyrene (PS) spheres (ø100 nm; concentration 0.025% in deionized water), spin-coated to the substrate (4000 rpm for 120 s)
- Metal sputter deposition (Co, Al, sputter rate 0.4 nm/min at 10^{-8} mbar)

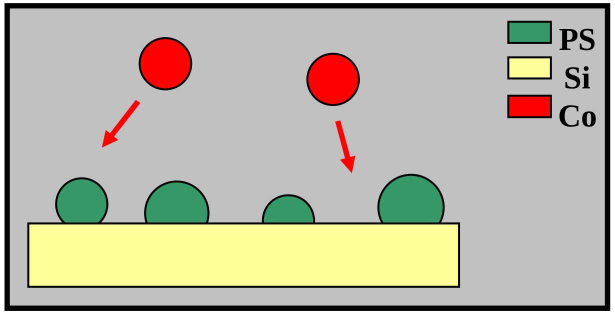

GISAXS setup with in-situ sputtering chamber @ BW4 (DORIS) HASYLAB-DESY

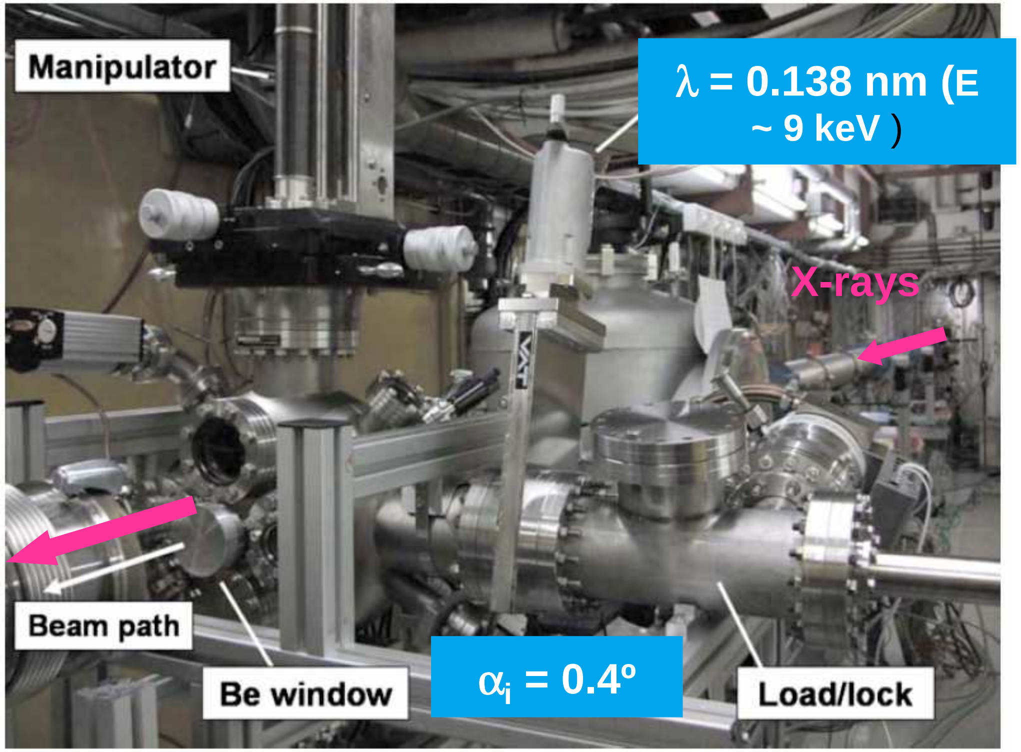

D_{SD} = 2.21 m

Sputtering with in-situ GISAXS

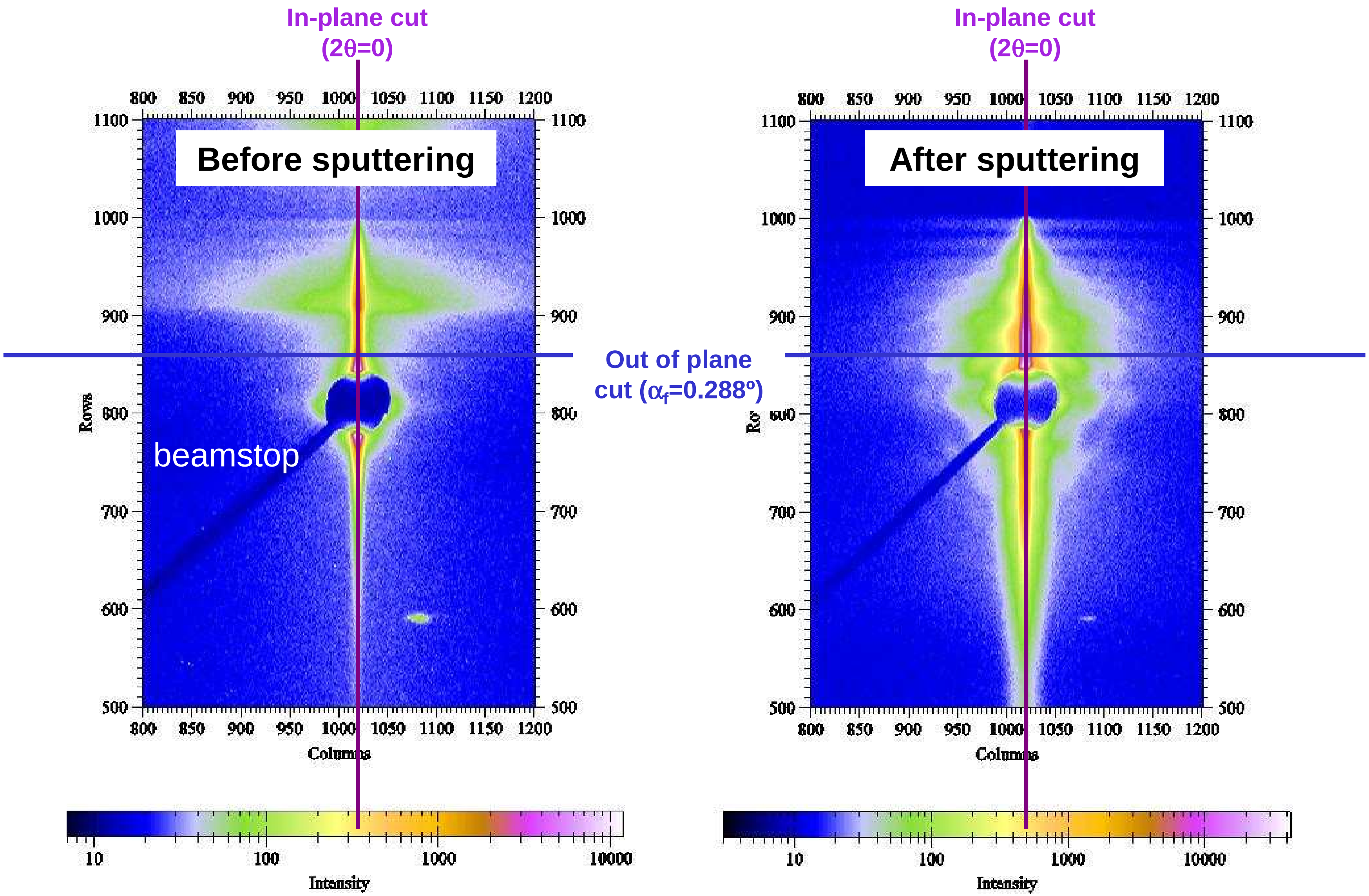

I_0
$h\nu$

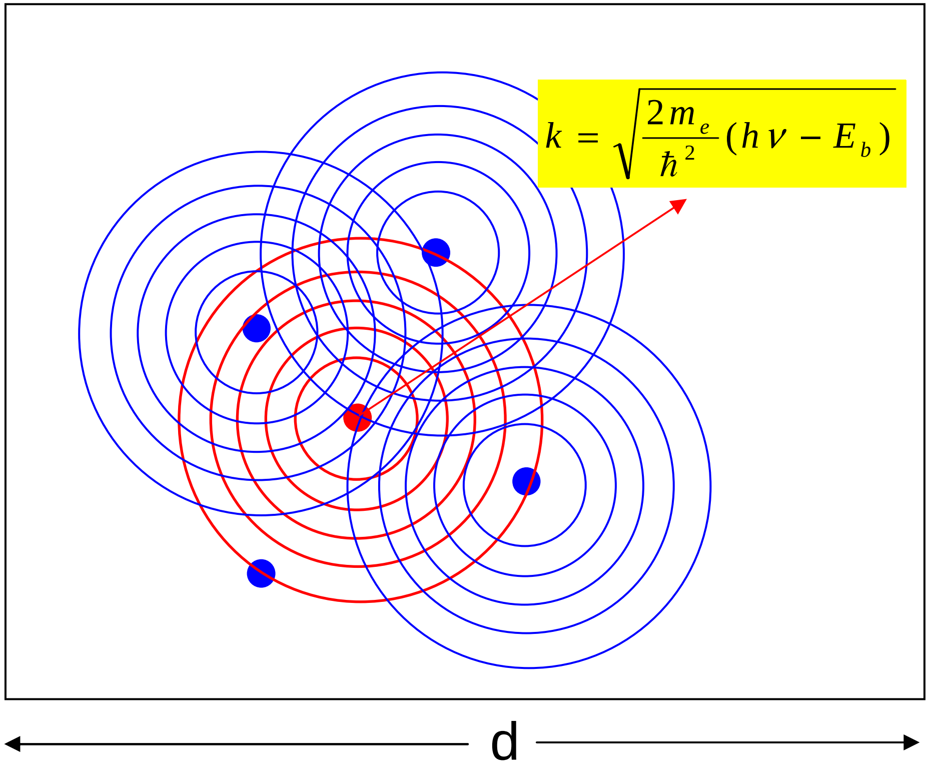

I_1
$h\nu$

Linear absorption coefficient μ

$$I = I_0 \cdot e^{-\mu d}$$

Detected Signal: Absorption or Fluorescence as function of energy of incident radiation

Photoionisation of a K-electron in the „red“ ad-atom →

Free electron: $E_{kin} = h\nu - E_{binding}$
→ Electron Wave with wavevector

$$k = \sqrt{\frac{2m_e}{\hbar^2}E_{kin}}$$

Fermis „Golden Rule“

$$\mu \propto |\langle\Phi_f|\, H\, |\Phi_i\rangle|^2 \cdot \delta(E_f - E_i - \hbar\omega)$$

Initial state

final state $\Phi_f = \Phi_{outgoing} + \Phi_{backscattered}$

X-Ray Absorption Spectroscopy Experiment Setup

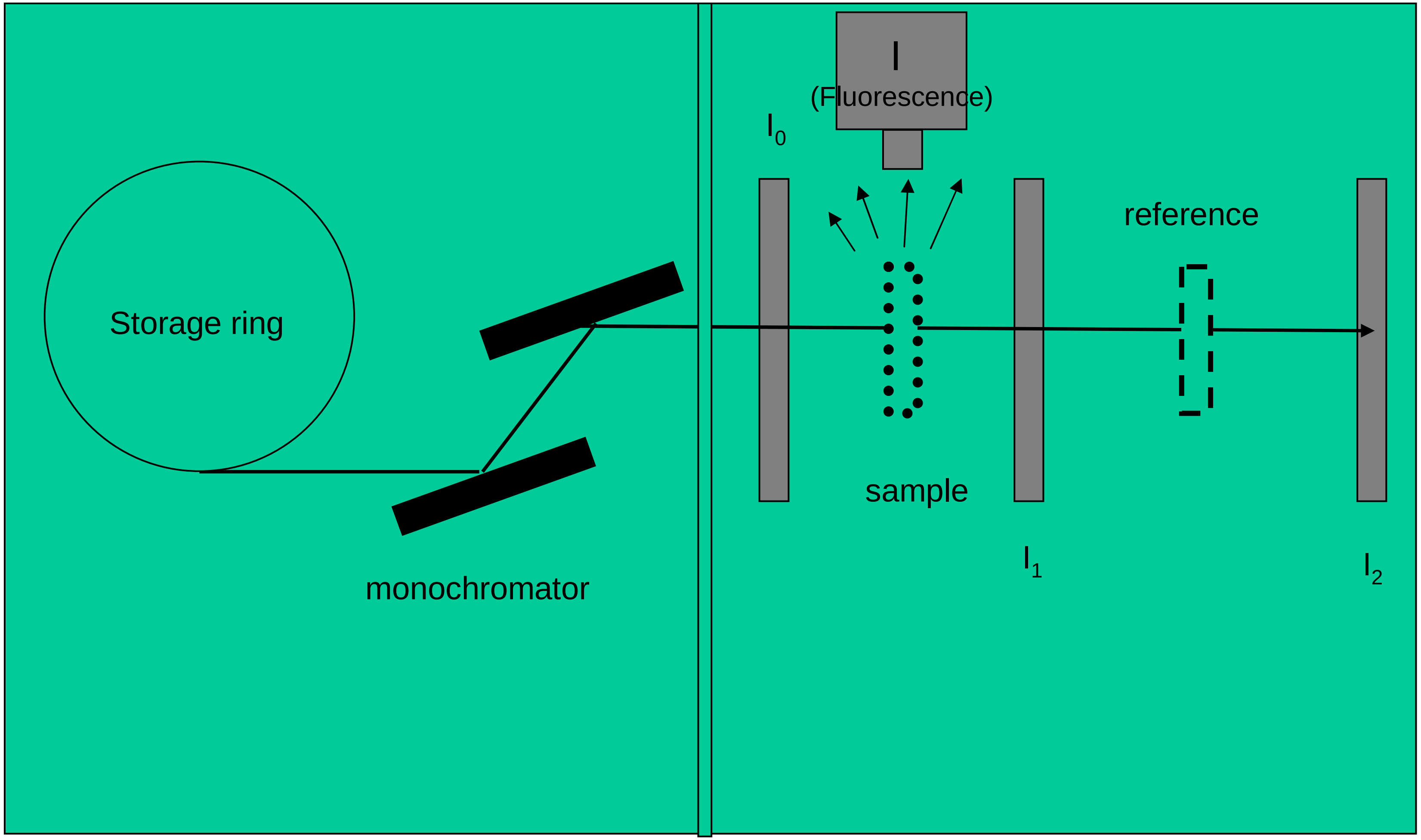

X-Ray Absorption Spectroscopy (EXAFS)

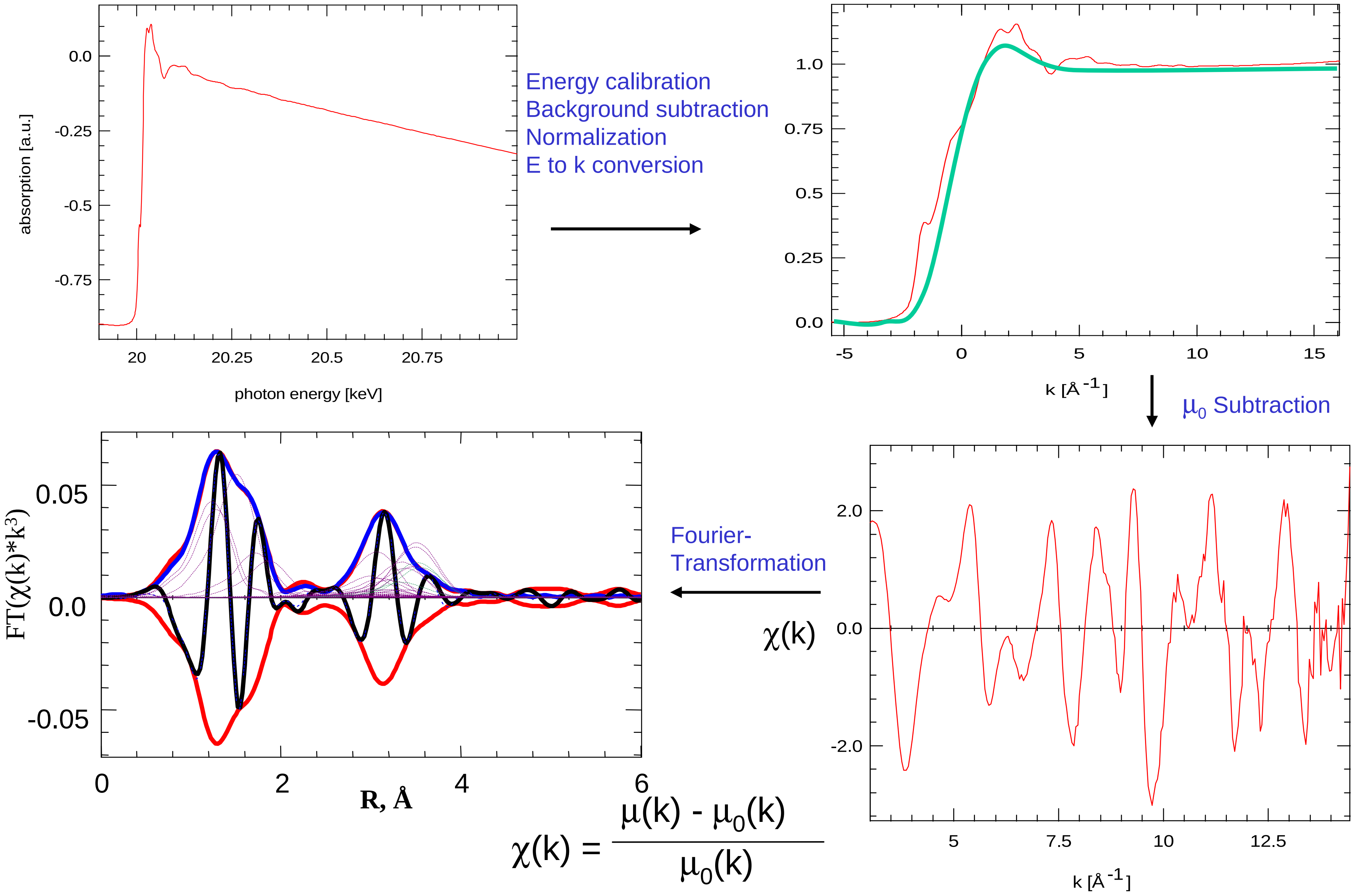

$$\chi(k) = \frac{\mu(k) - \mu_0(k)}{\mu_0(k)}$$

Near Edge X-Ray Absorption Spectroscopy (XANES)

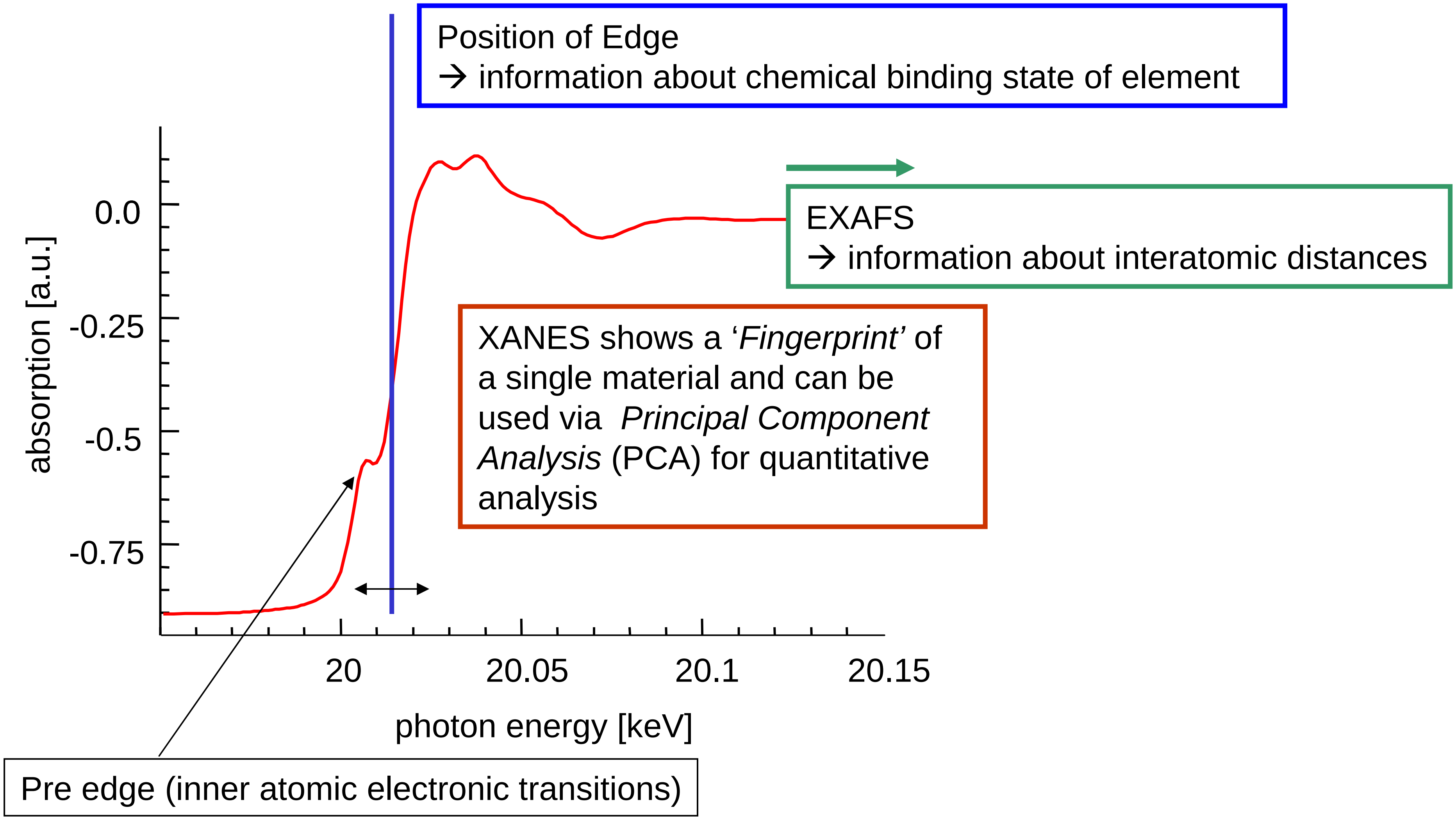

Instrumental development: QEXAFS (piezo scanning)
Study of solid state transformations in catalysis

Activation of a $CuO/ZnO/Al_2O_3$ catalyst for methanol synthesis:

- In-situ reduction in H_2 gas flow at elevated temperatures
- 50 ms time resolution
- Detailed analysis of transient chemistry (here Cu_2O)
- Experiment done at BW1

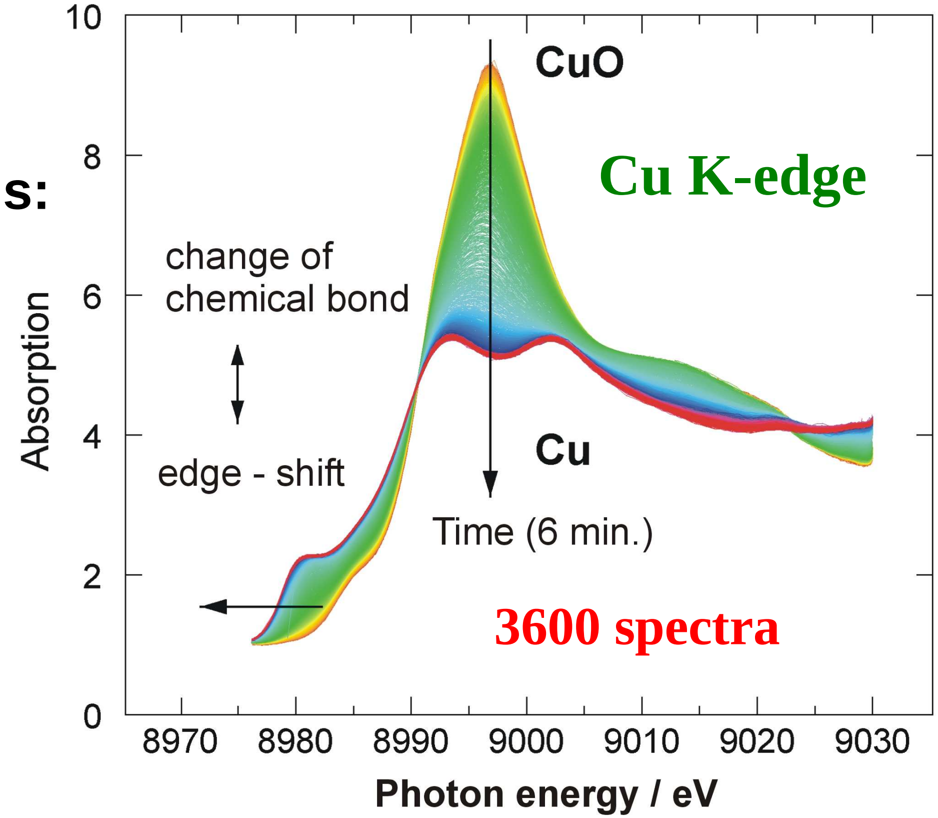

R. Frahm, B.S. Clausen et al.

Extended study:
J.-D. Grunwaldt et al., J. Phys. Chem. B **105**, 5161 (2001)

3D imaging with confocal X-ray Microfluorescence

Micro X-ray Fluorescence on Daphnia Magna (water flea)

Principle

beamline L

detection **incident beam**

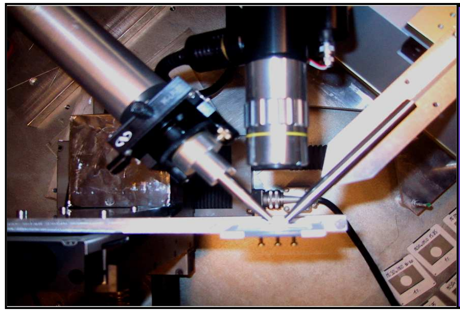

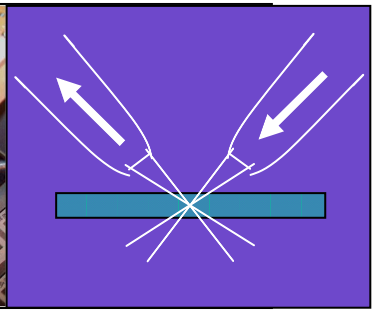

Focus 10 µm

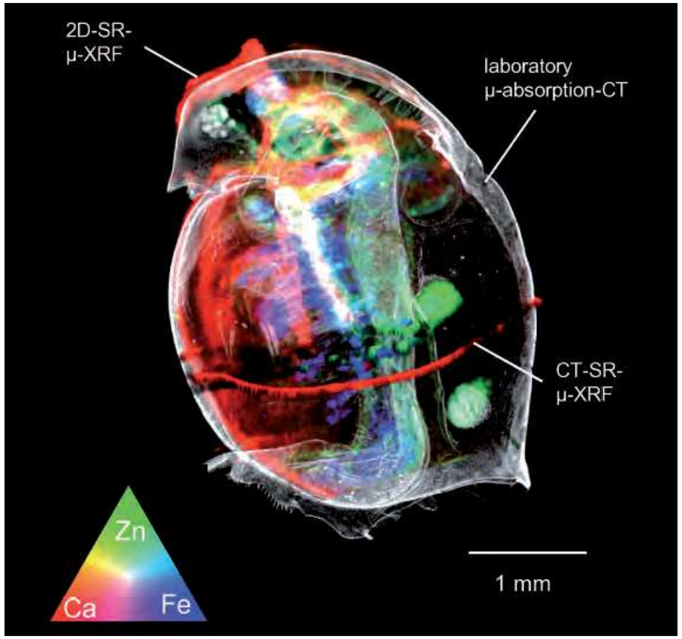

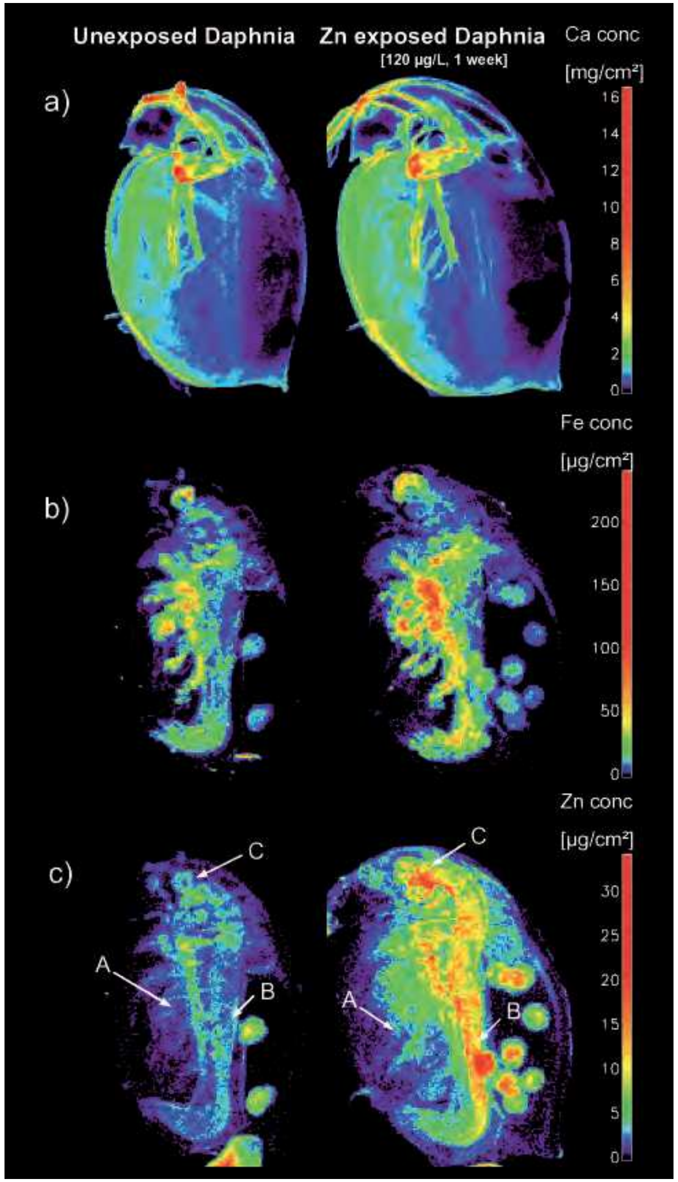

Vincent van Gogh: Meadow with flowers

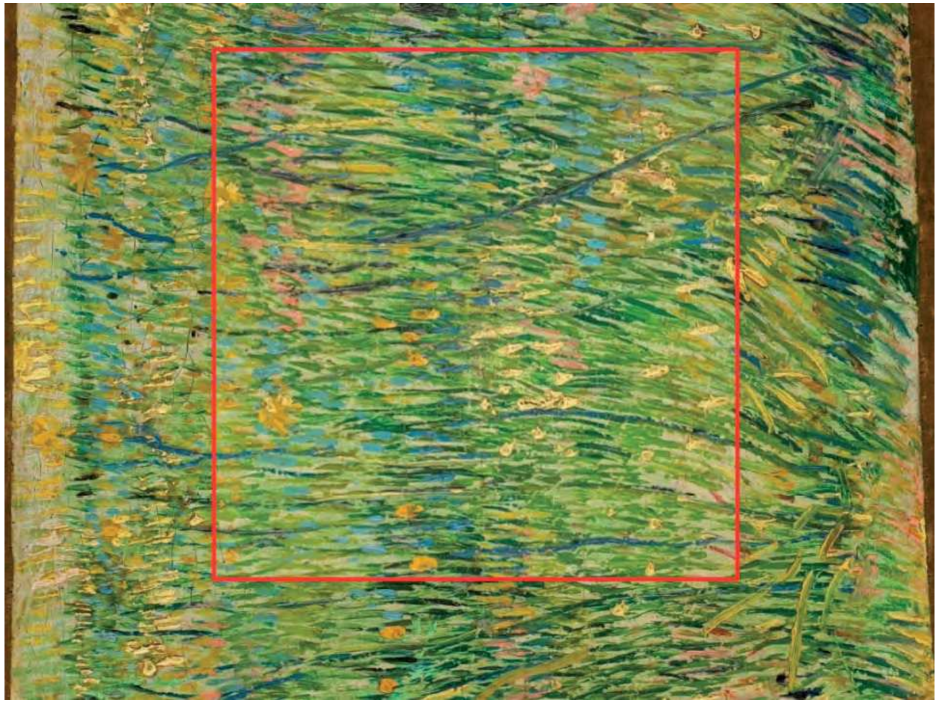

Typical fluorescence spectrum in a single pixel

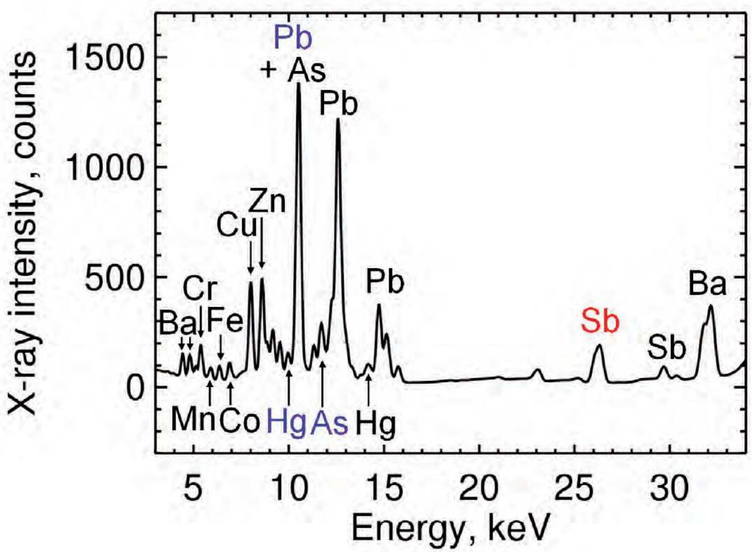

Raster scanning along 90000 pixels with 0.5 mm resolution

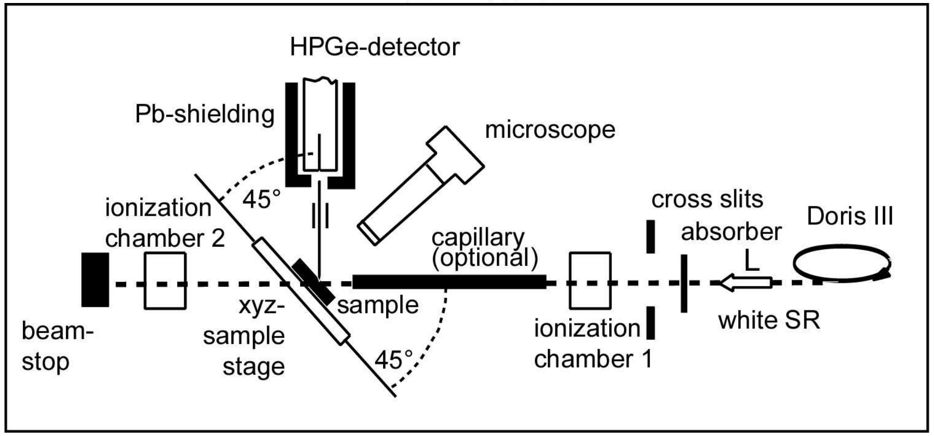

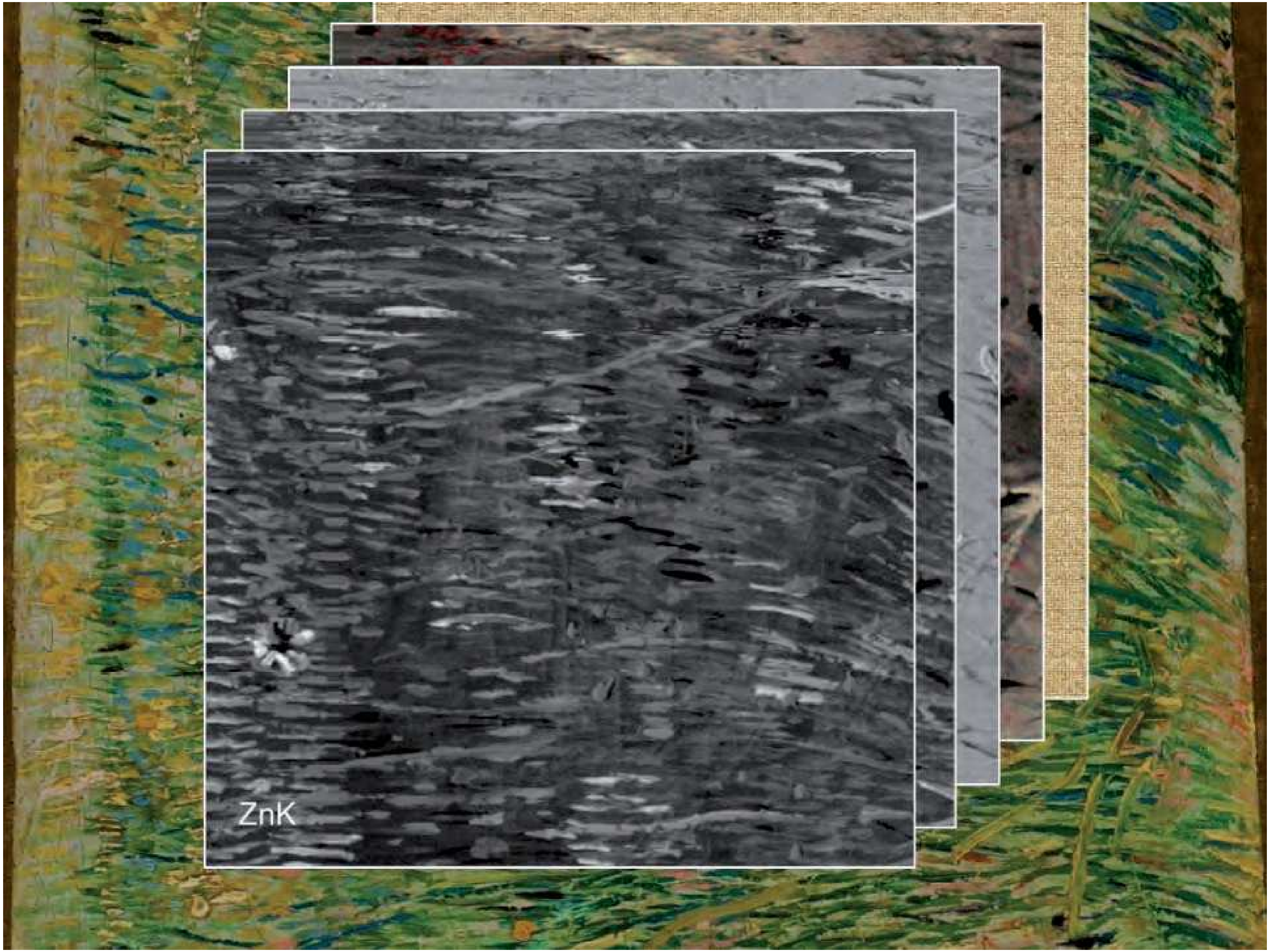
ZnK

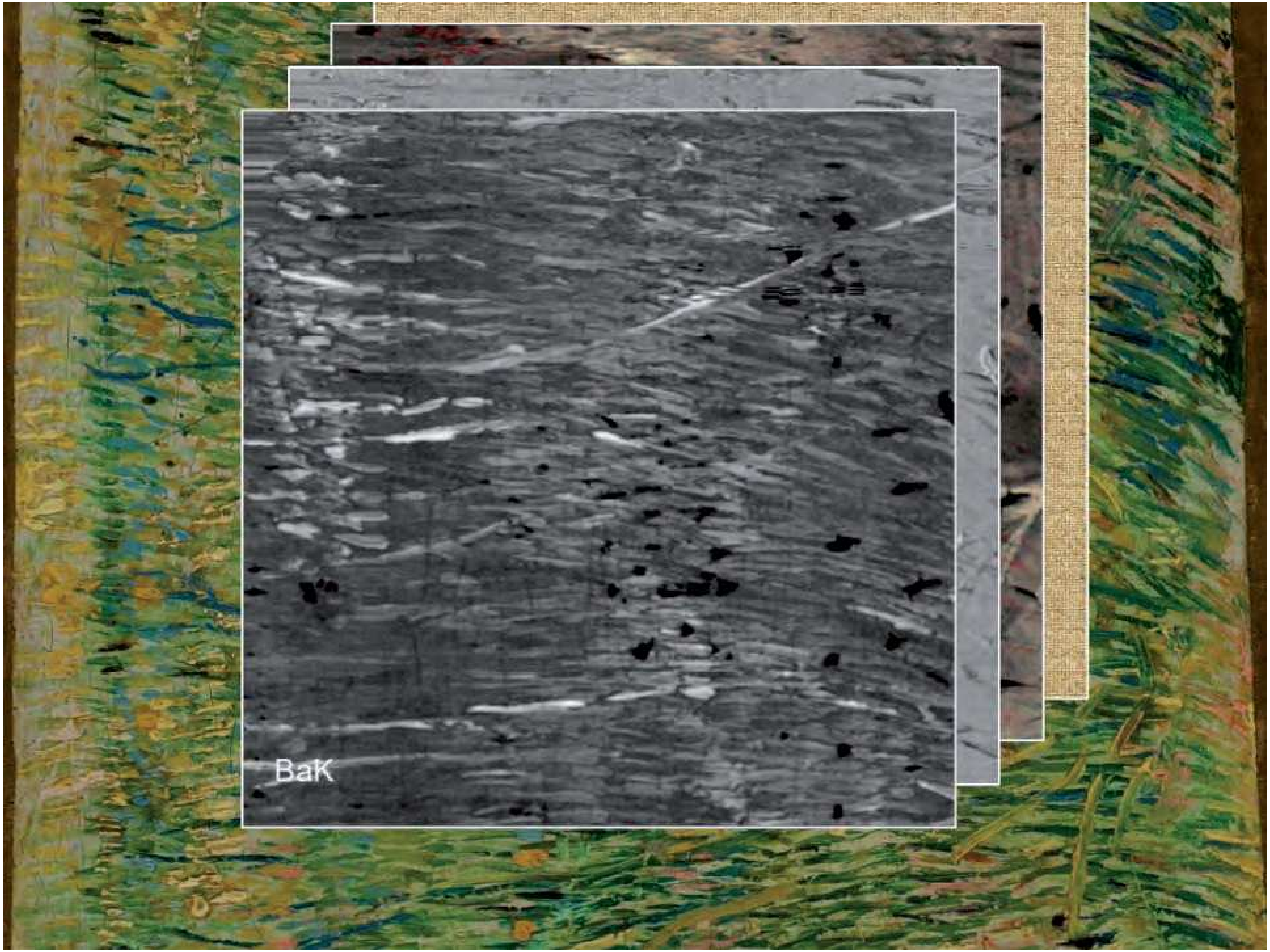
BaK

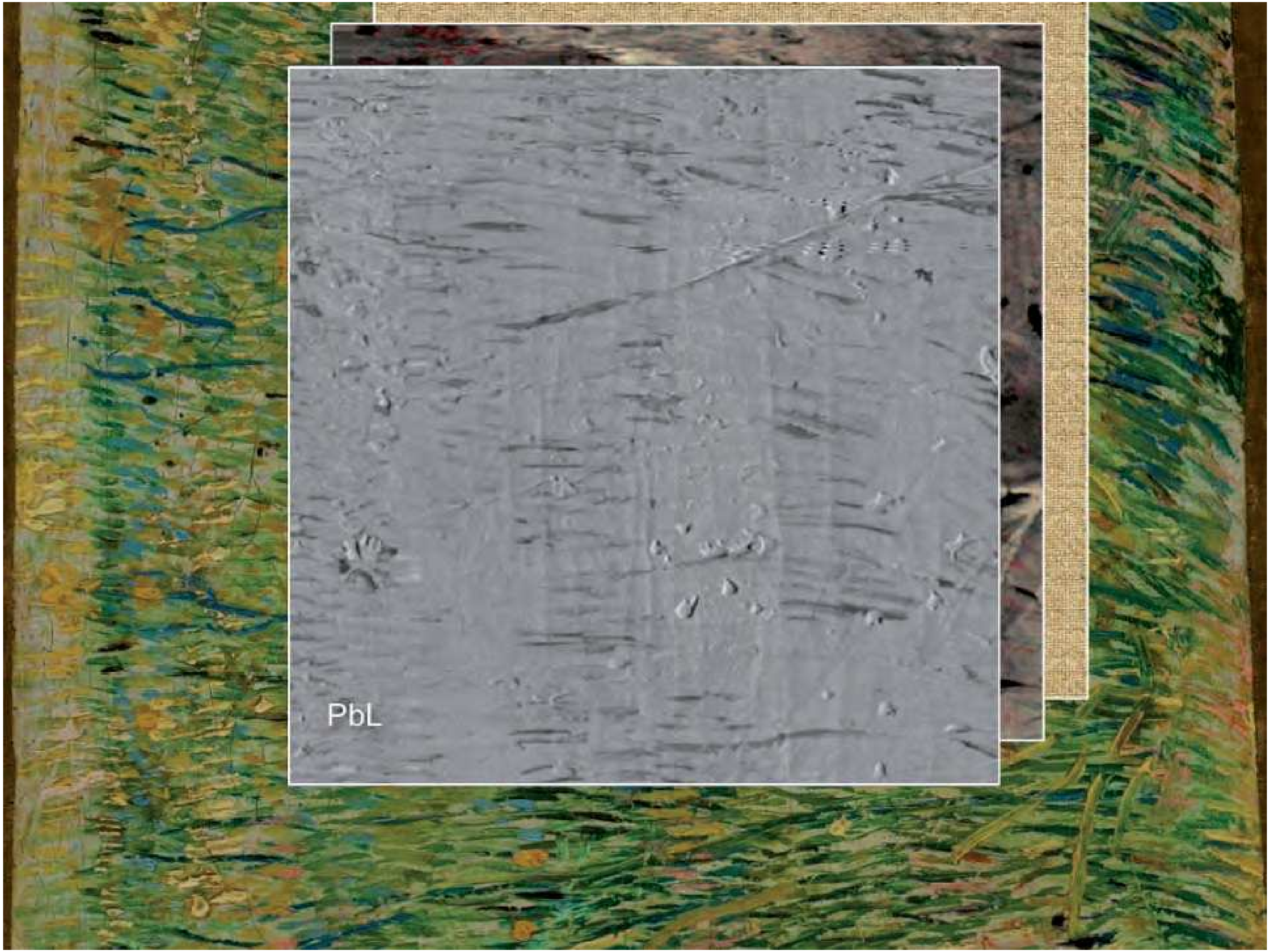
PbL


SbK + HgL

Activities of GFZ (Geoforschungszentrum Potsdam) at DESY

1750t press for in situ studies of large sample volumes.
Maximum pressure: ~ 25 GPa
Temperature: > 2000 K

Study of material under the conditions of the earths lower mantle.

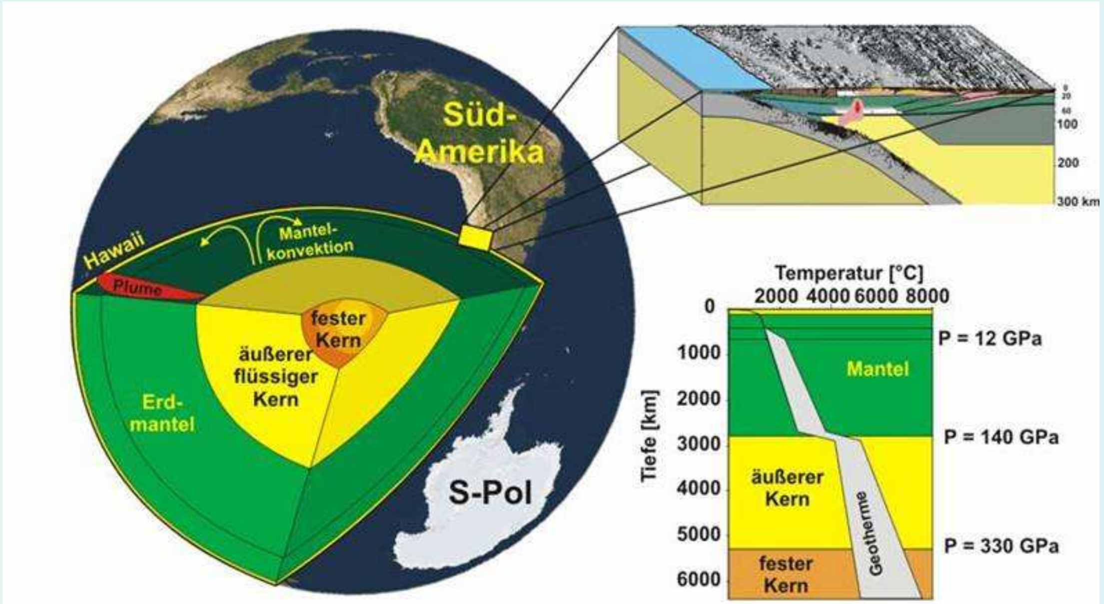

Inelastic X-ray scattering under High Pressure

Speed of sound of Fe under pressure (ESRF: 2 ph/min)

P=28GPa

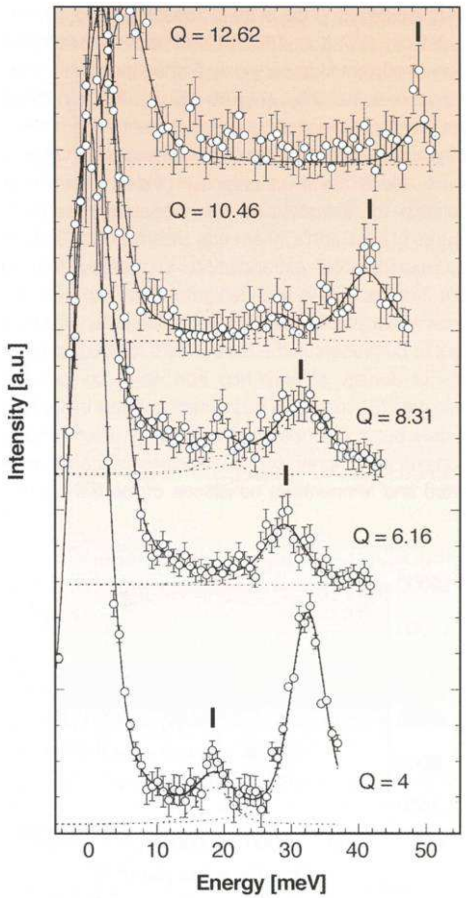

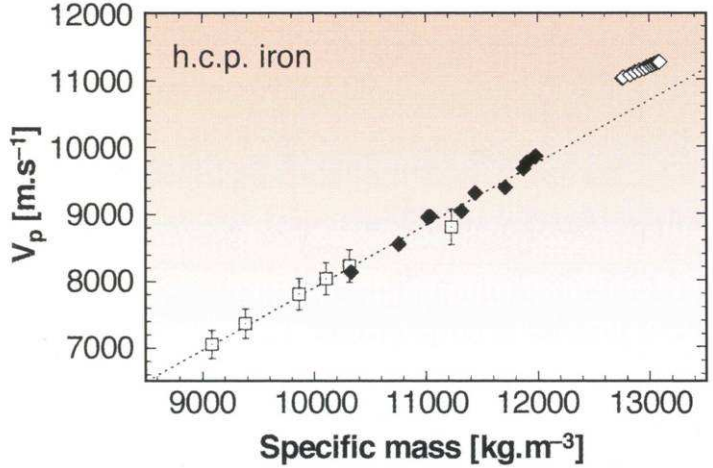

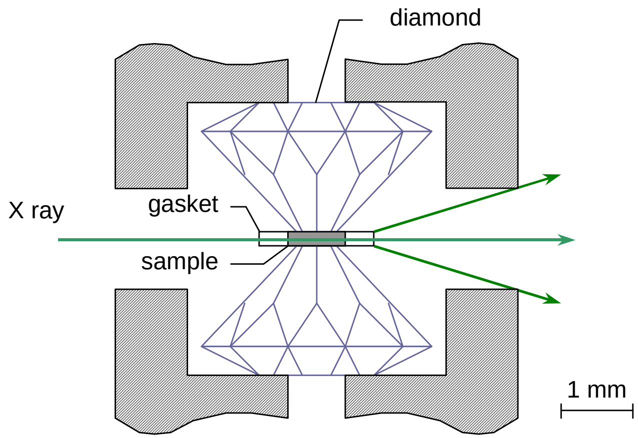

G. Fiquet et al., Science (2000)

Hydrothermal Diamond Anvil Cell

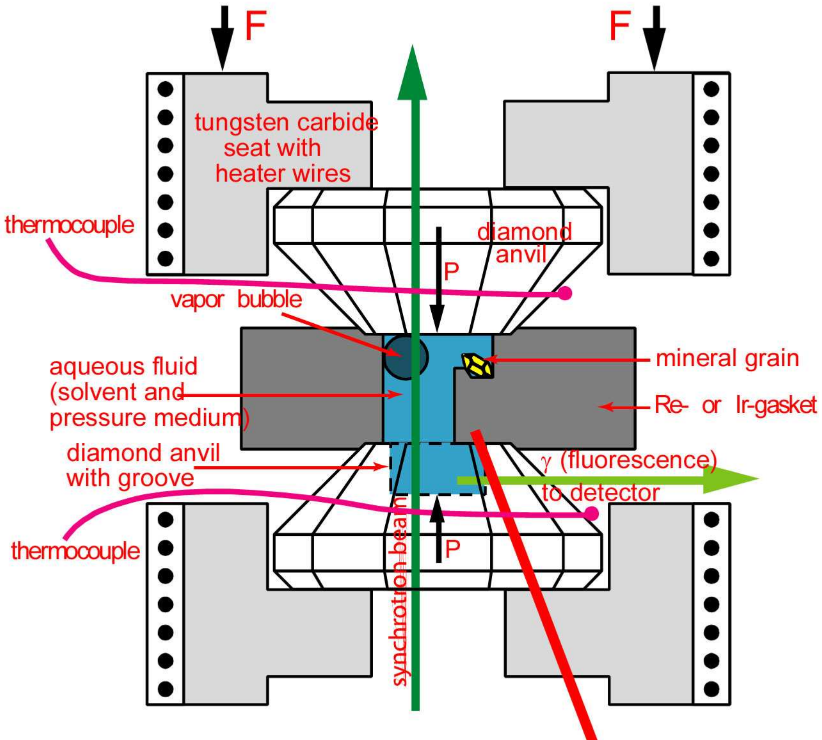

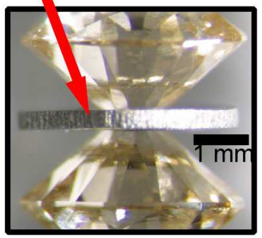

diameter of sample chamber: 300 µm
height of sample chamber: ca. 100 µm

SR-XRF:
In-situ determination of mineral solubilities at elevated temperatures and pressures (up to 800°C & 1.5 GPa)

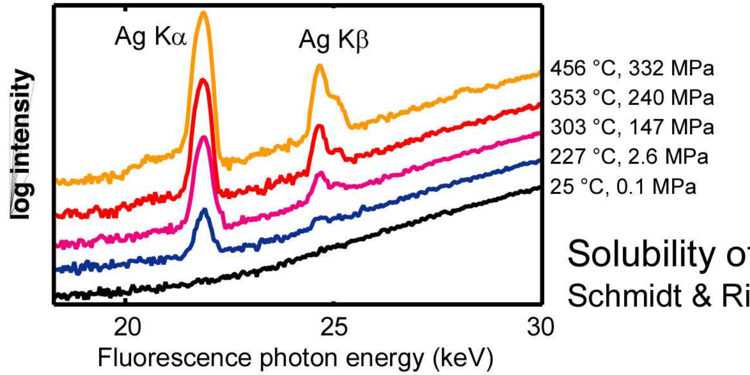

Solubility of AgCl in water
Schmidt & Rickers 2003

Background:
Fluid-mineral equilibria control the mobility of elements during geologic processes

This method is applicable for extremely low solubilities

C. Schmidt and K. Rickers, Am. Mineralogist **88**, 288 (2003)

Parallel Beam X-Ray Tomography

Spatial Resolution: 10 µm

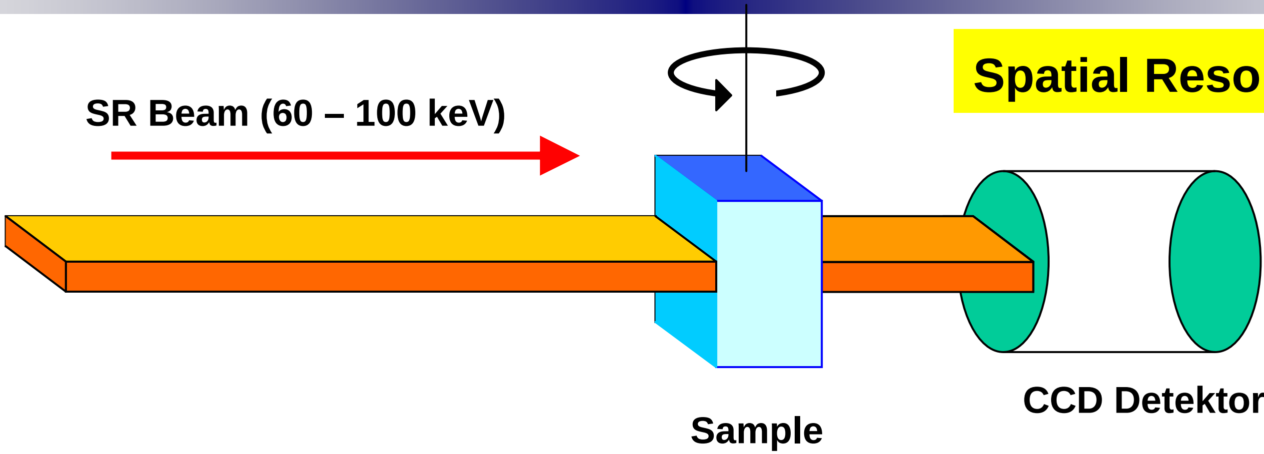

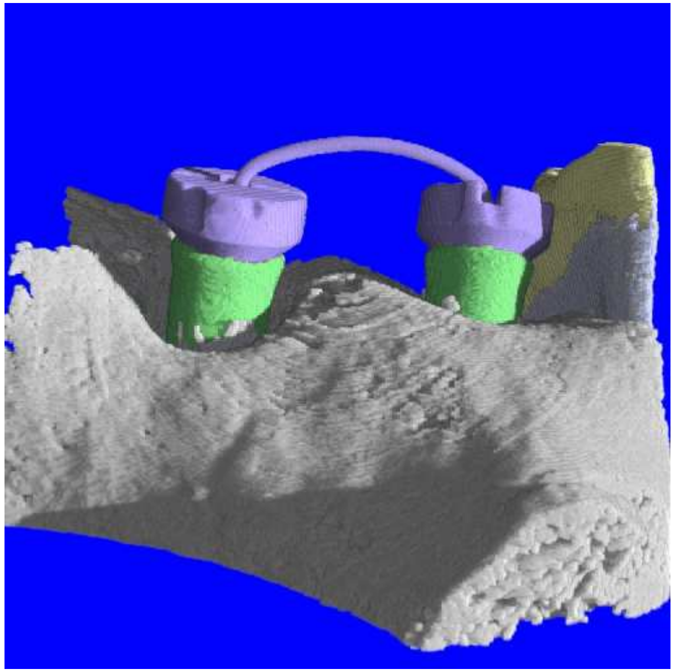

Sample: LED at 60 keV

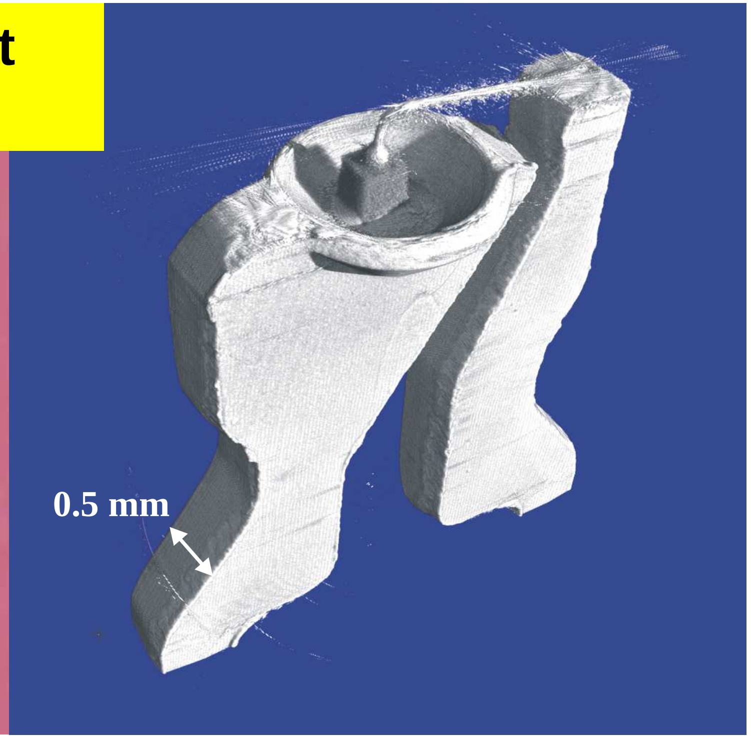

Photoelectric Effect at Ultrahigh Intensities (FLASH, 13.5 nm]

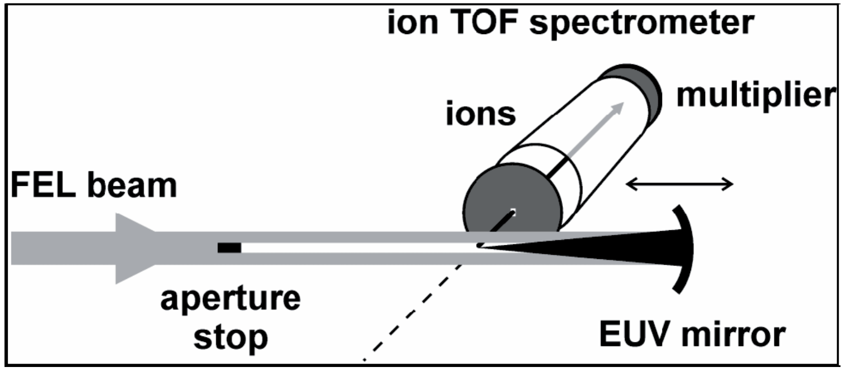

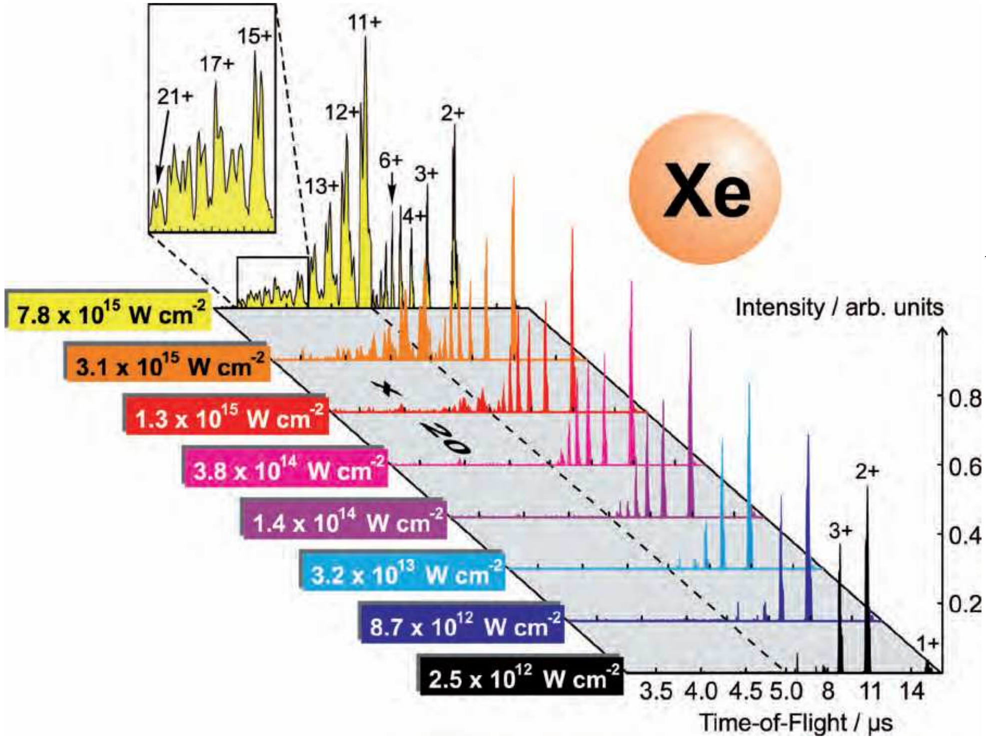

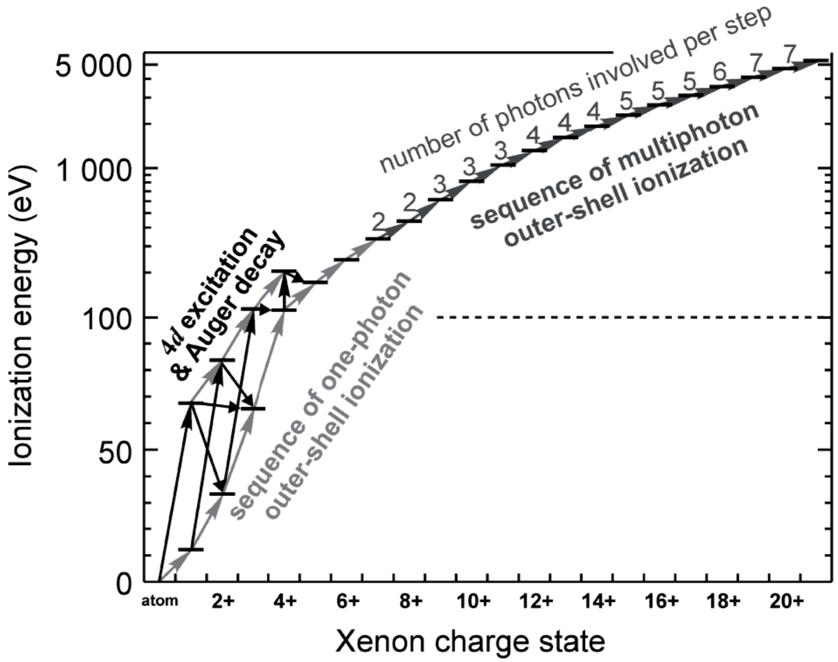

Dramatic changes in the ion charge state at high power densities

One atom has to absorb more then 50 photons

Phys. Rev. Let. 99, 213002 (2007)

Ultrafast Coherent Diffractive Imaging at FLASH

Resolution 50 nm

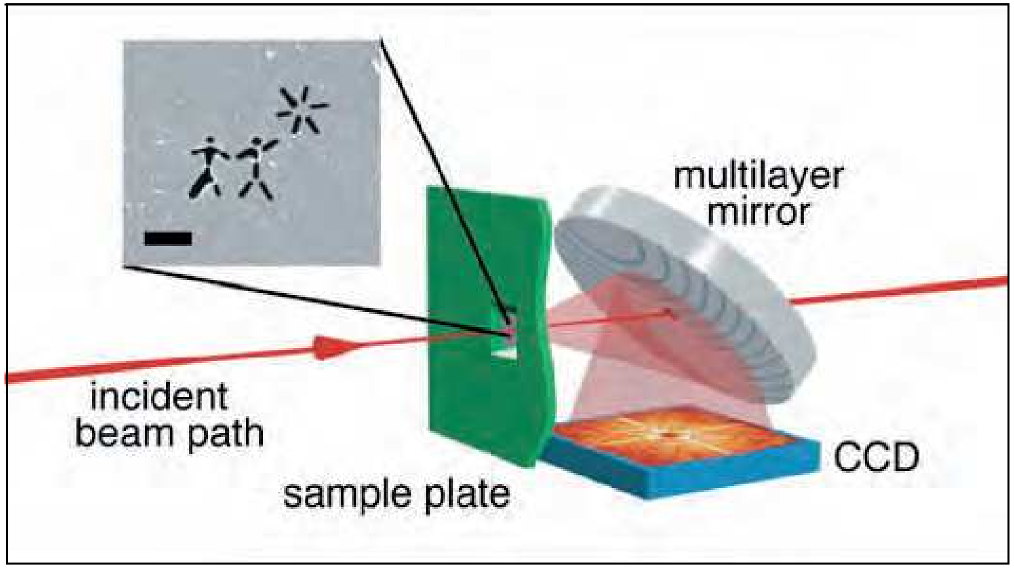

Nature Physics 2, 839 (2006)

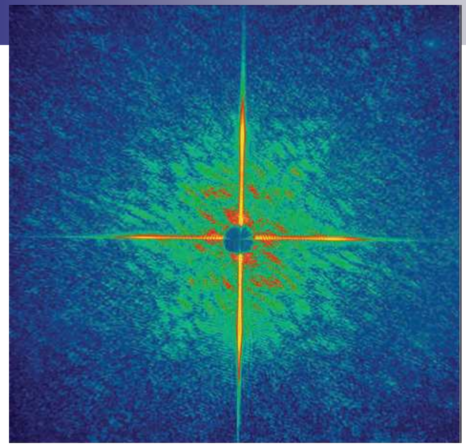

1st shot

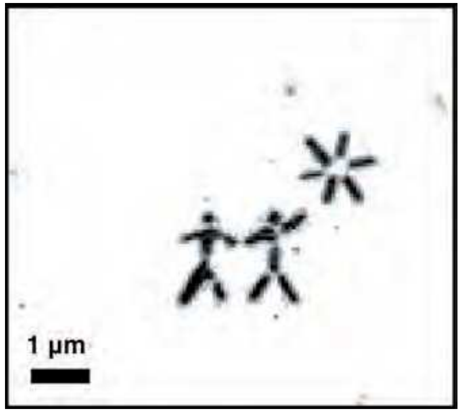

Image Reconstructed From 1st shot

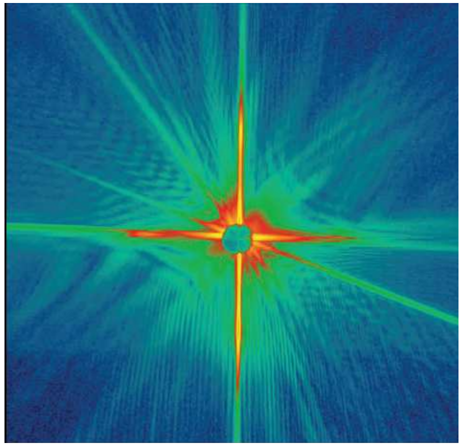

2nd shot (target destoyed)